Simulating smoldering and flaming combustion spread in wildfires through cellular automata modelling: the case of the 2020 Peel region wildfire.

Thesis – Luc Hermans – 6892787
Responsible Professor: Dr. Ir. Ron van Lammeren
Supervisor: Dr. Ir. Arend Ligtenberg
1-March-2020

In loving memory of
Trees Asmussen – de Quillettes

Simulating smoldering and flaming combustion spread in wildfires through cellular automata modelling: the case of the 2020 Peel region wildfire.

Abstract

This thesis aimed to end the mosaic like division of knowledge on different aspects involved in wildfire events that inhabit both smoldering and flaming combustion types. While not all these aspects could be addressed an extensive view on wildfire science theory, modelling theory and the Dutch wildfire context is presented. Furthermore, this work presents the first wildfire modelling framework that successfully includes the phenomena of revegetation and smoldering to flaming combustion transfers in simulations at the field scale. The proposed framework, FENIX, was subsequently applied to simulate the Peel region wildfire event of early 2020. This application was done by coupling the FENIX framework with spatial data obtained and manipulated through a Geographic Information System. While the framework was able to successfully simulate different wildfire behavior phases, simulations could not successfully predict the timing of these phases and the final wildfire extent. This is due to limitations in both the framework itself and available data.

Key words: Wildfire Modelling, Cellular Automata, Geographic Information Systems

Thesis – Luc Hermans – 6892787 – Word count: 22456
Responsible Professor: Dr. Ir. Ron van Lammeren
Supervisor: Dr. Ir. Arend Ligtenberg

Contact information writer:

l.d.hermans@students.uu.nl – luc.d.hermans@gmail.com
+31639848688
Jan Evertsenstraat 109-2 1057BT,
Amsterdam, The Netherlands

Table of contents

§1. Introduction

§1.1 General introduction

The October 6, 2020 update of the California Department of Forestry and Fire Protection (Cal Fire) marked the "milestone" of the first so-called *Giga fire* (the situation where a single fire complex burns more than 1.000.000 acres) in the state of California, United States. The 2020 wildfire season is therefore one of the most destructive wildfire seasons ever in the state (CalFire, 2020). Earlier this year the western part of Australia also saw an extreme wildfire season, which later was known as the *Black Summer*. This season destroyed over 11 million hectares of land nationwide (Burgess, Burgmann, Hall, Holmes, & Turner, 2020). The complete impact of Climate Change on the severity of these wildfire seasons is hard to estimate. However, extreme weather events such as record-breaking heat or extended dry periods certainly have an impact on the amount of fires, the length of the wildfire season and the area that burns during such a season (Burgess et al., 2020; Halofsky, Peterson & Harvey 2020). That Climate Change is of impact in itself is emphasized by a wide range of studies (I.E. Haider et al., 2019; Rein & Belcher, 2013). These studies often point towards the positive feedback between greenhouse gas emissions through wildfires for Climate Change (Restuccia, Huang, & Rein, 2017). This situation means that more and bigger wildfires result in more emissions, which lead to more and even bigger wildfires. The annual report on the pan-European wildfire season composed by The European Forest Fire Information System (EFFIS) mentioned the role of climate change for the first time in the reporting on the 2018 fire season (San-Miguel-Ayanz et al., 2018). However, the full impact of Climate Change remains unknown.

Alongside the destruction of nature put in numbers through surface measurements these heavy wildfire seasons also destroy a lot of habitat for fauna and directly affect their population therefore putting the biodiversity of the region at risk (Burgess et al., 2020). The fires also have a huge economic impact with regards to the destruction of residences and companies. In some cases, wildfires take lives of fire fighters or civilians who are trapped by the quickly progressing fire fronts. While these fires prove to form an immediate danger, they also indirectly affect the health of millions of people through their smoke pollution. Some studies even relate wildfires directly to mental health issues due to the risk of being evacuated and the risk of losing homes (Burgess et al., 2020).

Wildfires can be of flaming character, such as in ground fire in a heath vegetation area. Another form of wildfires is characterized by smoldering combustion (Rein, 2009). Smoldering wildfires have received less attention as opposed to flaming wildfires therefore there is a lack of academic knowledge about these smoldering wildfires (Rein, 2016). Smoldering happens mostly in organic layers such as peat, formed by decaying organic content. Peat as a soil holds enormous amounts of greenhouse gasses; more CO_2 is stored in peat layers then in rainforests (Nusantara, Hazriani & Suryadi, 2018; Rein & Belcher, 2013; Restuccia et al., 2017; Turetsky et al., 2015). When a smoldering fire happens, the stored greenhouse gasses are released into the atmosphere, a 1997 Indonesian peat fire accounted for around 15% of the global annual fossil fuel emission. This is about the same share as the emissions of the European Union (Christensen, Fernandez-Anez, & Rein, 2020a; Rein, 2009). Understanding the dynamics behind smoldering wildfires is key in effective forest management to prevent events and limit extents of future massive smoldering wildfires.

Solid forest management and prescribed controlled burning help to limit the impact of forest fires (Davies et al., 2016). Furthermore, education is a strong weapon in the war since almost nine out of ten wildfires occur due to direct or indirect human influence (Stoof, Tavia, Marcotte, Stoorvogel, & Ribau, 2020). Along with education on ignition of wildfires, a better understanding is needed in order to better estimate the impact of wildfires in specific ecosystems (Davies et al., 2016). The 2020-wildfire season proved to be extremely destructive, yet most wildfires do not affect more than three hectares of land and are contained relatively quickly after the initial attack by fire fighters (Arienti, Cumming, & Boutin, 2006; Cardil, Lorente, Boucher, Boucher, & Gauthier, 2019).

Extreme wildfire seasons are not limited to North America and Australia. Research into the specific situations for pan-European countries has taken flight since the installation of The European Forest Fire Information System (EFFIS) in 2000. The 2018 fire season in Europe was characterized by extreme draught and unusual warm periods. This meant that even in the Netherlands, a country widely known for problems in water management, wildfires are proving to become a natural hazard of increased risk (Oswald, Brouwer & Willemsen, 2017). This fire season along with unusually big wildfires over the previous decade such as the *Strabrechtse Heide* (2010) fire and the V*eluwe* fire (2014) resulted in the first-time contribution to the EFFIS annual fire season report by the Netherlands after the 2018 wildfire season (San-Miguel-Ayanz et al., 2018). A more recent EFFIS publication incorporates statistics on Dutch wildfire for a longer period of time (Kok & Stoof, 2020).

As said, the 2018 wildfire season was extreme in Europe and in the Netherlands. To put this in numbers the total count of wildfires in 2017 was 28, whereas the total count of wildfires in 2018 equals 193 wildfires in the Netherlands (Brandweeracademie, 2019). Compared to other countries wildfires in the Netherlands are relatively small, however due to the dense population and the resulting close interaction of built-up area and nature even these small scale wildfires can be a direct (and indirect) danger to assets and health of nearby residents (Oswald et al., 2017). Since the previous decade, the Dutch Institute for Physical Safety (*Instituut Fysieke Veiligheid*) is working on the development the Dutch Wildfire Spread Model (*Natuurbrandspreidingsmodel*) (NBVM). This model is meant to predict the spread in real time in order to improve the understanding and the use of firefighting assets in order to get the wildfire under control effectively. The model is operational as of 2013 (IFV, 2016). Currently improvements on the Dutch wildfire spread model are made to incorporate more fuel types and a more diverse vegetation map (Oswald et al., 2017). A set of semi-structured interviews is conducted to fill possible gaps on contemporary Dutch development in wildfire modelling that academic publications might have until now.

These improvements in research and understanding of wildfires will not mean that large wildfires will not happen in the Netherlands. In the late days of April 2020, biggest wildfire ever recorded in the country struck the southeastern region on the border between the Noord-Brabant and Limburg provinces. This fire affected an area of 710 hectares and resulted in the deprivation of air quality for a large region and immediate evacuations in the villages of Griendsveen and Liessel (EFFIS/WILDFIRE Database, 2020; Omroep Brabant, 2020; Stoof et al., 2020). The geographical extent of the Peel region wildfire is shown in image 1. One of the complex characteristics of this particular wildfire was that it was partly burning in a peatland-composed area. Smoldering combustion in peatland and its behavior in fire is not researched as widely as other soil types, partly due to its complex characteristics of underground fire progression (Davies et al., 2016; Mutthulakshmi et al., 2020).

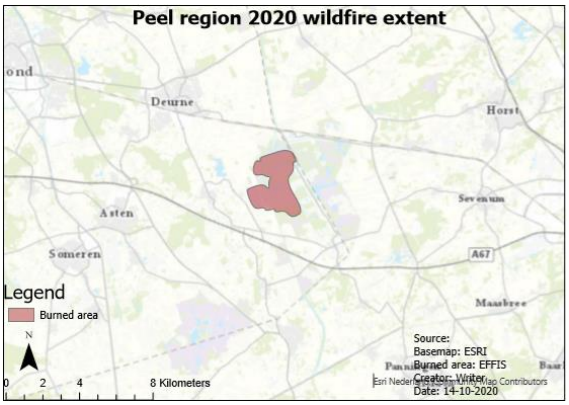

Image 1. Peel region 2020 wildfire extent
Source: EFFIS (2020)

In the academic world wildfires receive increasing attention due to the extent of contemporary wildfires and their societal impact. Recent studies focus on fire spread rates in smoldering combustion and findings of these studies are incorporated in wildfire spread modelling (Christensen et al., 2020a; Purnomo, Bonner, Moafi, & Rein, 2020). This thesis tries to combine knowledge from highly specified fields such as physics and data science in order to better understand what impact modelling can have on wildfire management. Furthermore, it tries to form a cohesive study on impacting factors on wildfires. While extensive studies are done on modelling on one side and impacting factors on the other, it is rare for studies to give an in-depth image of both at the same time. By combining knowledge from experts, an extensive literature review and a data-driving modelling approach this thesis aims to couple the mosaic-like destirbution of knowledge that characterizes wildfire research. The 2020 Peel Region wildfire will be the central case study in this thesis. Therefore, the Dutch situation on wildfire modelling and data registration will be discussed in depth.

§1.2 Research objectives

The objective of the final thesis is twofold. The first main objective is to shed light on current knowledge and developments concerning contemporary wildfire spread prediction specifically for peatland regions. This will be a qualitative research component, expert interviews and literature study will be combined to later form the basis for the second part of the research. This second research component is a quantative data driven investigation of the capabilities of cellular automate modelling in the simulation of smoldering and flaming peatland wildfires in the Netherlands. The second part will be addressed via modelling of the aforementioned Peel region fire of early 2020 through a cellular automate model. The choice for a cellular automate model is made because of its simplicity. Other models might have better performance in relation to wildfire spread explanation. However, these other models, which will be addressed more in depth, require a lot of computing power, which was not available for this thesis. With this in mind, the choice is made to build a cellular automate model. A drawback to the cellular automata approach is that it is a rather crude form of modelling. Some important characteristics of wildfire spread might be better captured by other forms of modelling, such as vector models based on partial differential equations. The different modelling approaches will be addressed in chapter three.

The goal of this thesis is to fill the gap in current academic literature on wildfire spread modelling concerning smoldering to flaming combustion transfers and the incorporation of revegetation at the field scale.

To sharply formulate the goal of the research the following research question and sub-questions are formulated:

§1.3 Research questions

To what extend can a smoldering and flaming peatland based wildfire spread be simulated from the real world into a data driven cellular automate model?

Broken down into six sub-questions:

1. *What are the influencing variables and characteristics with relation to wildfire fire front progression in smoldering and flaming combustion?*
2. *What modelling theories are deployed in contemporary wildfire spread models?*
3. *What are the specific characteristics of the Peel region 2020 wildfire?*
4. *What is the current state of modelling and data collection for wildfires in the Netherlands?*
5. *To what extend can processes in smoldering and flaming wildfires be simulated to model wildfire front fire spread over a hypothetical field?*
6. *To what extend can a cellular automate based model be used to explain the spread of the 2020 Peel region wildfire in the Netherlands and which factors are most important to the model output?*

§1.4 Scope

This research does not include the effects that forest management and firefighting have on front fire propagation. A recent study has shown that the incorporation of fire lines is doable (Mutthulakshmi et al., 2020). In line with this further research could focus on the integration of firefighting activities through the combination of cellular automata modelling and agent-based modelling to form new understanding of how firefighting activities can influence front fire propagation. Ultimately, this can result in a training tool for fire commandants.

Moreover, this research will not be about ways to improve our data gathering. While numerous ways exist to improve our classification of fuel types and forest dynamics this is not the focus of this study (I.E. Chuvieco et al., 2004; Fortin, 2020; Kötz et al., 2004).

Effectively and accurately explaining wildfire front fire spread is a highly multidisciplinary field of expertise and should be addressed as such (Bakhshaii & Johnson, 2019; Davies et al., 2016; Stoof et al., 2020). A single MSc thesis will not change the models we use worldwide and will not compete with contemporary models developed by climate institutes which can bring together scientist from a multifold of different disciplines, however these models and their limitations will be input for the discussion section (for more information on contemporary models see (Bakhshaii & Johnson, 2019). The aim of this thesis is to shed light on the fundamentals of wildfire modelling and to start a discussion on where to put the focus of subsequent academic research with a close link to the situation specific to the Netherlands. This thesis follows a deductive approach. This means theory will be the starting point used to address the case.

§1.5 Reading guide

To structure this thesis the work is divided in ten chapters, these chapters are visualized in image 2. The second chapter, concerning fire science theory as indicated in red in the image will address the first sub-question. The third chapter, concerning modelling theory as indicated in black in the image will address the second sub-question. The fourth chapter will address the methodology to answer the subsequent sub-question underlying the main research question. The fifth chapter, concerning the study area and the introduction of the case as indicated in green in the image will address the third sub-question. The sixth chapter, concerning the Dutch context as indicated in yellow in the image will address the fourth sub-question. The seventh chapter of this thesis will address the data that is used and will provide insights into the quality of that data. The eighth chapter, concerning results as indicated in brown in the image will address the fifth and sixth sub-question of the thesis. The subsequent ninth chapter of this thesis will present an extensive discussion concerning wildfire research, findings from the thesis and it will identify possible areas of future results. The lasts chapter will provide the conclusion to the main and sub-research questions as presented in section 1.3.

Image 2.
Reading guide

§2. Fire science theory

§2.1 Introduction

This chapter on fire science theory will introduce the most important concepts underlying wildfire phenomena. The chapter will be built up from the very basics of combustion theory. Subsequently, forms of combustion in wildfire phenomena will be identified. Thirdly, the impact of fuel will be considered. With this knowledge as a foundation, subsequent sections will address the most important influences on wildfire spread. This chapter aims to give the foundation upon answering the first sub-question as defined earlier in section 1.3.

§2.2 Fire and combustion

Fire is one of the most important natural phenomena in the world. Management of fire and the concept of controlled combustion are at the base of the success of humankind as a species, serving both domestic needs and industrial functions. However, unchecked a fire can quickly evolve in a direct danger with great material damage and sometimes human suffering (Drysdale, 2011; Rein, 2016). There are numerous chemical reactions underlying a combustion process. Nonetheless, the global reaction of a solid fuel combustion can be expressed by the process of pyrolysis (eq. 1), the base reaction and either a heterogeneous reaction (eq. 2) or a homogenous reaction (eq. 3) (Rein, 2016).

Pyrolysis: base reaction

Fuel (solid) + Heat -> Pyrolyzate (gas) + Char (solid) + Ash (solid) (eq. 1)

Subsequent possible reactions:

Heterogeneous reaction:

Char (solid) + O_2 (gas) -> Heat + CO_2 + H_2O + other gasses + Ash (solid) (eq. 2)

Homogeneous reaction:

Pyrolyzate (gas) + O_2 -> Heat + CO_2 + H_2O + other gasses (eq. 3)

A combustion process that follows the pathway of pyrolysis and a heterogeneous reaction, involving both solids and gas, expresses itself as a smoldering combustion and happens in the char that is left from the pyrolysis base reaction. One of the most illustrative examples of a smoldering combustion happens in burning cigarettes. The orange head is a visual indicator for the heat produced by the process. A combustion that follows the pathway of pyrolysis and is succeeded by a homogeneous reaction, involving only gas, will express itself as a flaming combustion. This form of combustion takes place in the gas phase and is therefore airborne (Rein, 2016). A candle fire can illustrate this where the homogeneous reaction takes place around the wick leading to visual indicators of heat that can have blue orange and yellow colors among others that are a result of the different burning gasses and difference in heat. The combined underlying process of pyrolysis allows combustion to transfer from a homogeneous to a heterogeneous reaction and the other way around (Santoso, Christensen, Yang, & Rein, 2020).

Smoldering combustion in comparison with flaming combustion produces less heat. Around 450-700 degrees Celsius whereas flaming combustion reaches temperatures ranging from 1500-1800 degrees Celsius. Concerning ignition a smoldering combustion needs far less heat mass. Spread rates for smoldering combustion are much lower compared to spread rates of flaming combustion where the former has a typical spread rate of 1 mm per minute and the latter 100 mm per minute (Santoso et al., 2019). Flaming combustion is widely researched and relatively well understood. Smoldering combustion is, also due to its complexity, not widely researched and therefore not thoroughly understood. The interplay between both forms of combustion is hugely complex and trying to model the exact chemical reactions and their relation to spread will not be feasible. However, in order to take decisions in the modelling phase of this thesis a good understanding of the occurrence of both types of combustions in wildfires is necessary. The proposed model will include both smoldering and flaming combustion and will attempt to simulate the transfers that happen between both combustion processes.

§2.3 Forms of combustion in wildfires

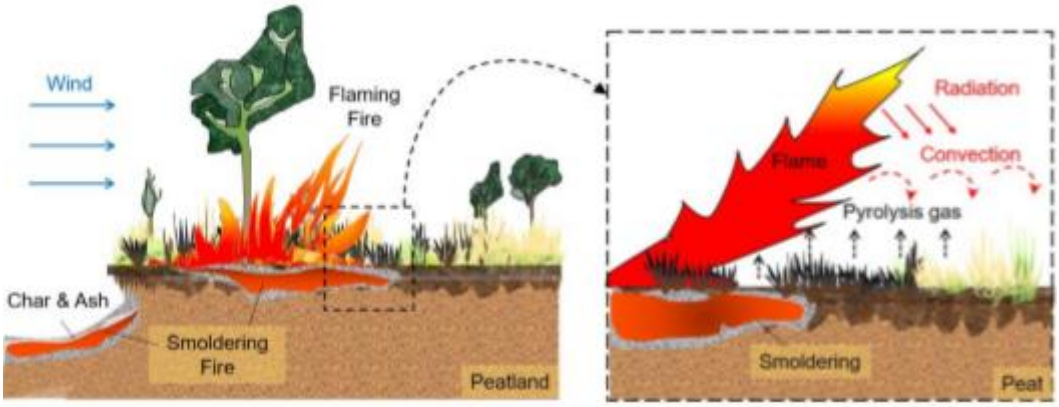

Image 3. Forms of combustion in wildfires (Source**:** Lin, Sun, & Huang, 2019).

Image 3 shows the combustion dynamics of a wildfire that takes place on a soil that allows for smoldering combustion. On the right hand side of the image, we can observe a schematic visualization of a wildfire with both a smoldering and a flaming form of combustion. The smoldering takes place at the surface and in the soil layer of the area. These subsurface fires consume the ground below the surface layer creating an instable surface structure that can break easily and is therefore very dangerous for fire fighters. A form of the instable soil can be seen in the left hand side of image 3 just left of the tree. This downward spread can progress in the soil for extended times. These time periods can last from weeks to months and in extreme cases even a year or centuries (Rein, 2009). These underground fires can subsequently progress in horizontal directions to climb back above the surface again, in the process initiating a new surface fire (Grishin, Yakimov, Rein, & Simeoni, 2009; Purnomo et al., 2020; Rein, Cleaver, Ashton, Pironi, & Torero, 2008a). A schematic visualization of this process is shown in image 4. A more in depth explanation of driving factors behind this smoldering combustion is presented in the subsequent section on fuel.

The flaming combustion front takes place on the surface layer of the area. The fuel for the fire, which will also be addressed more in depth in the subsequent section on fuels, for the flaming combustion front is formed by the vegetation in the area. A ground fire is formed at the base of the vegetation. Due to its horizontal nature, fire can climb the trunks of trees and form crown fires while the fuel mass of the tree is being consumed. These crown fires in relation with strong winds can shoot burning embers over significant distances. When retuning to surface level, these embers can ignite a complete new and unexpected fire front. This effect is called spotting fire spread. Due to lack of sufficient previous research on modelling this phenomenon, spotting fire spread will not be considered in the proposed model.

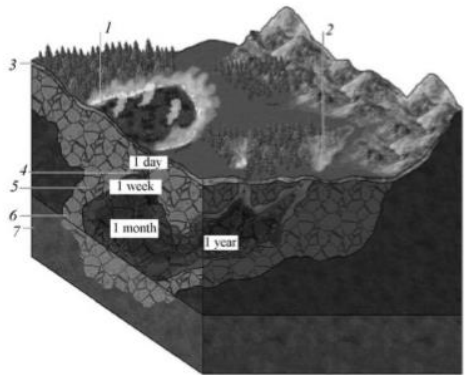

Image 4. Underground smoldering combustion spread.
(Source: Grishin et al., 2009).

§2.4 Fuel

Smoldering combustion is supported in soils with a low Inorganic Content (IC) such as peat. By definition peat is a form of soil, which is composed in a situation where a rate of decomposition is lower than the growth rate (Christensen et al., 2020a). Peat reserves extst in many different climates. Big peat reserves can be found in countries with dominant tropical climates such as Indonesia. Other big peat reserves can be found in the tundra climate of Siberia and the sub-arctic region. Substantial reserves occur in Europe (Rein & Belcher, 2013; Davies et al., 2016). 80% of world's peatland is located in moderate zones (Grishin et al., 2009).

As stated smoldering combustion is less researched as opposed to flaming combustion. The research into smoldering combustion began around 1985 with the work of Ohlemiller. Around the year 2000, a new interest in the subject was shown (Rein, 2016). The last decade is characterized by the work of professor Rein who emphasized the importance of understanding smoldering fire with regards to fire management but also with climate change. Subsequently, he laid the basis for modern smoldering combustion research. Very recent studies have, however been successful in identifying the behavior of smoldering fire in organic soil layers such as peat. The behavior is influenced by bulk mass (p), inorganic content (IC) and moisture content (MC) (Christensen et al., 2020a; Huang & Rein, 2015; 2017; 2019). Oxygen supply plays a crucial role in the smoldering combustion spread process, especially concerning burning depth. A recent study states that peat cannot be ignited when oxygen inflow is not sufficient (Huang & Rein, 2019). Numerous recent studies aim to find the effects of moisture content on fire spread rates in horizontal, vertical and global directions (Amin et al., 2020; Christensen et al., 2020a; Huang & Rein, 2019; Prat-Guitart, Rein, Hadden, Belcher, & Yearsley, 2016; Rein, Garcia, Simeoni, Tihay, & Ferrat, 2008b). The general rule is that with a higher moisture content peat is less likely to support smoldering combustion, therefore slowing the spread rate. The composition of peat, with respect to inorganic content, bulk density and moisture content relies heavily on how the peat layer is formed (Taufik, Veldhuizen, Wösten & van Lanen, 2019). Furthermore, moisture content of peat is dependent on the hydrological composition of the area (Wösten, Brouwer, Veraart, 2020). The complex

phenomenon of fingering spread behavior of smoldering combustion fronts in peat will not be considered in this thesis because it only occurs under very specific conditions (Fernandez-Anez, Christensen, Frette, & Rein, 2019). Due to the relative small amount of heat energy needed for ignition some natural fuels such as peat layers might self-ignite under the right conditions, this self-ignition is not incorporated in the proposed model (Santoso et al., 2019; Restuccia et al., 2017).

As stated flaming combustion happens on the surface layer of the area. More specifically, the fuel for the flaming combustion is vegetation. Different compositions of vegetation such as young heath, broadleaf forest and coniferous forest have different rates of burning. Rothermel (1972) formulated the key understanding of burning rates in his now famous *a mathematical model for predicting fire spread in wildland fuels*. Based on his work and subsequent research numerous fuel models have been developed for a wide array of vegetation compositions. In example, for the Netherlands alone Oswald et al. (2017) identify 21 fuel models that are relevant for the Dutch Wildfire Spread Model (NBVM).

Wildfire spread rates will be incorporated in the proposed model based on Purnomo et al. (2020). This stochastic approach allows the model to mimic the uncertain nature of wildfire spread. Vector based models, which will be addressed more in depth in the modelling section can have a more deterministic character. However, to limit computational requirements a discrete cellular automaton can be made stochastic through bond percolation. Due to limited computing power available for this thesis, the choice is made for a stochastic form of cellular automata. This will be further elaborated on in the next chapter.

§2.5 Wind

The effects of airflow on spread rate in smoldering fire has only recently been investigated in the work of Christensen, Hu, Purnomo and Rein (2020b). For the effect of wind three scenarios were experimentally observed and measured after which conclusions on the impact of airflow on spread rate have been derived. The study found that in a situation where the airflow is forward, at an angle of 0 degrees, both the horizontal and the in-depth spread rate increase heavily. Where the wind was perpendicular, at an angle of 90 or 270 degrees, the horizontal and the in-depth spread rate increase slightly. The last scenario with an opposed airflow, at an angle of 180 degrees, no change in spread rate was observed (Christensen et al., 2020b). Due to complexity and computational reasons, the effects of airflow on spread speed in smoldering combustion will not be included in the model.

In flaming fires, wind has significant effect on horizontal spread rates. Due to the less complex character of flaming combustion, the influence of wind on flaming combustion spread rates can be easily expressed. Forward wind heavily increases fire-spread rates, fire spread rates that face opposed wind direction decrease (Encinas, Encinas, White, Del Rey, & Sanchez, 2007a; Kyrafyllidis & Thanialakis, 1997). The effect of wind on flaming combustion spread rates will be considered in the model. This thesis chooses to decouple the spread rate and the wind parameter to limit the need for model optimization, thereby decreasing computational requirements (Purnomo et al., 2020).

§2.6 Slope

Similar to the effect of airflow, the effect of slope on smoldering combustion spread rates have only recently been researched. The same article by Christensen et al. (2020b) studied this effect empirically and experimentally. The study concluded that horizontal spread rate increases by around 21% with an angle of 20 degrees compared to a flat fuel bed at 0 degrees. Downhill slopes decrease the horizontal spread rate slightly and the spread rate was insensitive to slope (Christensen et al., 2020b). Due to complexity and computational reasons, the effects of slope on spread speed in smoldering combustion will not be included in the model.

In flaming fires slope has significant effect on horizontal spread rates. Due to the less complex character of flaming combustion, the influence of slope on flaming combustion spread rates can be easily expressed. Upward slope heavily increases fire spread rates this happens through the phenomenon of climbing fires. Fire spread rates that face downward slope and descend decrease (Encinas et al., 2007a; Kyrafyllidis & Thanialakis, 1997). Due to the flat topography that characterizes the Netherlands, the effect of slope is not considered in the model.

§2.7 Revegetation

Areas left behind by a flaming surface fire form fertile grounds for new vegetation to grow. Relative big amounts of CO_2 and other nutrients such as nitrogen accelerate the growth process of plants. The wide availability of nutrients stimulates growth of vegetation immediately after a fire event has taken place. This process is often dominated by a few plant species (Greene, Hebblewhite and Stephenson, 2012). The effects of a wildfire even to the organic soil layer is a rather different story. Affected soil layers take much longer to recover. Where revegetation might take place within weeks or days after the initial wildfire event, recovery of the soil layer takes years or even decades (Bowd, Banks, Strong and Lindenmayer, 2019).

When considering flaming fire fronts, the grow back rate of days is not likely to have impact on the final spread outcome. Therefore, this phenomenon is often not considered in wildfire modelling. Because smoldering fires can sustain for longer times revegetation becomes relevant and might form conditions where rekindling of revegetation is possible (Mutthulakshmi et al., 2020, Rein, 2016; Santoso et al., 2019). Moreover, rekindling does not only rely on regrowth of certain species but also on the leftover fuel which remained unburned after the initial wildfire front has progressed through the area (Stoof et al., 2020). Because of this twofold and uncertain character of possible rekindling, either through revegetation or through unburned fuel, revegetation will be incorporated in the model via a probability. As stated, regrowth of the organic soil layer is a lengthier process and is therefore not considered to be of impact in the model.

§3. Modelling theory

§3.1 Introduction

The third chapter of this thesis will address modelling theory. First, the definition of modelling is considered. Subsequently, key concepts of modelling are addressed in the third and fourth section. The fifth section seeks to present the current situation of wildfire spread modelling. Based on findings from this section, the sixth section will address the theory of cellular automate modelling. The final section will present the conceptual model for the FENIX wildfire spread modelling framework. The next chapter will address the applied methodology underlying this framework.

§3.2 Definition of modelling

Heywood, Cornelius and Carver (2011) define a model as an abstract description of a real-world event or process. A core principle in modelling theory is that not all underlying processes of a real world event can be considered. By simplifying the relations and interplays at hand modelling techniques try to help in understanding and managing real-world phenomena. Choices in what input is selected and what modelling approach is used relies heavily on the goal of the model. Different approaches of modelling can serve the needs of different questions. According to Tobler (1970), a model should always serve its purpose and should be kept understandable and explainable. The inherent inaccuracy of modelling does not mean that models are impossible to be improved; rather the improvement of modelling certain phenomena and the application of new techniques can help in building a more robust understanding of real-world phenomena. Moreover, when multiple modelling approaches are available, the different approaches can be used separately or combined to achieve a certain goal with certain needs. This noble pursuit of perfection is beautifully put in words by Fortheringham et al. : “We continually strive to produce more accurate models but the goal of a perfect model is elusive.” (2002, p.9). A widely known statement by Box and Draper also addresses the fundamental inclusion of omissions in modelling: “Essentially, all models are wrong, but some are useful” (1987, p.424).

Besides the inherent imperfect nature of models, the application of the theory is also highly dependent on the perspective of the modeler. Composing a model brings about questions on assumptions made and focus that is applied. Differences can even be found in the jargon different specialist use to describe similar concepts and as much as thirteen different definitions of the word model exist in the English language (Inoue, 2005). These differences become crucial when addressing a topic as highly multidisciplinary as wildfires. Now these differences are not a limitation, contrastingly they are a blessing. By combining different perspectives, new answers might be revealed about modelled phenomena. This work takes the perspective of the geographer, focusing on the general processes that occur in peatland-based wildfires. However, where possible, the knowledge from earlier works on specific phenomena within the process will be applied and incorporated.

§3.3 Deterministic versus stochastic modelling

In mathematical based models, a distinction must be made between deterministic and stochastic modelling approaches. The deterministic approach describes the situation where a model assumes exact relationships and therefore outputs are calculated precisely based on inputs and the relationships. Deterministic modelling leaves no room for random variation in the results, this means that a given input will always produce the same output. Furthermore, a deterministic approach assumes certainty in the model output (McClave, Bensonm, & Sincich, 2008). A stochastic or probabilistic approach tries to capture the essence of a random phenomenon. These stochastic models are often estimated with historical data on a certain phenomenon, deriving a probability of that same phenomenon happening again. Stochastic models incorporate the concept of randomness in the computation. Therefore, a stochastic model is likely to produce different results for a given set of inputs, although the same output might still be a possible outcome. The incorporation of uncertainty in stochastic modelling approach assumes that different solutions or outcomes might occur (McClave et al., 2008). Furthermore, probabilistic theory, and thus stochastic modelling, allows for the modelling of unconsidered influencing factors into a model. This uncertainty principle allows stochastic models to be closer to a real world phenomenon when such a phenomenon is not governed by a general rule and allows the influence of non-modeled aspects in the model (Inoue, 2005; Takama, 2005; Takama & Preston, 2008). Ignition of organic soils and wildfires can be seen as such phenomena (Frandsen, 1997; Purnomo et al., 2020). Since the proposed model aims to simulate the processes of wildfires, a highly uncertain phenomenon, the choice is made to take a stochastic modelling approach.

§3.4 Static versus dynamic modelling

Models can be either static or dynamic. A static model is a model that gives an output for a single point in time. Examples of static models are Multi-Criteria Analysis and Geographically Weighted Regression models (Fortheringham et al., 2003; Heywood et al., 2011). A dynamic model is a model that updates its output with each new time step. These dynamic models are used for example in environmental and climate modelling (Heywood et al., 2011; Malamud & Turcotte, 2000). Since the proposed model aims to simulate the processes of wildfires, a temporal phenomenon, the choice is made to take a dynamic modelling approach

§3.5 Modelling approaches in wildfire spread modelling

Modelling techniques have been applied to study wildfire spread for a long time. Often these models have the goal to predict wildfire front spread in a physical landscape under the influence of various weather conditions. Fuel, wind and topographic composition (Height, slope, ascent) are most often perceived as the most influential variables in wildfire spread modelling. These models help in understanding the phenomenon and can be used in many different ways. During a wildfire event, a model can directly aid the deployment decision process by fire fighters. After the wildfire event, findings from the fire fighters can be used for validating the model. Understanding the model and the dynamics of wildfire spread can be used in forest management and education. Ultimately, these models can be used to raise awareness for problems associated with wildfire spread (Kyrafyllidis & Thanialakis, 1997).

Wildfire models can be subdivided in two general approaches. Firstly, the vector or wave models which are calculated over a continuous plane. These vector models assume spread happens through a growth law and forms in standard geometries. Vector models can incorporate Huygens wave propagation principle and apply that to the continuously growing fire front, which can be visualized as an ellipsoid. These models elegantly incorporate our understanding of physics through partial differential (McDermott & Rein, 2016; Purnomo et al, 2020). The development of these mathematical equations with regards to flaming fire progression for certain fuel types happened mainly in the 1970s and the model proposed by Rothermel (1972) is still the foundation for contemporary fuel modelling (Bakhshaii & Johnson, 2019). However, our formulation of models for specific forms of fire spread are still developed and improved upon (Alexander & Cruz, 2006; Bakhshaii & Johnson, 2019). New technologies for observation further strengthen our understanding of the physical processes in smoldering and flaming combustion (Amin et al., 2020). With no external influences a fire would, by laws of the underlying wave propagation principle, take a circular shape. Vector models have proven to be very successful in accurately predicting spatial patterns involved in wildfire growth. Modern models such as the FARSITE model and the Dutch Wildfire Spread Model are based on this vector modelling approach (Oswald et al., 2017; Yassemi, Dragićević, & Schmidt, 2008). While more successful in their predictions vector models are computationally more intensive as opposed to the grid based approach (Purnomo et al., 2020; Yassemi et al., 2008). This long computation time is a direct result of the amount of computations that are needed to solve the partial differential equations that predict the fire front propagation. Furthermore, in these computations, time and space are continuous, this can lead to complex geometries, which might take a long time to render on a contemporary computational device. Often the state of the art vector models such as the Wildland-urban interface Fire Dynamics Simulator (WFDS), the Coupled Atmosphere-Wildland Fire-Environment model (CAWFE) and the FIRETEC model, are computationally too intensive to have a real time application (Bakhshaii & Johnson, 2019).

Secondly, grid based approaches in a cellular grid are used for wildfire spread modelling. These grid approaches divide the area into equal cells that have a discrete state. Bond percolation is a mathematical process to define probabilities in a grid (Broadbent & Hammersely, 1957). Bond percolation states that the transition behaviors of cells is probabilistic and can be applied to wildfire spread modelling (Favier, 2004). The advantage of incorporating uncertainty in the model brings the model closer to the real world phenomenon of wildfire spread and its uncertain nature (Purnomo et al., 2020). Through the incorporation of these probabilities, phenomena that are not considered in the model are still accounted for (Inoue, 2005). A more classic grid cell approach can be illustrated by a cellular automate model with a deterministic local rule. This rule is used to update the cell state for each time step based on the given local rule. Due to its deterministic character, a given input will always have a certain output. The grid approach is referred to as cellular automata and will be explained more in-depth in the subsequent section. Future research should try to combine the vector and grid based modelling approaches (Alexandridis, Vakalis, Siettos, & Bafas, 2008; Matthulakshmi et al., 2020; Yassemi et al., 2008).

Both approaches have to incorporate simplifications of the wildfire phenomenon. A subtle distinction between both approaches is however that the former is constructed by continuous mathematical calculations, whereas the latter is based on computations.

As stated, wildfires based on noncombustible soils are often of a small extent and tend to have a short duration. Modeling these specific types of wildfires can very purposefully be done using the vector approach of partial differential equations. However, lengthy fire events such as wildfires based on organic soils are not feasible to be modeled by this approach at the field scale. With these events, the grid-based approach is still feasible and is therefore more useful, even with its inherent higher level of simplification.

Based on these modelling approaches and the available computing power for this thesis a cellular automate modelling approach is chosen. Cellular automata will be further explained in the subsequent section. The proposed model will be of stochastic and dynamic character through the incorporation of probabilities and time.

§3.6 Cellular automata

Cellular automate modelling theory found its origin in the work of Stanislav Ulam and John von Neumann in the late 1950's (Inoue, 2005). Their work focused on the motion of liquid within a cell grid. The motion of the liquid was modeled to be influenced by the motion of the liquid in their neighboring cells. A few decades later, English mathematician John Conway developed his concept of the game of life based on the theory of cellular automate modelling. This work was popularized by two publications of Gardner in 1970 (Inoue, 2005). The game of life forms an example of a two-dimensional cellular automate with a deterministic character. The rules of the game of life can be summarized in two sentences. First, if a cell is 'dead' it is reborn only if it has exactly three 'alive' cells in its neighborhood. Second, if a cell is 'alive' it dies if it has less than two or more than three 'alive' neighbors. Without going into the details of the game of life, it is important to address the generational concept. As visualized in image 5. The generational pattern of the game of life considering a given initial configuration is shown for 12 generations.

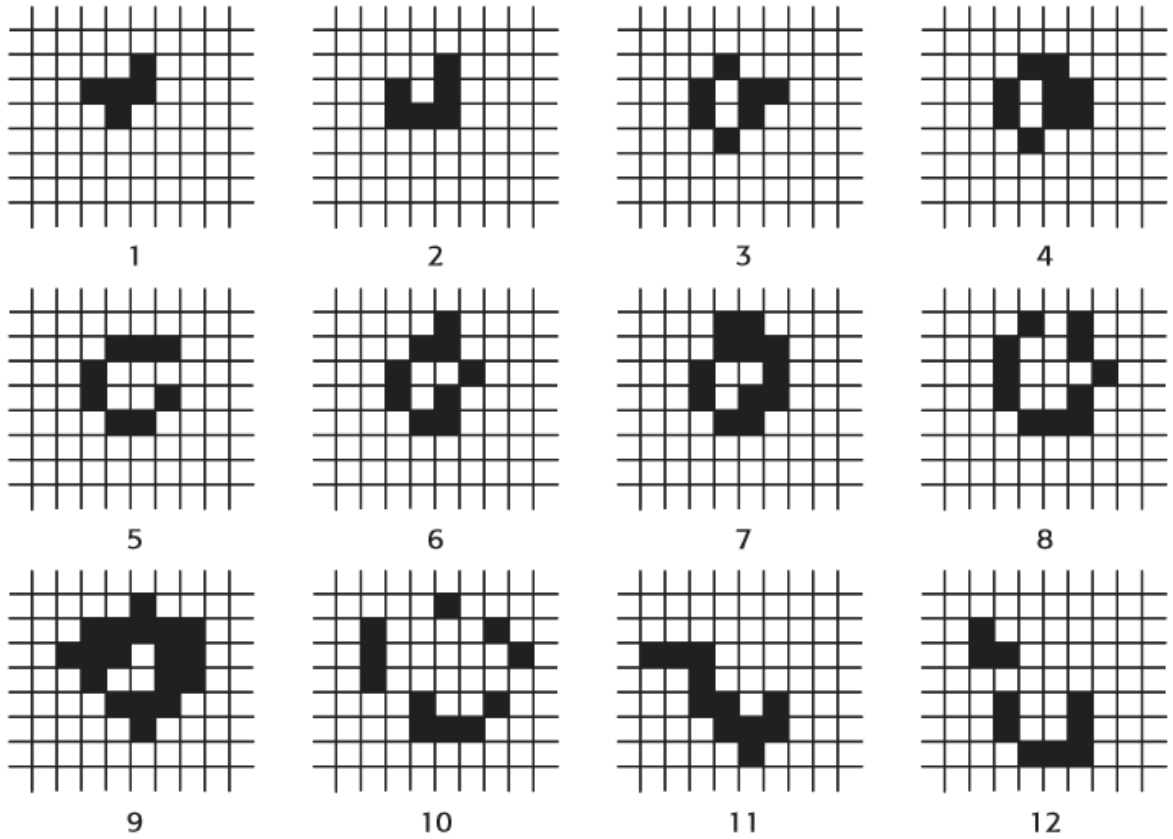

Image 5. Generational pattern with the rules of the game of life for twelve generations (Source: Inoue, 2005 P.7).

More recently, Stephen Wolfram drastically pushed research into cellular automate modelling working out his extensive framework of the results of certain change rules for a one-dimensional array. Wolfram claims that cellular automate are capable of successfully modelling the world as long as the answer to a given question can be determined by a Turing machine (Wolfram, 2002). A few interesting examples of generational patterns for Wolframs one-dimensional cellular automate are visualized in image 6.

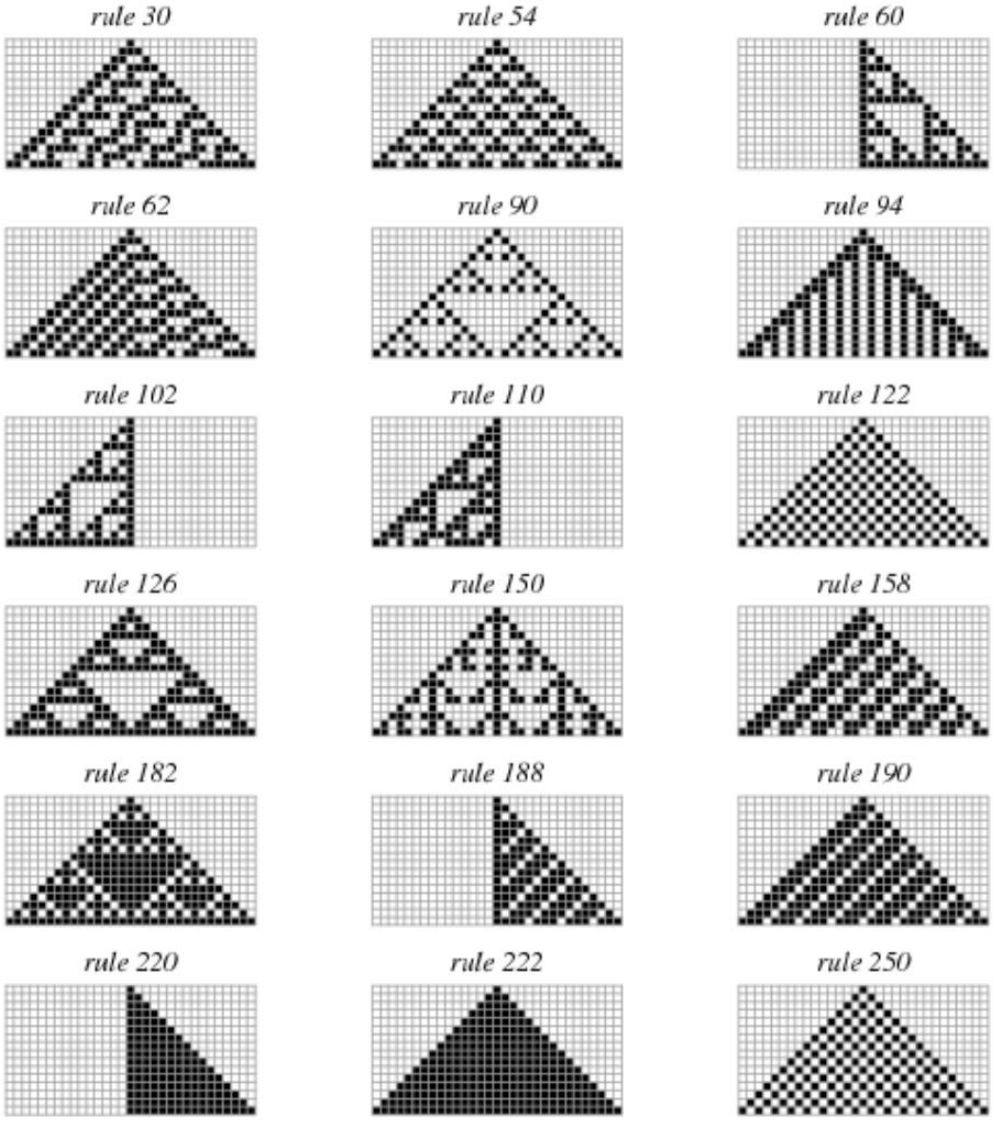

Image 6. Generational patters for Wolframs one-dimensional cellular automate. (Source: WolframMathworld, 2021).

Cellular automata models can be used for a wide variety of phenomenon modelling, the grid and transition rule approach allow for the incorporation of factors that change over time. This makes it a solid approach for modelling natural hazards as a broad group but wildfire front fire progression in specific (Malamud & Turcotte, 2000; Longley, Goodchild, Maguire, & Rhind, 2005). The cellular automata approach forms an alternative to other computationally more intense modelling approaches, such as modelling through partial differential equations. Cellular Automata models tend to run fast even on older hardware and therefore prove to be a powerful approach to model highly complex phenomena like wildfires (Karafyllidis & Thanialakis, 1997).

The fundament of cellular automate modelling can be described with four concepts. The first concept is that the Euclidian plane of the model is divided into a grid with a fixed number of cells. This plane can represent a place or area on earth, but cellular automate modelling is not confined to geographical applications (Wolfram, 2002). These cells can be square but among other variations also hexagonal, as is shown in image 7 on the right. (Encinas, White, Del Rey, & Sanchez, 2007b; Karafyllidis & Thanialakis, 1997; Longley et al., 2005; Trunfio, 2004). Cellular automate models based on hexagonal grids need more computing power and are therefore not widely used (Encinas et al., 2007b; Alexandridis et al., 2008).

Secondly, the cellular automata model cells are influenced by neighborhoods. These neighborhoods consist of nearby cells that influence the central cell state. The way a neighborhood is defined can differ. Most popular in cellular automata modelling are the Von Neumann-neighborhood and the Moore-neighborhood, as shown in image 7, middle and left. This cell state forms the third principle of a cellular automate and characterizes the cells condition at a given time interval. I.E. this might mean that a cell state can be either “Burned” or “Unburned”.

Lastly, the interaction between the neighborhood and the cell state at a subsequent time step is calculated through the use of a local rule. This local rule is the mathematical equation or logical operation that is used in order to determine the cell state at a subsequent time step (Karafyllidis & Thanialakis, 1997). While Cellular automata models are often deterministic, bond percolation allows for the incorporation of probabilities. Bond percolation technique is used in order to incorporate uncertainty into the local rule. This results in transitions based on probabilities rather than deterministic local functions (Purnomo et al., 2020). This changes the model to a stochastic approach. The proposed model in this thesis will take such a stochastic approach through a bond percolation based cellular automate model.

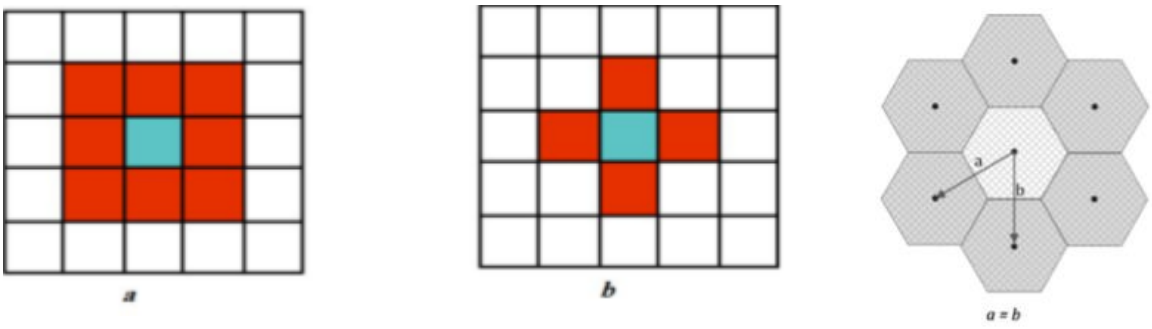

Image 7. Neighborhoods.
Left: Moore neighborhood, Middle: Von Neumann neighborhood, Right: Hexagonal neighborhood
Source: (Gazmeh, Alesheikh, Karimi, & Chehreghan, 2013; Sabokbar, Roodposhti, & Tazik, 2014)

Cellular automate based models are used to model a wide range of phenomena. Examples are, natural hazards, plant competition, spatial dynamics of urban and regional land use, epedemic propagation and vaccination and wildfire spread prediction (Malamud & Turcotte, 2000; Yassemi et al., 2008). Due to its computianol low costs, resulting from their discrete nature, cellular automate models prove to be a good alternative modelling approach compared with computationally heavy vector models (Karafyllidis & Thanailakis, 1997).

§3.7 Conceptual model for wildfire spread simulation (FENIX)

The goal of the wildfire spread model of this thesis, hereafter referred to as FENIX is to combine the theory of peatland-based wildfires and the theory on wildfire models into one wildfire spread model. This model must consider the ignition of smoldering fire by flaming fire. The model must be computationally feasible on a normal personal laptop. For flaming fire the effects of wind needs to be considered as well. Further, the model must incorporate a revegetation principle and therefore the uncertainty of smoldering fires igniting a flaming wildfire.

A model was formulated using a bond percolation driven cellular automate model that consist of two separate layers, one for the smoldering and one for the flaming fire spread. The FENIX-model is derived from the KAPAS model presented by Purnomo et al., which was published in October 2020. KAPAS was the first ever wildfire model that predicted both smoldering and flaming wildfire spread at the field scale (a couple of hundreds of hectares). The KAPAS model was built to be used in tropical environments (Purnomo et al., 2020). FENIX is the first wildfire spread model that considers revegetation and smoldering to flaming combustion transfers at field scale. The model is subsequently applied to predict the fire spread of the 2020 Peel region wildfire that burned over 700 hectares in the southeast part of the Netherlands. The states and rules of FENIX are visualized in image 8.

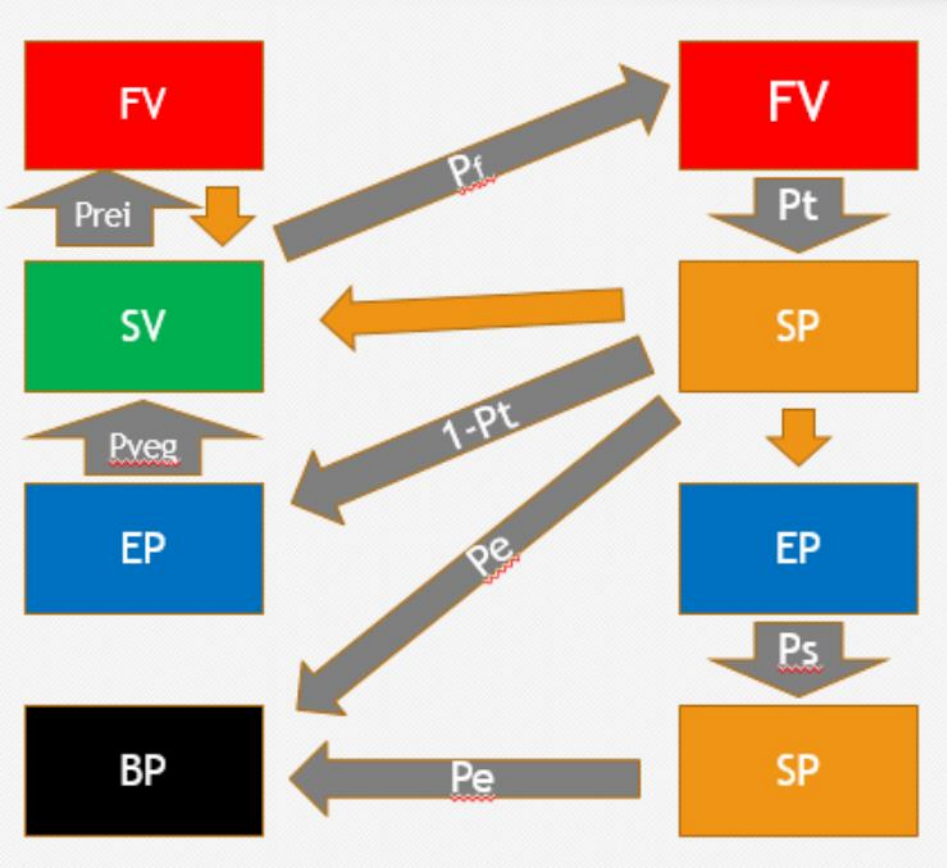

Image 8. Conceptual model FENIX

§4. Methodology

§4.1 Introduction

As stated, this thesis follows a dual approach to answer the research question. The qualitative part of the thesis will be used to aid the answers to sub questions three and five. As such, this part, which will be executed using semi-structured interviews, will influence the choice of used data for the final application of the framework and to build a broader understanding of the Dutch context (Bryman, 2016). The remaining part of this chapter will address the methodology that is applied to create the FENIX wildfire spread model. Since FENIX is based on the modelling theory of cellular automata, the chapter will explain the fundamental concepts of this approach section by section. The first section will introduce the composition of the grids and the neighborhood that are used within the FENIX model. Secondly, the cell states within both layers will be elaborated on. The third section will introduce the change rules between the grids and their cell states. The fourth section will address the mathematical foundation of the change rules and it will elaborate on how each influencing factor as identified in the theory section is incorporated in the FENIX wildfire spread model. The before last section of the chapter will introduce the calibration phase of the model. The final section will introduce the validation strategy for the FENIX wildfire spread model.

§4.2 Grids, Neighborhood and time steps

To initialize a cellular automate model a grid has to be defined on which the computations can take place. Because FENIX considers both smoldering and flaming combustion, two equal grids are needed. One to represent the top layer where the flaming combustion takes place and one to represent the soil layer where the smoldering combustion takes place. This multiple grid approach was first introduced by Alexandridis et al. (2008) to account for spotting fires, later this approach was applied to smoldering phenomena in wildfire spread modelling (Purnomo et al., 2020). Following the work of Purnomo et al. (2020), the area each cell occupies is equal to 4.5 square meters. In a cellular automate, time is considered to be discrete. In the FENIX model, each time step is equal to five minutes or 300 seconds. This means that each hour consists of twelve time steps and each day equals 288 time steps. The choice to follow both the grid size and the time step of the KAPAS framework as proposed by Purnomo et al. (2020) is due to their calculation of the constant probability for flaming fire propagation in shrub vegetation based on Rothermel (1972). This probability will be further elaborated on in section 4.6.

For spread phenomena, FENIX considers a first order Moore neighborhood. This means that each cell influences and is under influence of its eight touching neighbors. Following standard notation in linear algebra, the horizontal axis of the grid is named the j-axis and the vertical axis is named the i-axis. In image 9 a hypothetical central cell with its Moore neighborhood and notations are visualized. The example that follows the work of Encinas et al. (2007a) the origin is placed to the left upper corner. The orange cells visualize the neighborhood under the influence of the central cell, which is visualized in black.

(i-1,j-1)	(i-1, j)	(i-1,j+1)
(i,j-1)	(i,j)	(i,j+1)
(i+1,j-1)	(i+1,j)	(i+1,j+1)

Image 9. Moore neighborhood and notations.

§4.3 Cell states

The cell states that are incorporated into FENIX are similar to the cell states in KAPAS. This decision is made because this set represents the simplest conceptualization of a smoldering and flaming wildfire, the possibility of flaming peat is left out due to its unlikeliness (Purnomo et al., 2020). Five cell states are proposed: Surface Vegetation (SV), Flaming Vegetation (FV), Exposed Peat (EP), Smoldering Peat (SP) and Burnt Peat (BP).

The model will be composed of two separate but interacting layers. Layer one represents the surface layer and can be inhabited by cell states SV, FV and EP. The second layer represents the soil layer and can be inhabited by cell states EP, SP and BP. The possible occurrence of EP in both layers is due to the fact that a top layer surface vegetation cell might burn out, however the underlying soil remains intact.

§4.4 Change rules

Because of the uncertainty involved in wildfire spread the choice is made for a bond percolation model. Bond percolation is the mathematical term for probabilistic connection within a grid. If a grid has open connections between one side to the other we can conclude that the grid percolates (Broadbent & Hammersley, 1957; Favier, 2004). This means that probabilities will be incorporated rather than deterministic local rules. FENIX has six probabilities that will be considered. These are listed below together with the transition they govern. It is important to note that only P_f and P_t are influenced by their first order Moore neighborhood. The other transitions can only take place within a cell in the FENIX framework.

1. P_f = SV -> FV
2. P_e = SP -> BP
3. P_s = EP -> SP
4. P_t = FV -> EP
5. P_{veg} = EP -> SV
6. P_{rei} = SP -> FV

The cell states and their change rules are visualized in image 8. The change probabilities and their formulas will each be addressed in the subsequent section.

§4.5 Formulas of probabilities

Where possible formulas for the probabilities of transitions between cell states are drawn from existing literature. Each probability will be addressed in relation to their underlying math assuming little to none background knowledge.

Probability for flaming fire propagation

Based on the KAPAS wildfire spread model as proposed by Purnomo et al. (2020) the probability for flaming fire spread is formed by a constant probability based on the work of Rothermel (1972) which is subsequently augmented by a wind parameter. This structure for the probability for flaming fire propagation (P_f) is given in equation 4.

$$P_f = P_R * P_w \quad \text{(eq. 4)}$$

In this equation P_R is the constant flaming combustion propagation that is derived from the work of Rothermel (1972) when the effects of wind are not considered (Purnomo et al., 2020). This framework accounts for the type of vegetation. Since it is out of scope of this thesis to formulate the exact fuel model the choice is made to follow the KAPAS framework and the underlying equation for P_R. Therefore, the FENIX model considers surface vegetation cells to be shrub and the spread rate to be 83.1cm/min. In equation 4. P_w is the augmenting wind parameter. Both P_R and P_w will be elaborated on below.

Probability of wildfire spread (P_R)

Based on the aforementioned calculation Purnomo et al. (2020) present a probability P_R equal to 0.03. This means that, if wind is not considered of impact and P_w is set at 1, each SV cell in the neighborhood of one FV cell have a three percent chance of becoming a FV cell at the next time step. Under the influence of more FV cells, a SV cell has a probability to become a FV cell given by the complementary event formula given below in equation 5.

$$P_{fc} = 1-(1-P_f)^k \qquad \text{(eq.5)}$$

In equation 5 k represents the number of neighbors with a FV state at the time step of calculation. P_{fc} indicates the combined probability of flaming fire spread under the influence of k neighbors. Given this theory, it seems that the presented P_R by Purnomo et al. (2020) suffers from a typo. As visualized on the left in image 10. The maximum probability to for a SV cell, in the situation where each of its eight neighbors is in a FV state, is just over 0.20 or 20 percent.

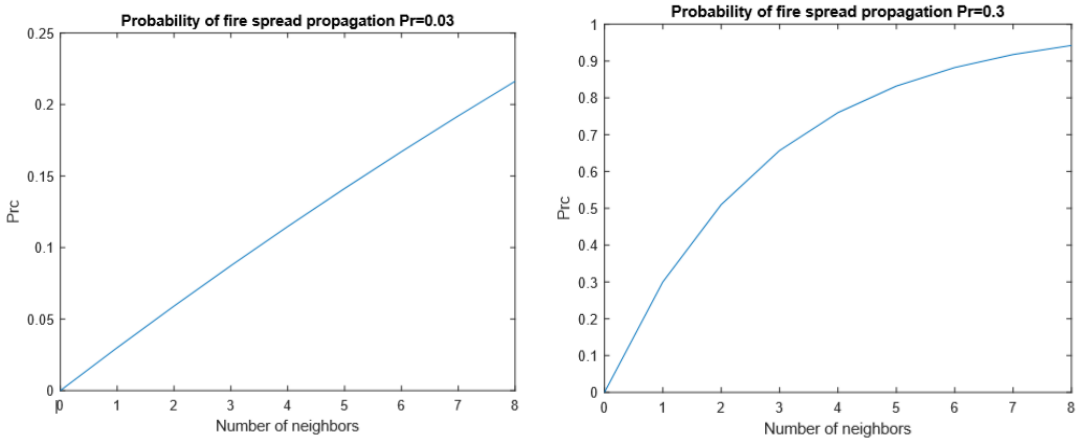

Image 10. Pf probabilities under the influence of k number of FV neighbors.

Thinking about the concept of a probability of wildfire spread it seems very unlikely that P_R = 0.03. Theory states that on average only three out of a hundred cells are ignited by a single FV neighbor. Since the word spread indicates growth, or at least a sustaining repetition, a minimum of $P_R = 1/8 = 0.125$ is expected. Considering this thought FENIX considers P_R = 0.3. The change in the probability for fire spread propagation (P_R) under the influence of multiple FV neighbors is visualized on the right side in image 10. This assumption will be tested in the calibration phase of the model, which is central in the subsequent section.

Augmented wind parameter

The influence of wind in wildfire spread modelling is one of the most important components with regards to flaming fire front propagation. First, the formulas as drawn from Alexandridis et al. (2004) will be presented. Subsequently the underlying core concepts will be explained in their relation with cellular automate modelling.

$$F_t = e^{(Vc2(\cos(\theta)-1))} \quad \text{(eq. 6)}$$

$$p_w = e^{(c1V)Ft} \quad \text{(eq. 7)}$$

In equations 6 and 7 e represents the mathematical constant for the derivate of exponential growth. e often referred to as Euler's number is an irrational constant meaning that it has an infinite number of decimals. The value described to e is 2.718281828… .

In equations 6 and 7 c1 and c2 are constants, which based on the work of Alexandridis et al. (2004) are equal to 0.045 and 0.131 respectively. In both formulas, V indicates the wind speed in meter per seconds at 6 meters above ground level. This height is the normal measurement height for a weather station. In equation 6 the Greek letter theta (θ) indicates the angle between the direction of the fire front spread and the wind direction expressed in degrees. The combination of these formulas allows the angle between the fire front propagation and the wind direction to be anywhere between 0 and 360 degrees. Earlier cellular automate models for wildfire spread prediction were often limited by only a few discrete values for cardinal and inter-cardinal wind directions (Alexandridis et al., 2004). Image 11 shows the general form of the probability P_w for arbitrary values of c1, c2 and V.

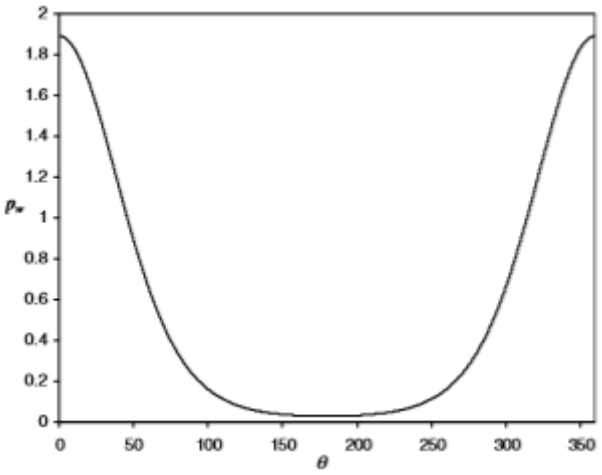

Image 11. Effect of the angle (θ) between wind direction and fire front propagation on P_w (Source: Alexandridis et al., 2004, p.196).

Wind direction can be expressed as any value between 0 and 360 degrees. The cardinal directions: north, east, south and west are indicated by degrees 0 (or 360), 90, 180 and 270 respectively. The inter-cardinal directions: northeast, southeast, southwest and northwest are indicated by degrees 45, 135, 225 and 315 respectively. However, in equation 6 θ represents the angle between the wind direction and the direction of the front fire spread. The implementation of this concept in the FENIX wildfire spread model will be addressed below and will be accompanied by an example to clarify.

With the definition of the Moore Neighborhood the wind parameter P_w can only influence the surrounding eight cells of a cell that is in FV state at a given time step. Combined with the notation of wind directions it is necessary to obtain the angular difference between that wind direction and the spread direction of the flaming fire front. This means that it is necessary to create an inversed direction matrix that will later be used to calculate the difference. The inverse direction matrix (Wi) is composed as visualized below in image 12. The center cell X represents the cell in FV state. Considering a wind direction of 60 degrees (about north east east) the absolute angular difference is as presented below in matrix Ad visualized in image 13. Given the formulas represented by equation 6 and 7, the results of P_w under a hypothetical wind speed of five meter per second are presented in the matrix P_w visualized in image 14. This results in a P_f for each of the cells as visualized below in matrix P_f as visualized in image 15.

Wi =

135	180	225
90	X	270
45	360	315

Image 12. Inverse angle matrix

Ad=

75	120	165
30	X	210
15	300	255

Image 13. Angular difference matrix

P_w =

0.7709	0.4688	0.3455
1.1471	X	0.3689
1.2247	0.9026	0.5491

Image 14. Example results P_w

P_f =

0.2312	0.1407	0.1037
0.3441	X	0.1107
0.3674	0.2708	0.1647

Image 15. Example results P_f

The FENIX wildfire spread model can incorporate changes in wind speed and direction at every time step. With the defined time step of 300 seconds this means that the framework has the capability to update the wind parameter twelve times per hour. Because of the decoupling of the wind parameter computing power to calculate P_f is limited (Purnomo et al., 2020).

Probability for flaming to smoldering combustion (P_t)

In accordance with the work of Purnomo et al. (2020), the probability for the transition of combustion between flaming combustion and smoldering combustion is drawn from the work of Frandsen (1997). In this work, Frandsen (1997) investigated the ignition probabilities of multiple organic soils through flaming ignition. Based on logistic regression the work provides the following equation to calculate the probability for the transition flaming to smoldering combustion. This equation is presented below in equation 8.

$$P_t = 1/(1+ e^{(-(B0+B1*MC+B2*ash+B3*rho))} \quad \text{(eq. 8)}$$

In this formula B0, B1, B2 and B3 are parameters that are specific for each soil type. MC indicates the moisture content in percentages. Ash indicates the percentage inorganic content and rho indicates the organic bulk density in kilograms per cubic meter. Following the work of Frandsen (1997), the B parameters for peat are as follows:

B0 = -19.8198
B1 = -0.1169
B2 = 1.0414
B3 = 0.0782

Following the work of Purnomo et al. (2020) the inorganic content of the soil layer is set at 3.7% and the bulk density is set to 222 kg/m^3. The resulting formula is given in equation 9 and the values for the transition probability for each percentage of moisture content is visualized in image 16. After considering both the inorganic content and the bulk density P_t remains with a sigmoid relationship with regards to the moisture content percentage.

$$P_t = 1/(1+ e^{(-(-19.8198+-0.1169*MC+1.0414*3.7+0.0782*222))} \quad \text{(eq. 9)}$$

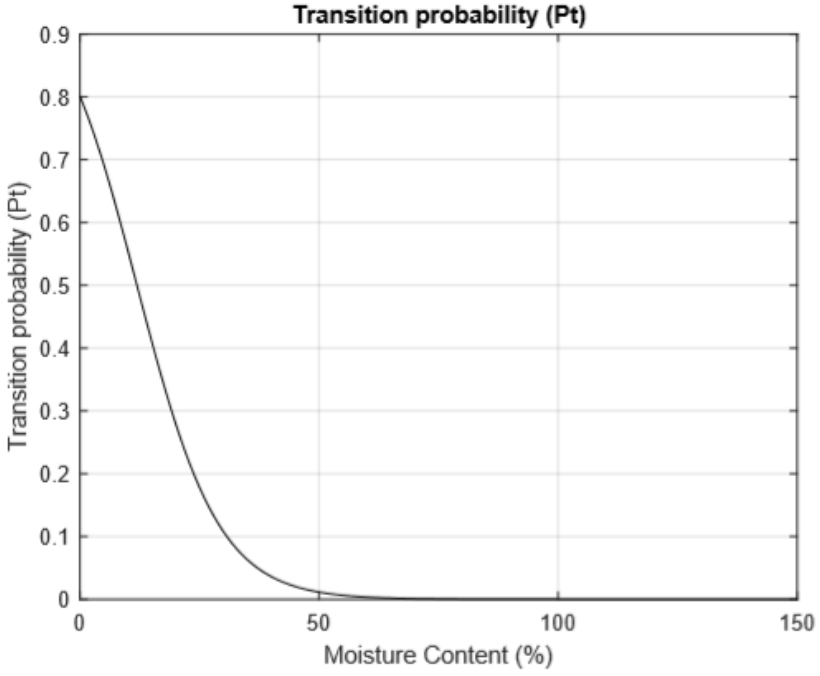

Image 16. Transition probability for different percentage moisture content

Smoldering spread probability (P_s)

The underground spread between smoldering peat cells and exposed peat cells is governed by the smoldering spread probability. A cell in smoldering peat state has a probability of P_s to ignite any exposed peat cell within its Moore neighborhood. Following the work of Purnomo et al. (2020), the formula to calculate P_s is stated in equation 10 below.

$$P_s = 1/(1+ e^{c3+c4MC}) \quad \text{(eq. 10)}$$

In this equation, c3 and c4 are constants with the values 9.58 and 0.057 respectively. MC indicates moisture content expressed in percentages. P_s has a sigmoid relationship with respect to moisture content. The smoldering spread probability for each percentage moisture content is visualized in image 17. The influence of moisture content percentage on smoldering spread and transition between flaming and smoldering combustion is investigated thoroughly in the work of Purnomo et al. (2020). This work considered multiple predictions for the constant c3 and c4. Ultimately, the values where chosen because of their relative good fit for peat with a low percentage of moisture content. Peat layers with this characteristic pose a great danger with regards to wildfires based on organic soils, therefore no changes in the constants were considered for the FENIX wildfire spread model.

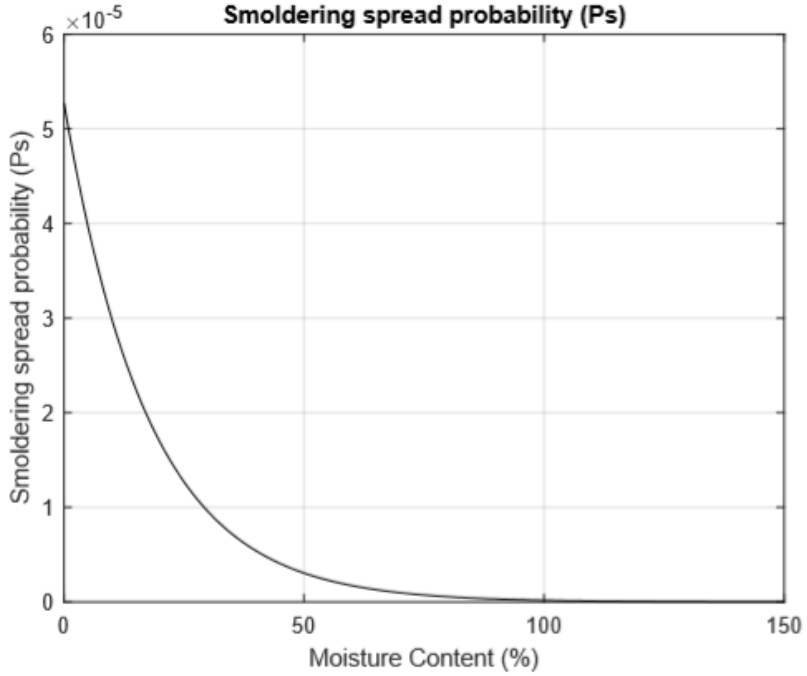

Image 17. Smoldering spread probability for different percentage moisture content

Extinction probability (P_e)

So far, the probability of a smoldering peat cell to become extinct has not been found in previous work. To indicate the persistency of smoldering combustion Purnomo et al. (2020) set the probability P_e to $5*10^{-7}$, this is an order of magnitude lower than the probability of smoldering spread. Considering the lack of research towards this probability, the FENIX wildfire spread model considers the same extinction probability. This issue will be further addressed in the discussion chapter.

Revegetation probability (P_{veg})

To the best knowledge of the author, the FENIX wildfire spread model is the first framework that considers the impact of revegetation at the field scale. The incorporation of the revegetation phenomenon is important in understanding the dynamics that exist in lengthy wildfire events such as those that are based on organic soils due to the perseverance of smoldering combustion. The transition from an exposed peat cell in the top layer, the situation where the initial state of surface vegetation has burned out, to surface vegetation is not only governed by the back growth time of vegetation but also by the amount of left over fuels that did not burn during this initial flaming phase. Because of the novelty of modeling this phenomenon, no previous work describing probabilities of revegetation was found. However, literature indicates that the process takes place over the course of a few weeks (Stoof et al., 2020). Putting this in relation to the length of the extinction of smoldering combustion the FENIX framework considered multiple revegetation probabilities in the calibration phase, which will be addressed in the subsequent section. Tests ranged from values between $5*-10^{6}$ to $1.5*-10^{4}$. The revegetation probability will be further addressed in the discussion chapter.

Reignition probability (P_{rei})

Similar to the phenomenon of revegetation, the phenomenon of reignition, or smoldering to flaming combustion transition, has not been considered in a wildfire spread model before. Santoso et al. (2019) have studied this transition for a wide range of materials that allow for smoldering combustion. However, a specific probability for peat soils and shrub vegetation has not been found in the literature. The FENIX modeling framework focusses on the incorporation of the phenomena of revegetation and reignition, finding the right specific probabilities is out of scope in this work. However, multiple values for the reignition probability have been tested in the calibration phase. In this phase, values for P_{rei} ranged between 0.001 and 0.0001. Furthermore, smoldering to flaming combustion transition can only take place between cells that are directly above one another.

§4.6 Model calibration

Before the model can be validated, it is necessary to calibrate the model. This modelling phase is necessary to check the behavior of different elements within the model. To guide this phase an extensive testing strategy is developed to increase replicability but also to eliminate outside factors. The total calibration phase consists of 30 tests. For each test, diagnostic information is gathered and recordings of the fire front progression are made. The tests are divided in four phases. The focus of each phase, the number of tests and their length are listed below:

- Ground fire progression calibration phase (Phase 1)
    - 10 tests
        - 5 tests with Pr = 0.03
        - 5 tests with Pr = 0.3
    - Length of each test is 5 days (t=1440)
- Wind influence calibration phase (Phase 2)
    - 9 tests
        - 1 test for each cardinal wind direction (North, East, South, West)
        - 1 test for each inter-cardinal wind direction (NE,SE,SW,NW)
        - Wind speed is set at 15 m/s at 6 meters above ground level.
        - One composed test with different wind directions per day.
            - This test will be on a 1001*1001 grid to make sure the fire does not leave the hypothetical plane.
            - Wind speed is reduced to 10m/s at 6 meters above ground level in order to get a wider flaming fire front.
    - Length of each test is 5 days (t=1440)
- Combined wind influence calibration phase (Phase 3)
    - 5 tests
    - Length of each test is 5 days (t=1440)
- Revegetation calibration phase (Phase 4)
    - 6 tests
        - Pveg = $5*10^{-5}$
        - Pveg = $5*10^{-6}$
        - Pveg = $5*10^{-7}$
        - Pveg = $1*10^{-4}$
        - Pveg = $1.25*10^{-4}$
        - Pveg = $1.5*10^{-4}$
    - Length of each test is 35 days (t=10080)
- Reignition calibration phase (Phase 5)
    - 5 tests
        - Prei = 0.001
        - Prei = 0.00075
        - Prei = 0.0005
        - Prei = 0.00025
        - Prei = 0.0001
    - Length of each test is 35 days (t=10080)

All tests will be held on a uniform fuel grid. This means that every cell in the Top layer has the cell state Surface Vegetation and the central cell will be ignited. Every cell in the Soil grid has a cell state of EP. In each calibration phase, the tested phenomena are isolated as far as possible. This means that every other aspect of the FENIX wildfire spread model are omitted. The choice for an odd number of cells per array is made in order that the exact central cell can be ignited at the initial state where t=0.

§4.8 Model validation

Validating is the process of assessing the fire spread model's accuracy and uncertainty. This process has to verify whether the mathematical processes in the model behave properly and as expected (McDermott & Rein, 2016). In order to facilitate this verifying process the FENIX framework is extended with the automated gathering of a wide range of diagnostic data visualizations. For each cell state in each layer total amounts and their percentages in relation to the total amount of cells in their layer are gathered at every time step. The results from this data gathering are subsequently and automatically graphed out against those time steps. To enrich this data, the FENIX framework also collects the diagnostic data about percentages and amounts for each day. Each day consists of 288 time steps. The resulting tables are made for both layers and are enriched with the amount differences for each day (Δ). Furthermore in accordance with the work of Purnomo et al. (2020) diagnostics are collected for φ_b which represents the sum of cells in cell state burned peat and smoldering peat divided by the total amount of cells in the soil layer. Finally, for each run of the FENIX wildfire spread model high quality recordings are made for both the top and soil layer. With a framerate of 20 frames per second, these recordings are capable of showing the results of the model run at each time step.

Validation of the model by comparing the final burnt area predicted by the model with the final extent of the wildfire in the Peel region early 2020 is not feasible due to extensive fire fighter deployment. Trying to fit the prediction to the actual situation without accounting for repression ruins the robustness of the model. However, a comparison can still be made in order to check for direction and the influence of this extensive fire fighter deployment. This validation step will only be done for the modeling of the actual Peel region wildfire event.

The FENIX wildfire spread model is developed in the MATLAB software environment. In order to increase reproducibility of this study, the code is incorporated in Appendix C. The results of the testing phases and the final calibration of the model will be presented in chapter eight of this thesis.

§5. Study area and case introduction

§5.1 Peel region

The Peel region is the region on the border of the Dutch provinces of Limburg and Noord-Brabant, crudely ranging between the settlements of Deurne and Asten on the western side to the settlements of Horst and Sevenum on the eastern side. The region is characterized by a mosaic soil structure where small forests, sandy heathlands and marsh peatlands form the main component. Historically, this region is known for marshy grounds and a harsh and hard to travers nature (Smulders & Bossenbroek, 2016).
Underneath a geological break line governs the long-term processes of nature, the Peelrandbreuk is visualized in image 18 and ranges from the municipality of Oss, through the eastern part of the Netherlands until Bonn, Germany. Along this break line, the strongest earthquake in Dutch history was measured. This earthquake had a strength of 5.8 on the Richter scale and happened near Roermond in April 1992 (Smulders & Bossenbroek, 2016).

Image 18. Peelrandbreuk (Source: Brabants Dagblad.nl, 2020)

§5.2 History of the region

The map from the late Middle Ages, shown in image 19 shows the impassible nature of the region as perceived in that time. Interestingly, this map has a slight northwestern orientation and is mirrored. The stretch of Peatland in 1850 is shown in Image 20 in brown. The situation in 1850 is especially interesting because industrialization took place in the second part of the nineteenth century in the southern part of the Netherlands (Smulders & Bonnebroek, 2016). Industrialization took place in urban centers like Eindhoven, Helmond, Weert en Venlo. Newly found factories and the rapidly increasing populations of these urban centers had a great demand for fuel. The peat layer of the Peel region proved to be a good natural fuel. The new peat sticking industry emerged in the region that lead directly to a better accessibility due to the emergence of new settlements. This land reclamation also lead to a dryer Peel region in general (Smulders & Bossenbroek, 2016).

Image 19. Late medieval map of the Peel region.

The map has a slight north eastern orientation and is mirrored.

(Source: Smulders & Bossenbroek, 2016).

The red areas in image 20 show the situation of the peat layer in the current situation. Surrounding areas are mainly used for agricultural purposes. The area indicated with number 3 shows the Mariapeel, this part of the Peel region was involved in an extensive wildfire with both flaming and smoldering combustion in 1980 (Stoof et al., 2020). The area indicated with number 2 shows the Deurnese Peel. This part of the Peel region was involved in the 2020 wildfire, central in this thesis. The area indicated with number 1 shows the Grote Peel. The national park is situated on this part, subsequent pictures in this chapter were made there.

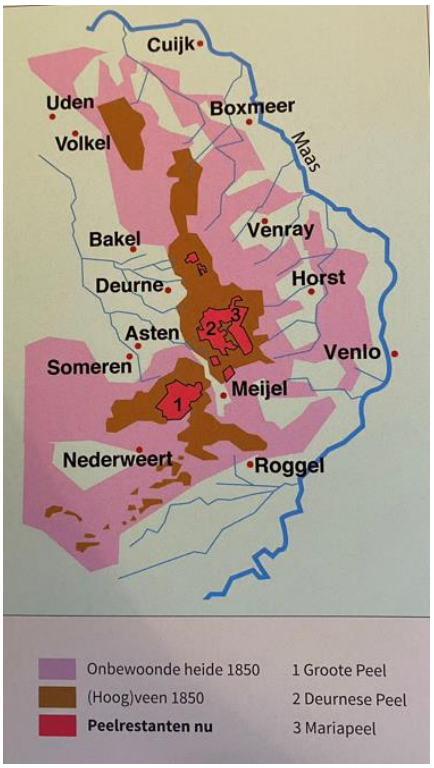

Image 20. Extent of the peat layers in different years
(Source: Smulders & Bossenbroek, 2016).

§5.3 Nature in the region

With regards to flora and fauna, the Peel region proves to be interesting as well. The region supports and interesting and fragile ecosystem. As stated the region supports both peat and heath lands. A big part of the region is protected under the Natura2000 legislation (Stoof et al., 2020).

The region is home to a wide variety of flora and fauna. Wildfires, like the one central in this thesis form a direct threat to the biodiversity of the region and the habitat of many plants. The most common tree in the region is the *Betula,* better known as the Birch tree. Further vegetation is dominated by *Pteridium aquilinum* and *Molinia caerulea,* Eagle fern and Moore grass respectively (van de Kam, 2020). A picture of peat supporting moor grass is shown in image 21. The summer and fall situation are shown in image 22.

Image 21. Peat vegetation November 2020.

The flora supports an interesting population of Fauna, the region host a lot of seasonal birds. A wide fold of insects, such as spiders and dragonflies can be found. Interestingly the region host a few species of amphibians but only one species of fish, namely the *Umbra pygmaea,* better known as the eastern mudminnow. Mammals can be found in the form of cattle, foxes, European badger, sheep and wild boars (van de Kam, 2020).

Image 22. Meerbaansblaak (situated in the Peel region)
left: October 2020, right: August 2020

§5.4 Peel region 2020 wildfire

The Dutch spring of 2020 was characterized by the absence of rainfall and an incredible amount of sun hours. The week of 20 April was not different. With a strong, dry eastern wind and lots of young vegetation that was still recovering from winter storms, conditions were perfect for wildfires to emerge (Stoof et al., 2020). That afternoon at 12:37, the first report of a wildfire reached the control room of the emergency services, a short three minutes later a second report of grey, white and black smoke reached the control room (Brandweer, 2020). The black smoke might indicate that the peat layer was already facilitating smoldering combustion. Considering this the fire might have initially started from this smoldering combustion state. From satellite imagery, the fire was observed to be burning at 12:17, the short time between emergence and time of report show the close relation between the nature-urban interface (Brandweer, 2020; Stoof et al., 2020). Shortly after the initial response, the emergency services scaled up to the situation of "very big wildfire". This resulted in the deployment of multiple fire departments of surrounding settlements such as Neerkant, Someren, Asten, Deurne and Helmond (Brandweer, 2020). Spotting fire spread phenomena also carried the fire to the western side of the Deurnese kanaal in at least two places, forming two new fire fronts. The Deurnese Peel proves to be an area that is very hard to reach with firefighting equipment. This situation made the fire very hard to get under control. One of the interviewees, who was an eyewitness to the fire, indicated that the wildfire showed extreme fire behavior (Appendix B.). The fire develops to become the biggest wildfire the Netherlands have ever seen. Burning an approximated area of 710 hectares. Deployment of four military helicopters to execute water bombings seem to only slow down the flaming fire front (Stoof et al., 2020). The rapid expansion of the fire front leads to the direct evacuation of houses along the Helenaveenkanaal, which borders the Deurnese Peel. After four days the flaming fire front ends, the wildfire as a structure however, continues underground as a smoldering combustion process. This process leads to heavy smoke and multiple new ignitions. Smoke from the smoldering process leads to a chain collision involving six cars on a nearby provincial road (Stoof et al., 2020). The smoldering combustion lasts until June 22nd and rekindling flaming fires happened until around June 10th.

The aftermath of the fire results in a lot of questions with local governments. Investigations on why this fire could results in such an extreme event were conducted. Further investigations aim to answer questions on process of fire fighter deployment and communication during the event. Ultimately, the cause is investigated. Although a piece of glass was found near the area observed by the satellite minutes after the fires emergence, the angle of the piece of glass towards the sun makes it unlikely to be the direct ignition source (Brandweer, 2020). Based on the observed black smoke and the work of Santoso et al. (2019) a hypothesis is formed that the wildfire event might have started with smoldering combustion. Considering this hypothesis, it might be that the piece of glass was sufficient to provide the peat with enough heat energy to ignite. Smoldering combustion needs less heat energy to ignite after all (Santoso et al. 2019). This hypothesis will be tested with the FENIX framework.

Both the interviewees indicated that the Dutch wildfire spread model (NBVM), which will be addressed more extensively in the next chapter, does not consider spotting fire spread phenomena (Appendix A & B). Therefore, the model did not predict new fronts on the west side of the Deurnese Kanaal.

Further research by the Wageningen Research University (WUR), investigates the impact of vegetation and nature management on the wildfire event (Stoof et al, 2020). The wide presence of *Pteridium aquilinum*, better known as eagles fern and *Molinia caerulea*, better known as moor-grass were further identified as a great benefactor of the quick flaming fire spread (Brandweer, 2020; Stoof et al., 2020). November 19th most of the investigations are published and handed to the governments who issued the investigations. The main results are pushing for more education and more specialized personal in the fire department. Stoof et al. (2020) also push for a better understanding of prescribed burnings and better nature management as a whole to decrease the chance of an extreme wildfire event such as the 2020 Deurnese Peel fire proved to be. Furthermore, a striking conclusion is made. An old investigation of a peatland fire happening in the nearby Mariapeel in 1980 proposes multiple points of improvement that, forty years later, have not been realized. These points of improvement are included in the proposed improvement points as presented in Stoof et al. (2020).

§6. Wildfire modelling and wildfire data collection in the Netherlands

The Netherlands are known for success stories with water management. With this in mind, the Netherlands are not often considered a place where significant wildfires happen (Oswald et al., 2017). However, due to the dense population and the close link of the nature urban interface even smaller wildfires can pose threats. A few relatively big wildfires occurred around 2010, which lead to societal and political attention for the problem. An encompassing project was launched by the Dutch fire department. The project aimed to improve knowledge of wildfires, of the sub-projects both the NBVM and the Dutch wildfire database (Appendix A &B). Data collection on wildfires had been stopped in 1997. This was done after a relatively calm period concerning wildfires. Around 2017 the data collection was started again and annual contributions to the EFFIS fire season reports are made. The Peel region wildfire of early 2020 resulted in both academic and media attention. National political attention seems to be limited.

The goal of the wildfire database is to collect all available data about a certain wildfire event. The database should become coupled with reports at the central control rooms of the emergency services. A platform for the coupling is being developed. Challenges with regards to reporting location, coupling of reports of the same event and classification in the control room system. Contemporary development of the database and the resulting challenges were addressed in an expert interview with the developer. A transcript of this interview can be found in appendix A. It is important to emphasize that the newly created database for wildfires is still in its infancy and many issues remain. For instance, the deployment of firefighting material is not allowed under restrictions of private data. The Dutch Institute for Physical Safety aims to improve data collection for smaller wildfires and thereby to increase their understanding of these phenomena. However, this collection has not been started at the moment of writing (Appendix A).

One of the biggest issues regarding spatial accuracy is the limitation of the emergency room system that a location must always consist of an address rather than a coordinate. For normal fires, this is not a big issue because the location of such event can be located very well along this approach. This is not the case for wildfires. A fire in a vast nature area such as the Veluwe or the Peel can be located kilometers from its actual location due to the need for an address (Appendix A).

Another project of the Dutch fire department that was initiated is the formation of a specialized team for wildfire investigation. This team focusses on finding the origin of a wildfire event. Furthermore, the team focusses on mapping the flaming front progression. However, due to limited availability of resources this team is not often deployed (Appendix A). Moreover, with respect to the Peel region wildfire, the specialized team was deployed when smoldering combustion was still happening in the area (Brandweer, 2020).

As stated, the conclusion towards the origin of the wildfire event in the Peel by the specialized team did not yield a conclusive answer into how the fire started. However, smoldering combustion was not considered as a possible start of the wildfire event (Brandweer, 2020). Considering this, a model run is presented in the results chapter where the ignition of the wildfire happens in the soil layer. These results will not give a definitive answer to how the fire started. However, the goal of the test is to see if such an ignition is possible within the proposed framework, which is based on fire science theory.

As stated, another important development within Dutch wildfire knowledge is the development of the wildfire spread model (NBVM). The NBVM was developed some years before the wildfire spread database. With the future incorporation of about 20 specified fuel models for Dutch vegetation types, the NBVM proves to be a full-grown wildfire spread model. The NBVM is based on a vector approach modelling technique which is also used the widely known FARSITE model. The NBVM focusses on surface flaming fire fronts (Oswald et al., 2017). While the internal processes of the model is complicated, the front-end application of the model is easy to use. The layout is based on Google Earth. At the time of writing, the NBVM uses the TOP10NL dataset to determine the vegetation in an area when a spread prediction is made. Contemporary developments and challenges of the NBVM were central in an expert interview with the product owner. A transcript of this interview can be found in appendix B.

Considering that the NBVM is based on a vector approach it comes with certain limitations. The model is computationally heavy and only calculates six hours into the future (Appendix B; Oswald et al., 2017). Furthermore, the model does not account for the effects of smoldering combustion. From studies after the fire and academic literature concerning wildfires based on organic soils it is known that this type of combustion plays a key role in these specific types of wildfire events.

Another limitation of the NBVM is that the model does not account for the effects of spotting wildfire spread (Appendix A & B; Stoof et al., 2020). The wildfire event central in this thesis did spread through this kind of wildfire phenomenon. This being said the NBVM proves to still be a good wildfire spread model. The model proved to be capable of predicting the progression of the fire front for the first six hours. Moreover, the model can be used for educational purposes and to raise awareness with third parties (Stoof et al., 2020).

The recently improved relationship between the Dutch Institute for Physical Safety and the European Forest Fire Information System provides a network needed to improve the understanding of wildfire events that take place in the Netherlands. Considering that wildfires were hugely ignored for almost two decades further emphasizes all these new initiatives by the Dutch fire department are already an enormous improvement.

§7. Data and data quality

§7.1 Introduction

This chapter will briefly introduce the datasets that play a role in the quantative part of the thesis. The datasets will be assessed on their explanatory power subsequently. As suggest by Longley and his colleagues (2005), the explanatory capacity can be best measured with a combination of aspects. Geospatial datasets are always to some extent incomplete and inaccurate. Common indicators for spatial data quality are positional accuracy, attribute accuracy, temporal accuracy, logical accuracy and completeness (Devillers et al., 2007). A framework proposed by Wang and Strong (1996) will be used in this thesis to make a quantified indication of data quality. However, the framework will be simplified because the data quality is not the focus of this thesis. All together, the simplified framework still emphasizes the need to think critically about which data is used and how reliable that data is.

The framework divides four quality indicators: representational data quality, accessibility data quality, contextual data quality and intrinsic data quality. Representational data quality focuses on the accuracy and interpretability of the dataset. Contextual quality, considers the relevancy, completeness, timeliness and the benefit of the dataset. Accessibility data quality considers the ease of acquiring the dataset. The last category is the intrinsic data quality. This category focuses on the objectivity and believability of the producing party (Wang and Strong 1996). The quantification of scores will be done over a 5-point scale with 1 indicating lowest score and 5 indicating the highest score. Because the focus of this thesis is the Peel region wildfire an arbitrary square study area is defined. The study area has an area of 4050 by 4050 meters and is visualized in image 23 together with the extent of the fire as given by the European Forest Fire Information System (EFFIS).

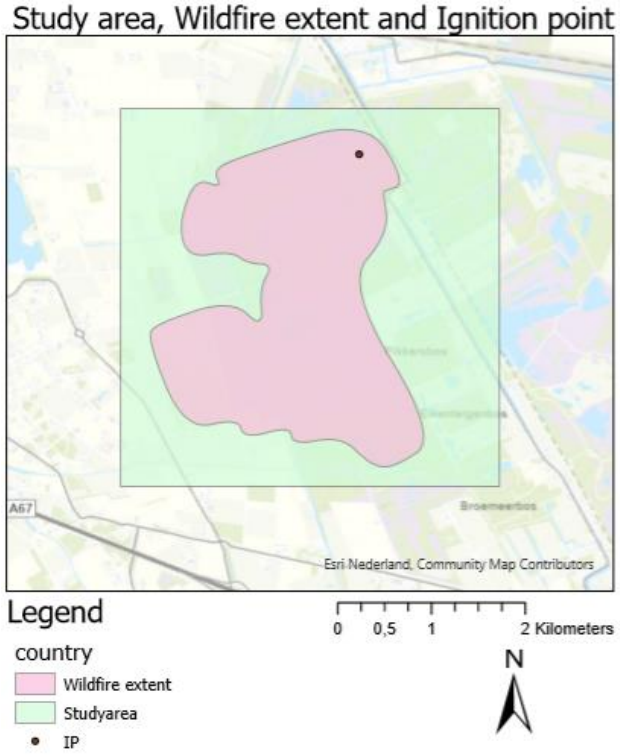

Image 23. Study area, wildfire extent and ignition point

§7.2 Topographic data

Vegetation plays a big role in fire spread as it forms the fuel for the fire. Information on vegetation can be obtained through de Basisregistratie Grootschalige Topographie (BGT) and the TOP10NL dataset, which is also used as input for the NBVM. The BGT is freely available and enclosed via the PDOK geo-data platform, therefore no additional data request is needed to obtain the data. Because this thesis aims to incorporate smoldering combustion as well data on soil types is drawn from the Basisregistratie Ondergrond (BRO).

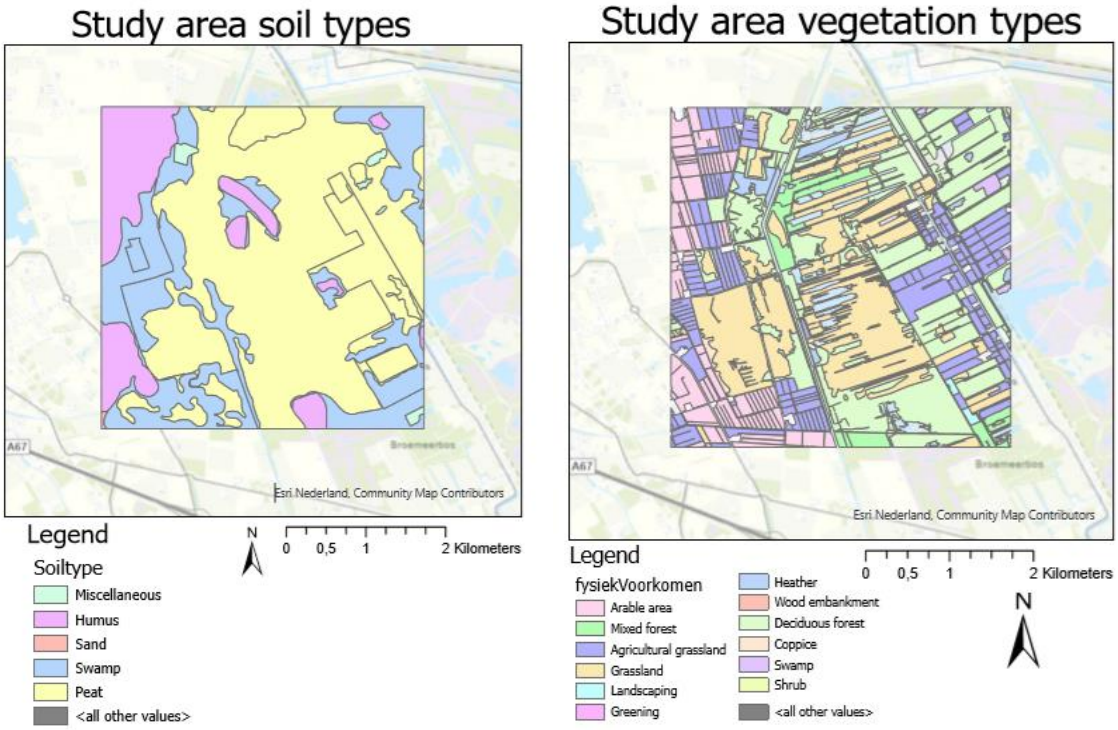

Image 24. Soil and vegetation types in the study area.

Data quality indicator	**Score (1-5)**	**Description**
Representational data quality	5	The dataset is easy to understand and due to its format has a high level of interoperability.
Accessibility data quality	5	Obtained via the PDOK platform the dataset is easily obtainable (without costs or data requests)
Contextual data quality	4	The dataset is published in June 2018. Since little changes in soil composition are expected this still yields a high score. Furthermore, the data is complete for the study area.
Intrinsic data quality	4	Multiple organizations within the Dutch government are responsible for the BRO. therefore the reputation of the producing parties is conceived to be good.
Total score	4.5	(Sum of scores / total possible score)*5. (18/20)*5 = 4.5

Image 25. Data quality score soil types

The given scores are rather arbitrary. However, with a total score of 4.5, as indicated and argued on in image 25, the data quality for the soil types provides the needed data for the application of the FENIX wildfire spread model. The score for contextual data quality was lowered due to the time of publication. Preferably, a more recently updated dataset was used, however only minor changes in the soil are expected. With regards to the lowered score for intrinsic data quality, the preferable situation was a single responsible party with a good reputation.

Data quality indicator	**Score (1-5)**	**Description**
Representational data quality	5	The dataset is easy to understand and due to its format has a high level of interoperability.
Accessibility data quality	5	Obtained via the PDOK platform the dataset is easily obtainable (without costs or data requests)
Contextual data quality	4	The timeliness of the data is impeccable with a publishing date of February 10th, 2021. However the data has some open spaces (where no vegetation is found)
Intrinsic data quality	4	Multiple organizations within the Dutch government are responsible for the BRO. therefore the reputation of the producing parties is conceived to be good.
Total score	4.5	(Sum of scores / total possible score)*5. (18/20)*5 = 4.5

Image 26. Data quality score vegetation types

Image 26 shows a high data quality score for the vegetation dataset. The lowered score for contextual data quality is due to the blank areas. The score for contextual data quality was lowered due to the time of publication. Preferably, a more recently updated dataset was used, however only minor changes in the soil are expected. With regards to the lowered score for intrinsic data quality, the preferable situation was a single responsible party with a good reputation.

It is important to note that the FENIX framework does not incorporate multiple states for vegetation types. Moreover, the framework is not capable to incorporate vector data formats. This means that the data for both the soil types and the vegetation types have to be converted to raster datasets. Because the data for vegetation types has empty spaces, a union transformation is done together with the vector layer of the study area. This results in a complete vector for the study area. However, the space that was empty in the vegetation dataset is now only perceived as not filled. No differentiation is made between areas that are for instance occupied by water, roads or buildings. Both the soil data and the vegetation data are converted into a raster format in order to be useable in the FENIX framework. The soil data is reclassified to only incorporate peat cells and incombustible area cells. The vegetation data is reclassified to only incorporate surface vegetation cells and incombustible area cells. The resulting maps are visualized in image 27 and 28.

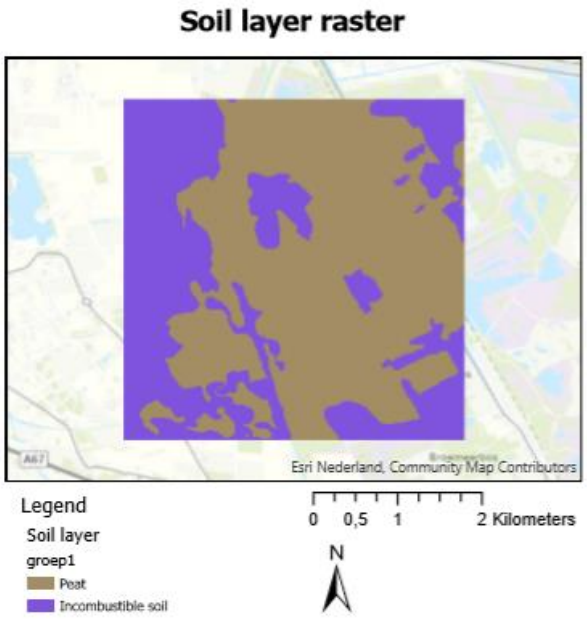

Image 27. Soil layer raster

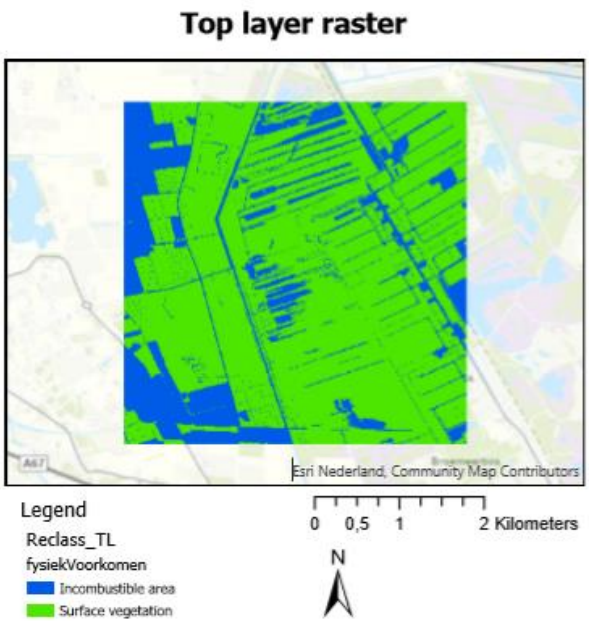

Image 28. Top layer raster

§7.3 Weather data

Weather data has a big role in wildfire progression, most importantly, wind direction influences the direction of the fire front. Furthermore, amount of rain and ground water levels are important factors with regard to the progression of wildfires. This data can be obtained through the data-portal of the Dutch Weather and Climate Institute (KNMI). Weather data from the period April until July is collected. The data is updated for every hour. With regards to meteorological data, only wind speed and wind direction are considered in the FENIX wildfire spread model.

Data quality indicator	**Score (1-5)**	**Description**
Representational data quality	5	The dataset is easy to understand and comes in a highly interoperable ASCII-file.
Accessibility data quality	3	The data platform of the KNMI faced some issues at the time of writing. After some searching the data was still found.
Contextual data quality	4	The dataset is published in January 2021 and contains all the weather data per hour for the period 2011-2020. However, the position of the weather station is not very close to the study area.
Intrinsic data quality	5	The KNMI is the Dutch national institute for weather and climate observations. Therefore, the reputation of the producing party is conceived to be good.
Total score	4.25	(Sum of scores / total possible score)*5. (17/20)*5 = 4.25

Image 29. Data quality score weather data

The high score for weather data quality and the given arguments can be found in image 29. The severely lowered score for accessibility data quality is due to the issues with the KNMI data portal. Even for a native Dutch speaker, it proved to be very hard to find the right place

to come by the dataset. The score for contextual data quality was lowered due to the position of the weather station Arcen, which is not very close to the study area.

§7.4 Wildfire data

The dataset for the fire data is derived from multiple sources. The extent of the wildfire and its spatial print are obtained via a data request at the European Forest Fire Information System (EFFIS). Furthermore, the ignition point is derived from the work of Stoof et al. (2020) and the specialized team of wildfire research of the Dutch fire fighter department (2020). Based on satellite imagery and subsequent field research the exact point of ignition was set to be situated at the coordinates: 51°26'0.06"N 5°53'0.78"O. The fire data, in relation to the defined study area is visualized in image 23.

Data quality indicator	**Score (1-5)**	**Description**
Representational data quality	5	The dataset is easy to understand and due to its shapefile-format has a high level of interoperability.
Accessibility data quality	3	A data request had to be made, the waiting period to obtain the data was several days. The ignition point had to be drawn from literature.
Contextual data quality	4	The dataset is complete and serves its purpose. The ignition point had to be drawn from literature.
Intrinsic data quality	4	EFFIS is the institute for wildfire research of the European Union. Therefore, the reputation of the producing party is conceived to be good. The ignition point was validated through field research, which improves the believability.
Total score	4	(Sum of scores / total possible score)*5. (16/20)*5 = 4

Image 30. Data quality score fire data

The data quality score for the fire data and its argumentation can be found in image 30. The relatively low score was that part of the data request was not answered. Furthermore, the location of the ignition point had to be drawn from literature (Brandweer, 2020)

Considering the high scores of the datasets in the proposed framework, it can be stated that if data was available, it is of high quality. However, it is important to note that there is also a lack of data, for instance with regards to firefighting activities during the wildfire event. An estimation was made that around 18.000 hours of active firefighting was deployed during the wildfire event. A further 550 hours of management hours were deployed together with another 550 hours of work in support services. Moreover, the deployment of the army and other parties involved are not known. This leads to a direct lack of data since the extent of the fire will be influenced by these extensive firefighting activities.

As stated earlier, reclassifications had to be made to the used datasets in order to make them interoperable with the FENIX wildfire framework. These data manipulations also lead to less accurate results. These inaccuracies are not to be described to lacking data, rather they are due to limitations of the proposed FENIX framework.

§8. Results

§8.1 Introduction

Chapter eight of this thesis sets out to present the results of the quantative part of the study. Structure wise it follows the phases as defined in the model calibration strategy, which is addressed in section 4.7. For each phase the relevant diagnostics and visualizations, with respect to the focus of each testing phase, are incorporated in the text. As stated for each test run high quality recordings are made. These recording can be requested with the author. After finishing the presentations of the results of the calibration phase this chapter will address the final calibration of the FENIX wildfire spread model framework. Ultimately, this chapter will present the results of the application of the FENIX model to the Peel region wildfire event of early 2020.

§8.2 Results model calibration phases

Phase 1: Flaming fire progression calibration phase

As stated in the methodology section the constant probability of flaming fire spread of P_R = 0.03 seems unlikely. Considering a typing error, the first calibration phase considers ten tests. Five test runs are executed with a P_R value of 0.03 and five other test runs are executed with a P_R value of 0.3. Each of the test runs where computed over the length of 5 days (t=1440). All of the test runs were computed over a hypothetical 501*501 grid where the central cell (251,251) is ignited at the initial time step (t=0). Relevant diagnostics are considered to be snapshots of the top layer after 1 day (t=288) and after 5 days (t=1440). Moreover, graphs indicating the amount of cells in cell state flaming vegetation (FV) and the percentage to the total number of cells are presented. The results of the five test runs considering P_R = 0.03 are presented below in images 30 until 34.

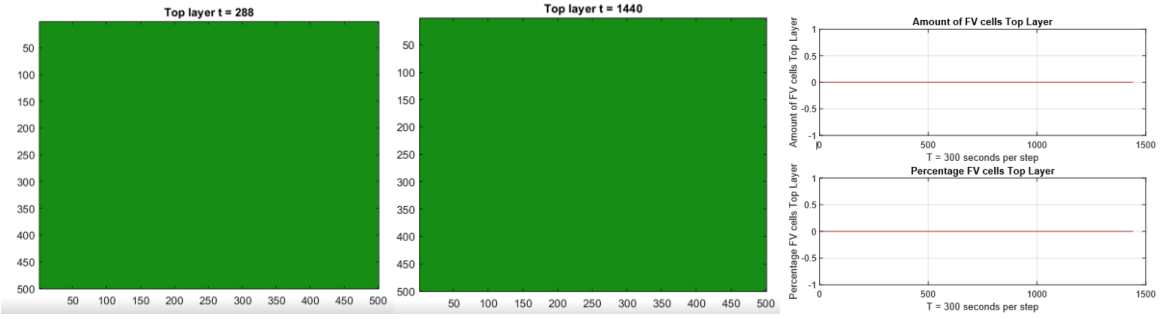

Image 30. Results test run 1.

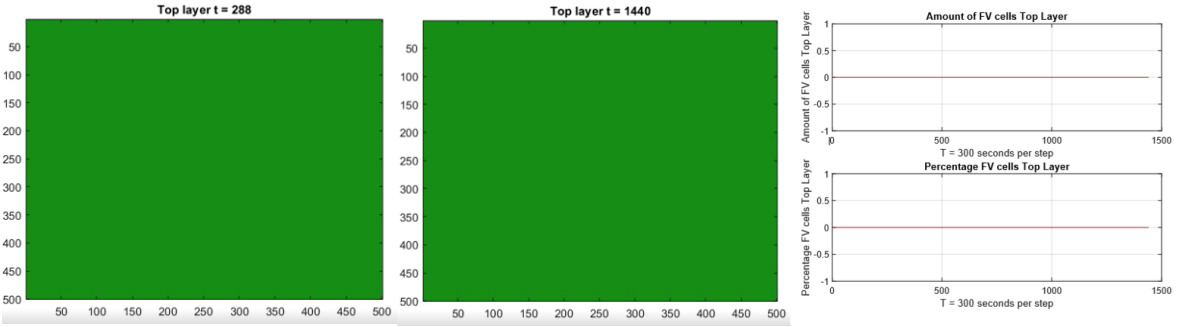

Image 31. Results test run 2.

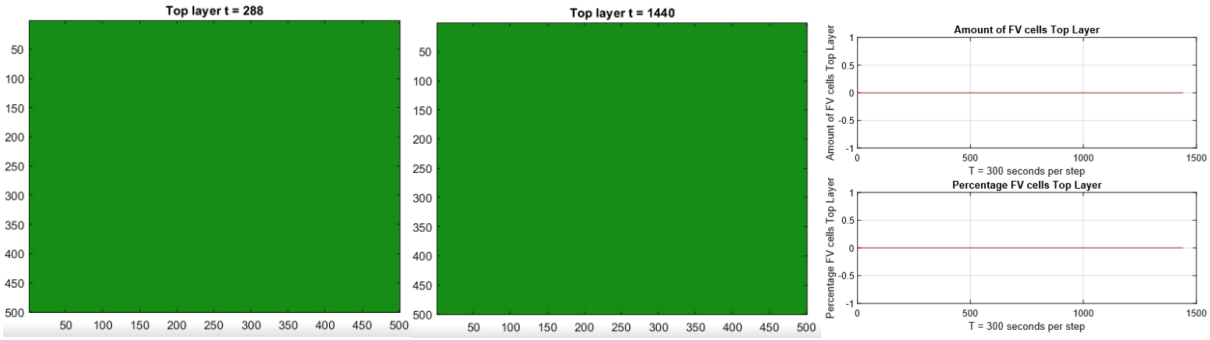

Image 32. Results test run 3.

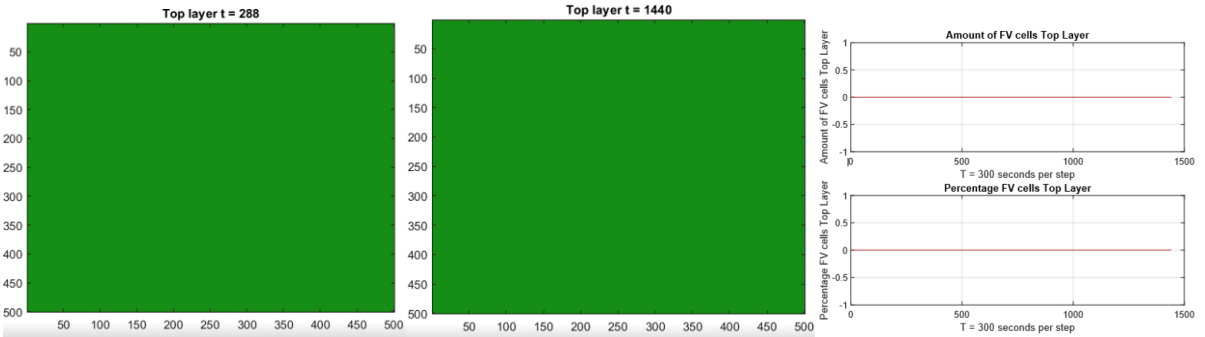

Image 33. Results test run 4.

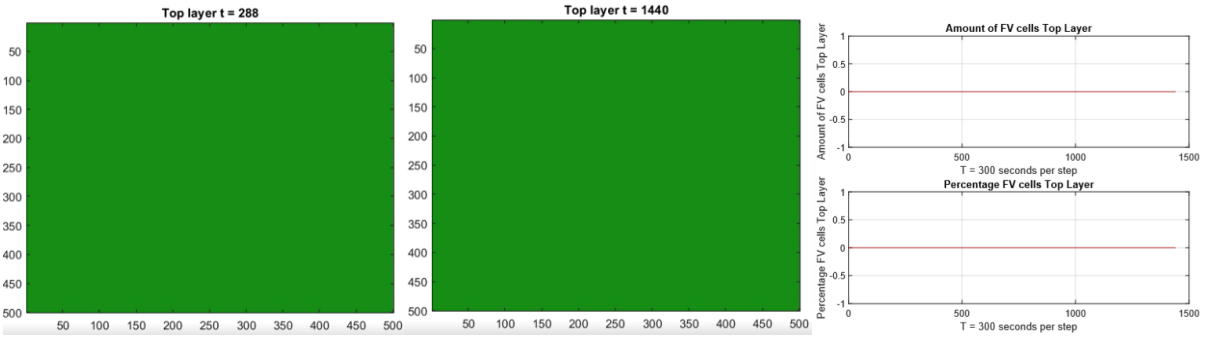

Image 34. Results test run 5.

Interpreting these results can be done rather straightforward. None of the test runs show any form of front fire propagation based on a P_R value of 0.03. The percentage and amount graphs start collecting data at the first time step. Therefore, with the central cell burned out, it is visualized that not a single cell was ignited after the initial phase. The next five test runs present the same diagnostics, however, in these runs the P_R value is equal to 0.3.

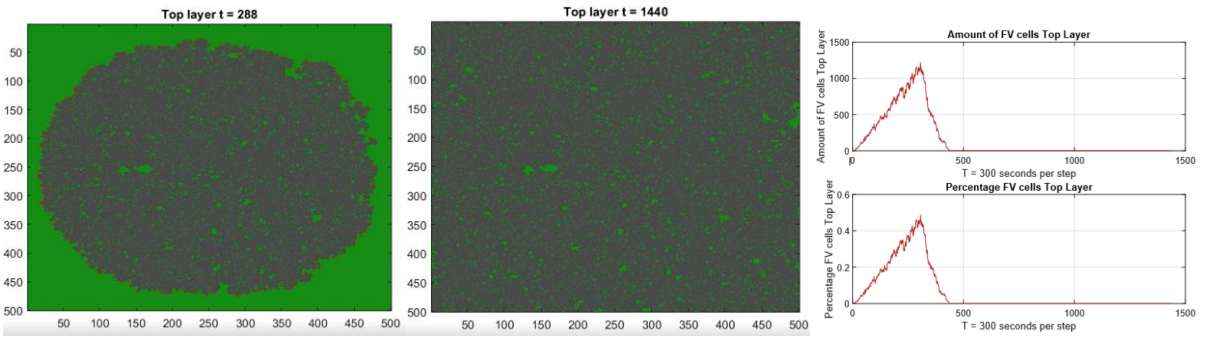

Image 35. Results test run 6.

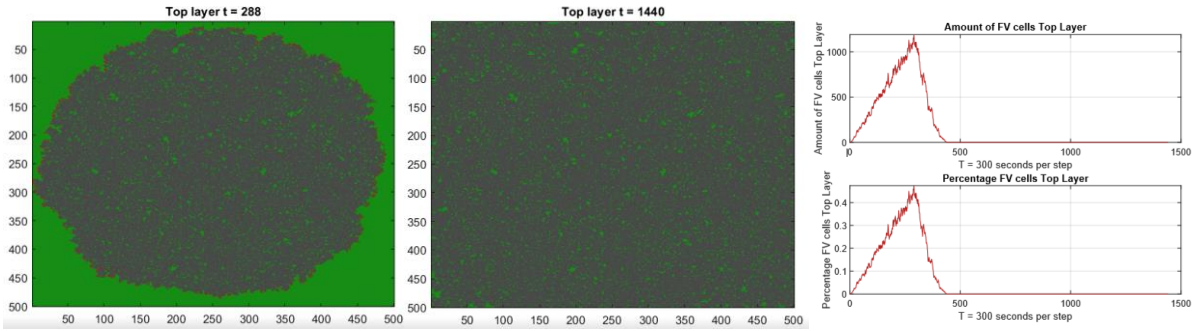

Image 36. Results test run 7.

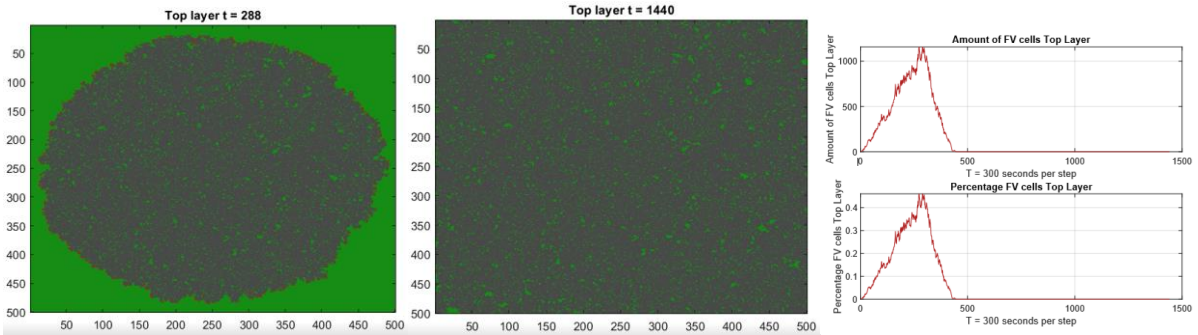

Image 37. Results test run 8.

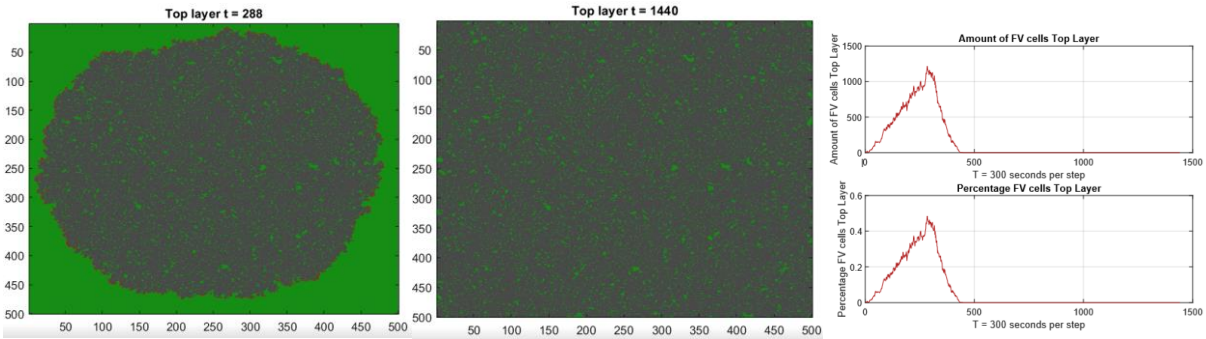

Image 38. Results test run 9.

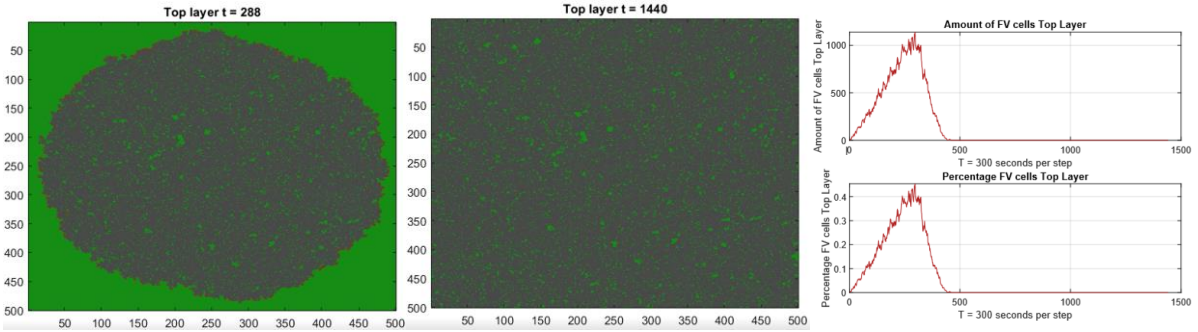

Image 39. Results test run 10.

As can be seen in the presented diagnostics in images 35 until 39 of the last five test runs a P_R value produces the expected result of flaming fire front progression. The circular shape is also expected because the influence of wind is omitted in the first calibration phase. The slightly different shapes after the first day are result of the probabilistic approach of the FENIX model and mimic the uncertainty of flaming fire front propagation.

Phase 2: Wind influence calibration phase

As stated in the methodology section, modelling the influence of wind can be tricky with regards to the translation of circular trigonometry into matrices. To calibrate and validate the influence of the wind a total of nine test were executed. The first four test focus on the flaming fire front progression to the cardinal wind directions. Translated to a wind angle east equals 90 degrees, south equals 180 degrees, west equals 270 degrees and north equals 360 degrees. Based on the first calibration phase P_R is set to a value of 0.03. To maximize the influence of the wind direction, wind speed is set at a very high level of 15 m/s at 6 meter above ground level. The presented diagnostics are the snapshot of the top layer after 5 days (t=1440) and the amount and percentage graphs of flaming vegetation cells over time. Results for the wind influence calibration phase for the cardinal wind directions are presented in images 40 until 43.

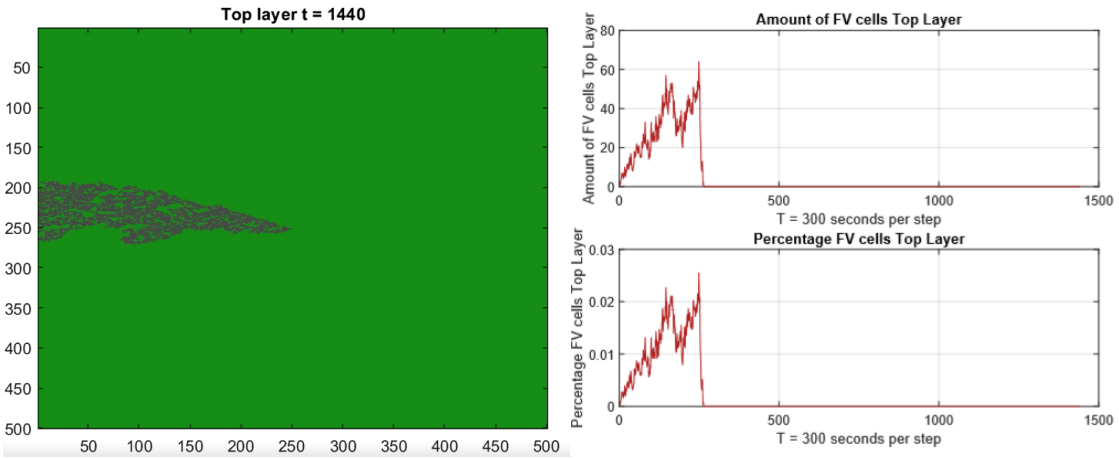

Image 40. Results test run 11 wind direction is 90 degrees (east).

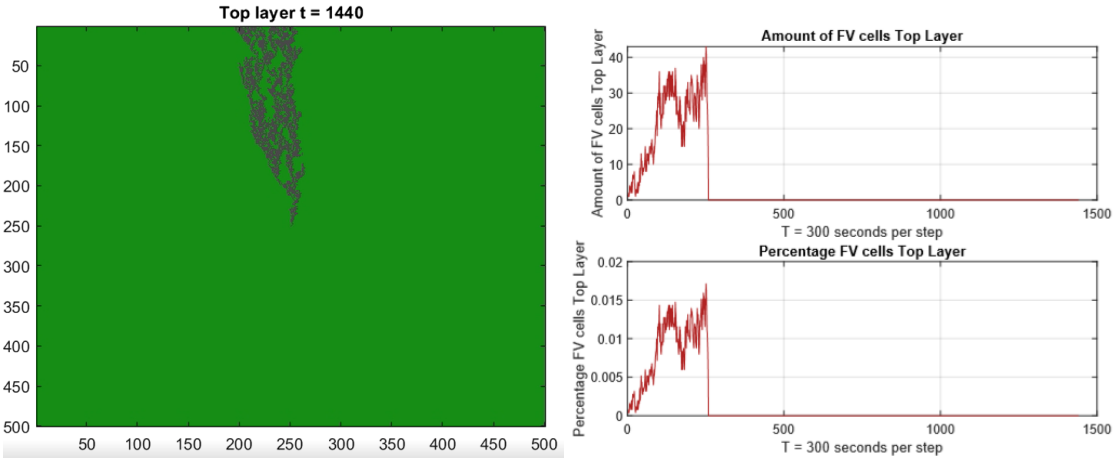

Image 41. Results test run 12 wind direction is 180 degrees (south).

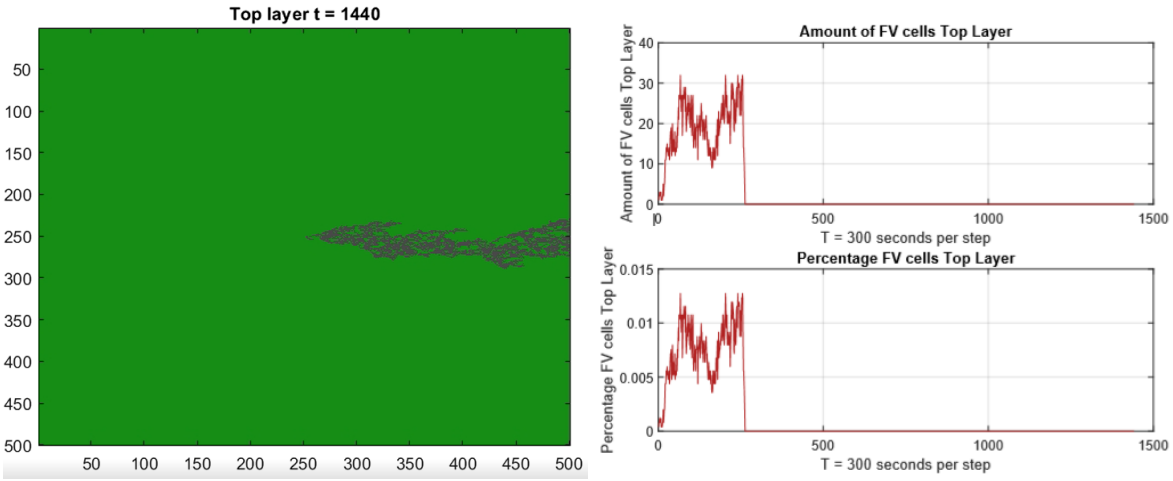

Image 42. Results test run 13 wind direction is 270 degrees (west).

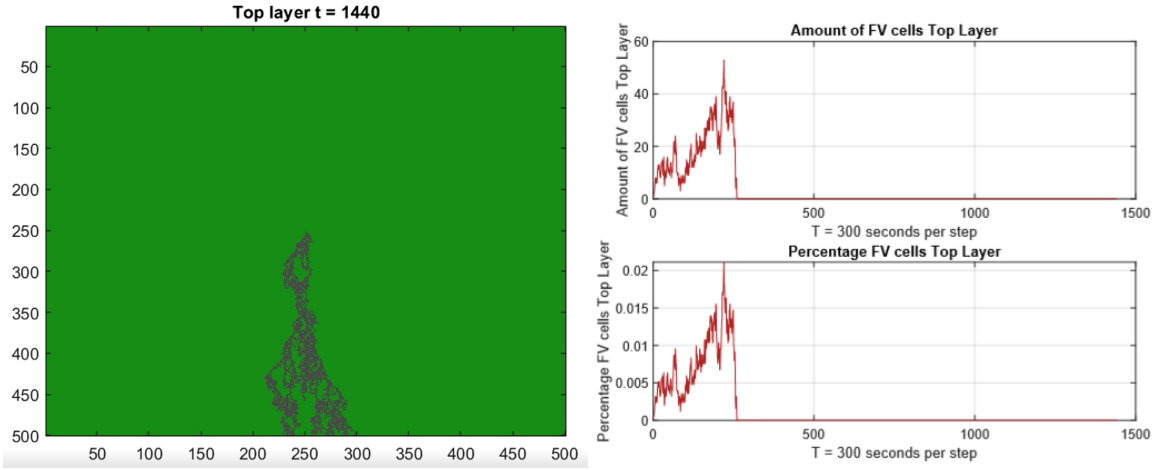

Image 43. Results test run 14 wind direction is 360 degrees (north).

As can be seen in the results as presented in images 40 until 43 the wind direction influences the flaming front progression in the expected way. The sudden fall of FV cell amounts and percentages indicates the situation where the flaming front goes out of bounds of the hypothetical field. The next four tests calibrate the influence of wind direction for the inter-cardinal wind directions. Translated to degrees southeast wind equals 45 degrees, northeast wind equals 135 degrees, northwest wind equals 225 degrees and southwest wind equals 315 degrees. Results of the tests for inter-cardinal wind directions are presented in images 44 until 47.

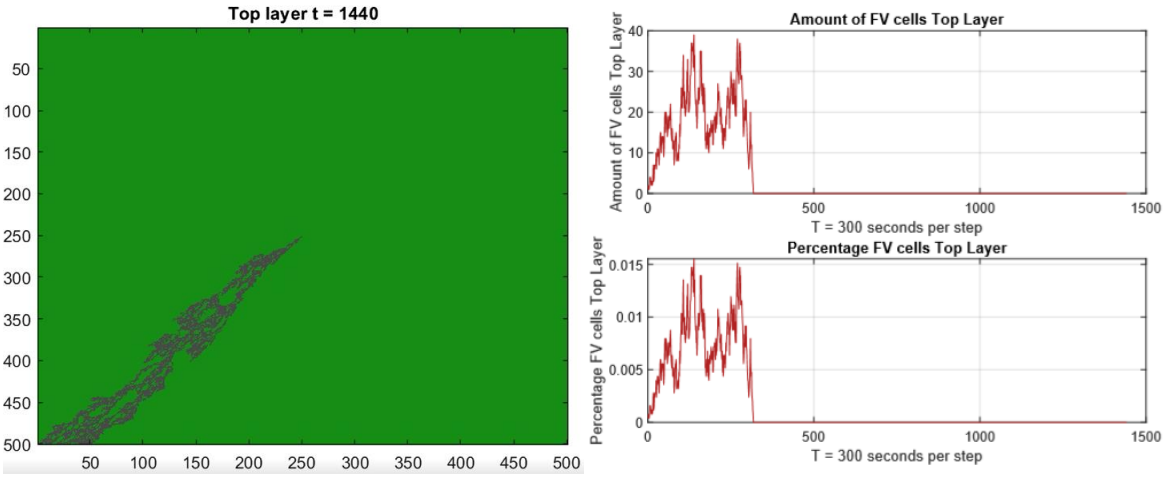

Image 44. Results test run 15 wind direction is 45 degrees (southeast).

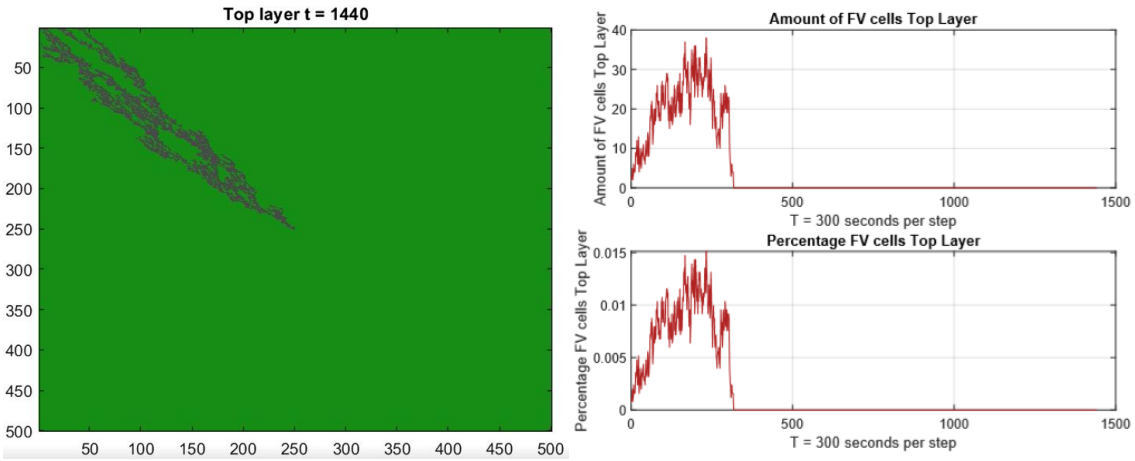

Image 45. Results test run 16 wind direction is 135 degrees (northeast).

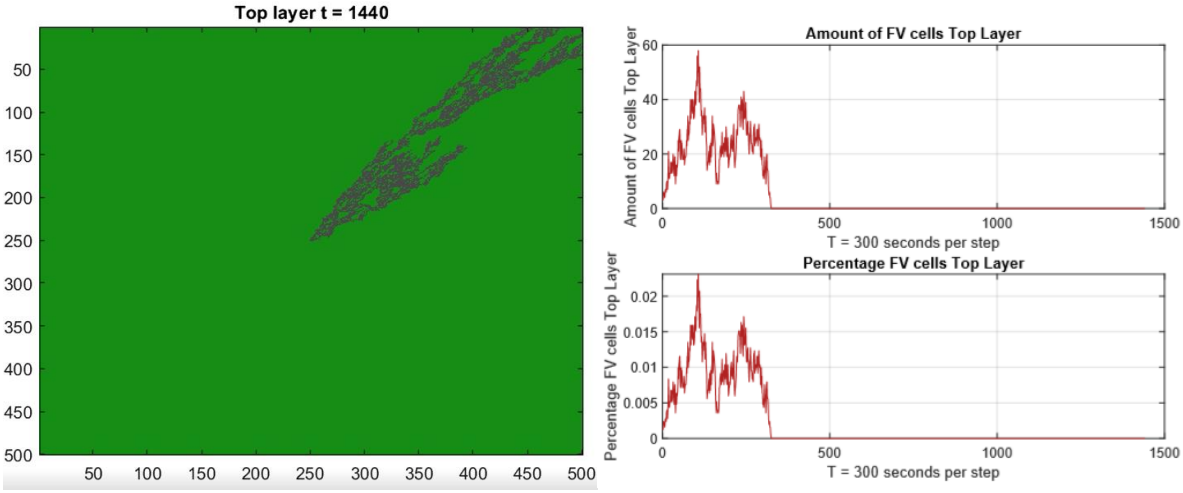

Image 46. Results test run 17 wind direction is 225 degrees (northwest).

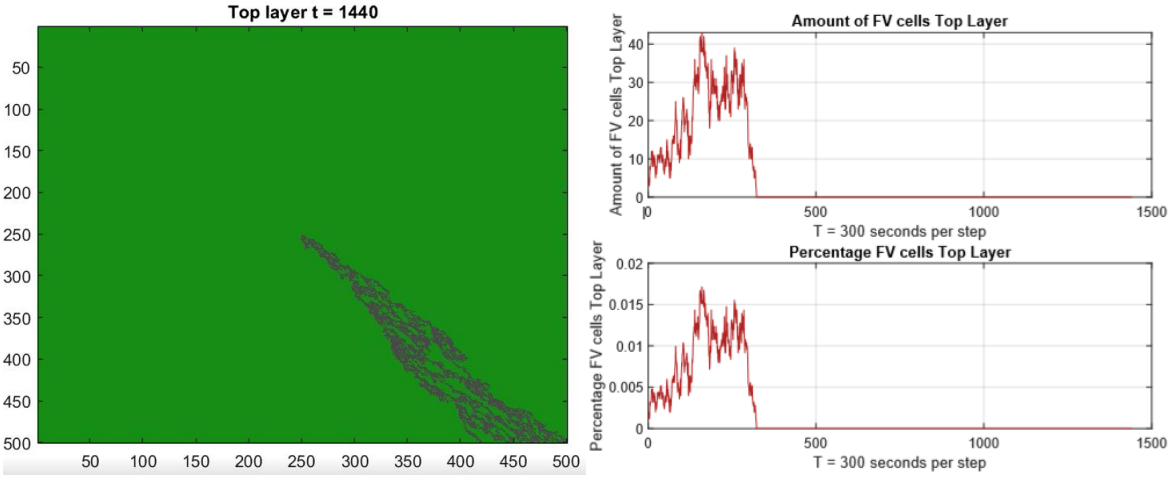

Image 47. Results test run 18 wind direction is 315 degrees (southwest).

As can be seen in the results as presented above, the wind influence for the inter-cardinal directions works as expected. The thin flaming fire front is due to the high wind speed, which was used to emphasize the effect of wind direction.

The last test of the wind influence calibration phase is a compound test where the wind direction is diversified for each day. The diagnostics for the resulting situation are presented below in image 48. The wind speed was brought back to 10m/s in order to get a wider flaming fire front progression. Further, the grid was extended to 1001*1001 to prevent the flaming front to leave the hypothetical plane. The first day had a northern wind. The second day had a western wind. The two subsequent days had a southern wind. The last day had an eastern wind.

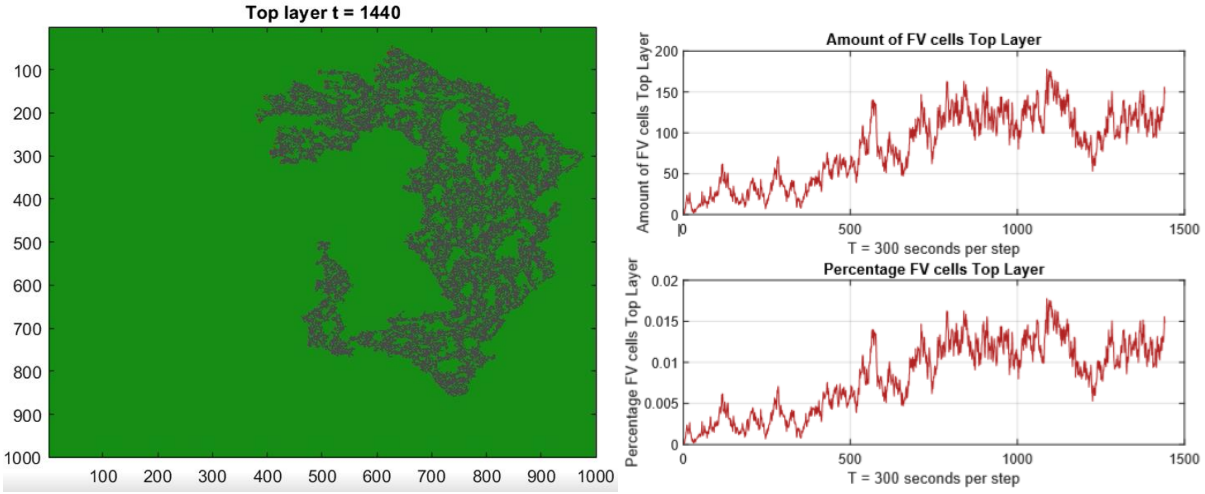

Image 48. Results test run 19 compound test for wind directions.

From test 11 to 19, it can be concluded that the influence of wind direction and speed is modeled with the expected results in the FENIX wildfire model framework. Therefore, no additional changes to the model were made.

Phase 3: Revegetation calibration phase

The FENIX wildfire spread model is the first model to incorporate the effects of revegetation phenomena for wildfires on organic soils at the field scale. Calibrating the framework to perfectly mimic this phenomenon is beyond scope of this thesis. However, derived from the probability of extinction as proposed by Purnomo et al. (2020) a range of values for P_{veg} was tested. Since the transition of a cell between the cell states exposed peat and surface vegetation is not only governed by growth back but also by leftover fuel the phenomenon is uncertain. Moreover, updating the probability with a number of time steps a cell has been in the state of exposed peat can be computationally intensive. The following diagnostics are selected for the calibration phase. A snapshot of the top layer after the initial burning period 2 days (t=576), a snapshot of the top layer at the end of the test at 35 days (t=10080). Furthermore, the graphs of amount and percentage flaming vegetation cells are included together with the same graphs for surface vegetation. Ultimately, a table is included with the diagnostics for the top layer at each day (each day equals 288 time steps). The phase consists of six test runs. With a highest $P_{veg} = 5*\text{-}10^{4}$ and a lowest $P_{veg} = 5*\text{-}10^{6}$. The results are presented below in images 49 until 66.

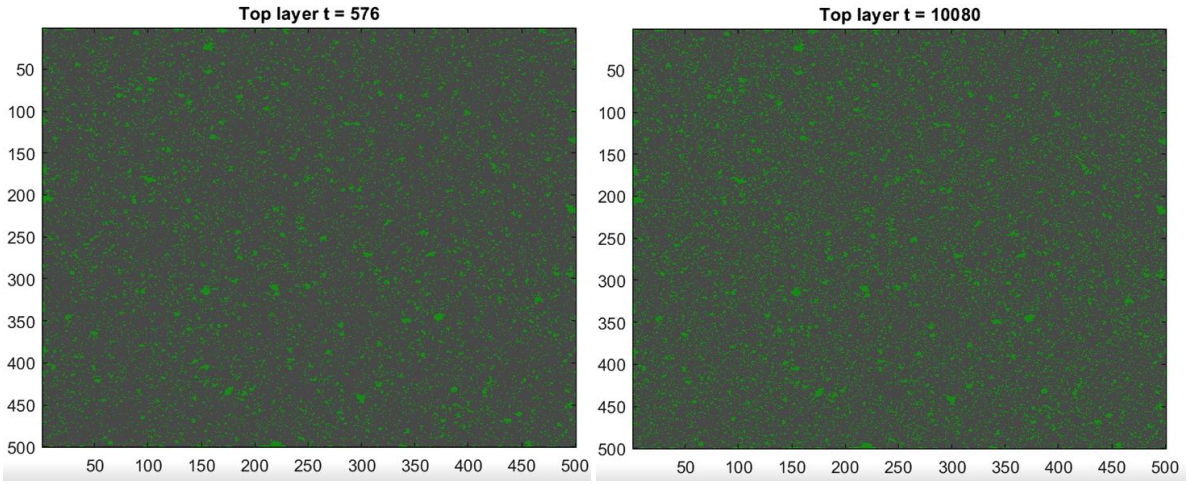

Image 49. Snapshots test run 20. Pveg = 5*-10^6.

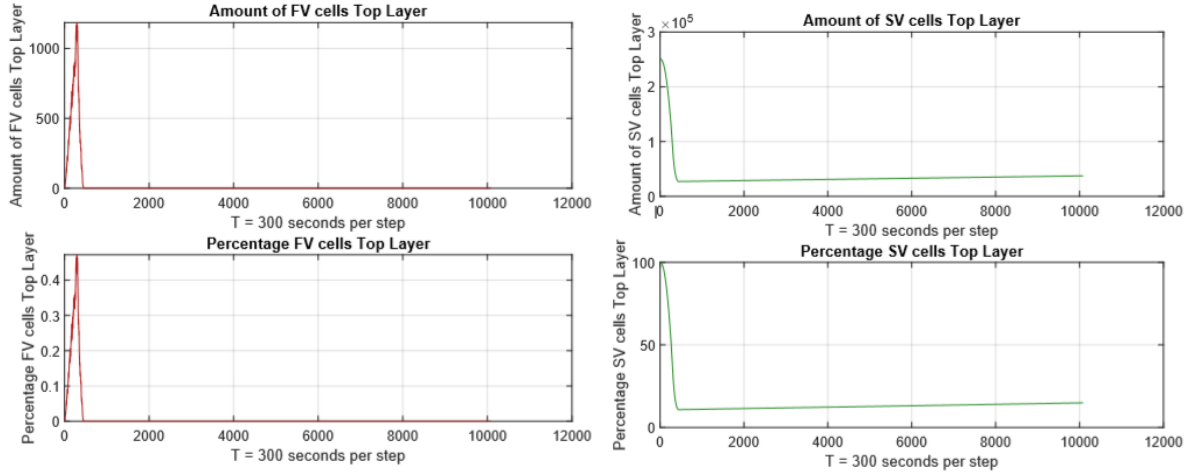

Image 50. Cell state diagnostics test run 20.

	Day	#FV	%FV	Δ#FV	#SV	%SV	Δ#SV	#EP	%EP	Δ#EP
1	0	1	0	0	251000	100	0	0	0	0
2	1	1132	0.4510	1132	102450	40.8166	102450	147419	58.7324	147419
3	2	0	0	-1132	27295	10.8745	-75155	223706	89.1255	76287
4	3	0	0	0	27595	10.9940	300	223406	89.0060	-300
5	4	0	0	0	27917	11.1223	322	223084	88.8777	-322
6	5	0	0	0	28267	11.2617	350	222734	88.7383	-350
7	6	0	0	0	28553	11.3757	286	222448	88.6243	-286
8	7	0	0	0	28860	11.4980	307	222141	88.5020	-307
9	8	0	0	0	29167	11.6203	307	221834	88.3797	-307
10	9	0	0	0	29515	11.7589	348	221486	88.2411	-348
11	10	0	0	0	29804	11.8741	289	221197	88.1259	-289
12	11	0	0	0	30105	11.9940	301	220896	88.0060	-301
13	12	0	0	0	30407	12.1143	302	220594	87.8857	-302
14	13	0	0	0	30690	12.2270	283	220311	87.7730	-283
15	14	0	0	0	30975	12.3406	285	220026	87.6594	-285
16	15	0	0	0	31248	12.4494	273	219753	87.5506	-273
17	16	0	0	0	31568	12.5768	320	219433	87.4232	-320
18	17	0	0	0	31867	12.6960	299	219134	87.3040	-299
19	18	0	0	0	32177	12.8195	310	218824	87.1805	-310
20	19	0	0	0	32494	12.9458	317	218507	87.0542	-317
21	20	0	0	0	32799	13.0673	305	218202	86.9327	-305
22	21	0	0	0	33117	13.1940	318	217884	86.8060	-318
23	22	0	0	0	33421	13.3151	304	217580	86.6849	-304
24	23	0	0	0	33728	13.4374	307	217273	86.5626	-307
25	24	0	0	0	34041	13.5621	313	216960	86.4379	-313
26	25	0	0	0	34361	13.6896	320	216640	86.3104	-320
27	26	0	0	0	34661	13.8091	300	216340	86.1909	-300
28	27	0	0	0	34999	13.9438	338	216002	86.0562	-338
29	28	0	0	0	35295	14.0617	296	215706	85.9383	-296
30	29	0	0	0	35609	14.1868	314	215392	85.8132	-314
31	30	0	0	0	35920	14.3107	311	215081	85.6893	-311
32	31	0	0	0	36230	14.4342	310	214771	85.5658	-310
33	32	0	0	0	36543	14.5589	313	214458	85.4411	-313
34	33	0	0	0	36864	14.6868	321	214137	85.3132	-321
35	34	0	0	0	37181	14.8131	317	213820	85.1869	-317
36	35	0	0	0	37484	14.9338	303	213517	85.0662	-303

Image 51. Top layer diagnostics per day.

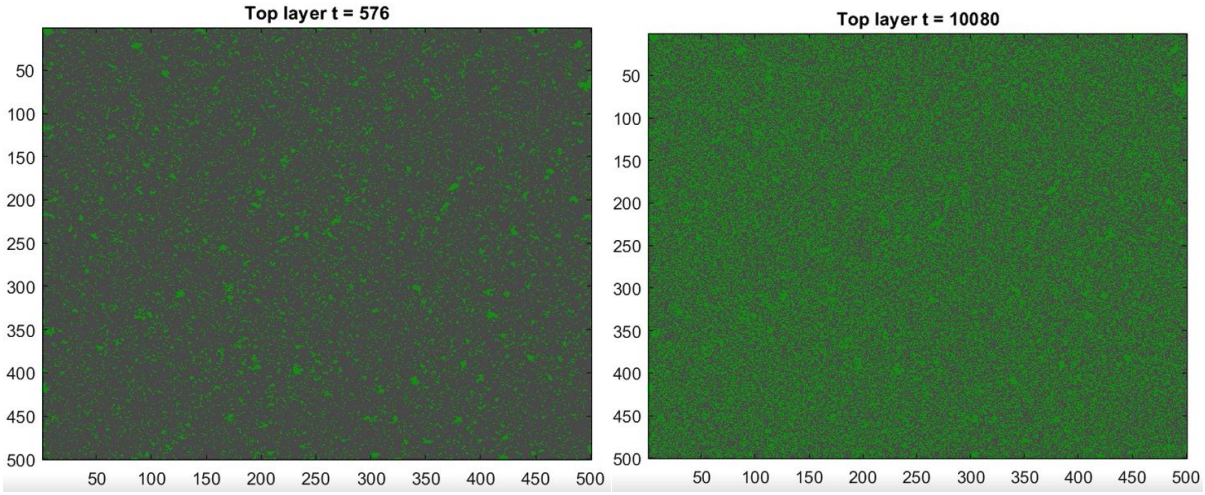

Image 52. Snapshots test run 21 P_{veg} = 5*-10^5.

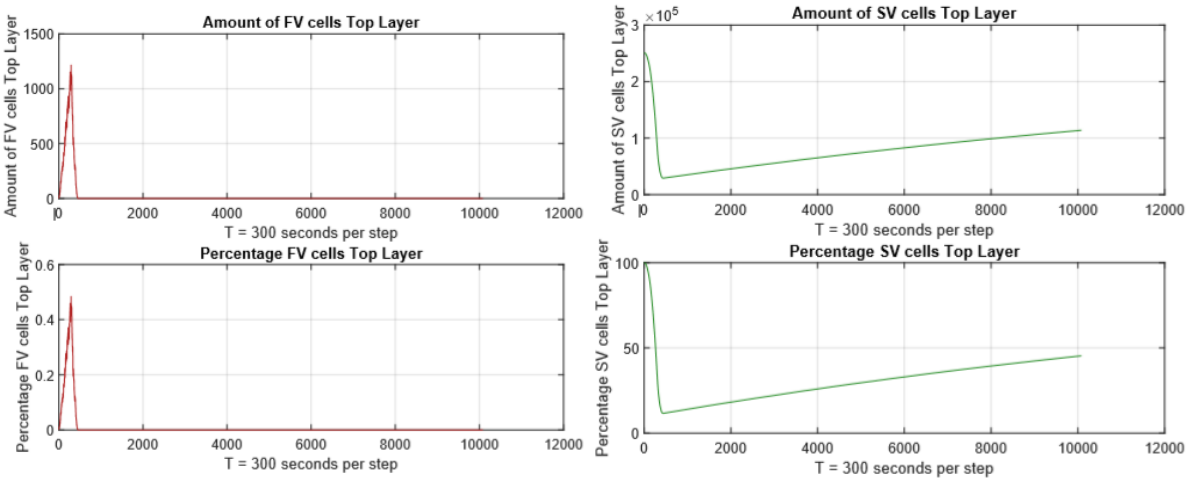

Image 53. Cell state diagnostics test run 21.

	Day	#FV	%FV	Δ#FV	#SV	%SV	Δ#SV	#EP	%EP	Δ#EP
1	0	1	0	0	251000	100	0	0	0	0
2	1	1079	0.4299	1079	100494	40.0373	100494	149428	59.5328	149428
3	2	0	0	-1079	30738	12.2462	-69756	220263	87.7538	70835
4	3	0	0	0	33767	13.4529	3029	217234	86.5471	-3029
5	4	0	0	0	36861	14.6856	3094	214140	85.3144	-3094
6	5	0	0	0	39987	15.9310	3126	211014	84.0690	-3126
7	6	0	0	0	42960	17.1155	2973	208041	82.8845	-2973
8	7	0	0	0	45842	18.2637	2882	205159	81.7363	-2882
9	8	0	0	0	48767	19.4290	2925	202234	80.5710	-2925
10	9	0	0	0	51676	20.5880	2909	199325	79.4120	-2909
11	10	0	0	0	54449	21.6927	2773	196552	78.3073	-2773
12	11	0	0	0	57243	22.8059	2794	193758	77.1941	-2794
13	12	0	0	0	60094	23.9417	2851	190907	76.0583	-2851
14	13	0	0	0	62845	25.0377	2751	188156	74.9623	-2751
15	14	0	0	0	65474	26.0852	2629	185527	73.9148	-2629
16	15	0	0	0	68198	27.1704	2724	182803	72.8296	-2724
17	16	0	0	0	70767	28.1939	2569	180234	71.8061	-2569
18	17	0	0	0	73362	29.2278	2595	177639	70.7722	-2595
19	18	0	0	0	75867	30.2258	2505	175134	69.7742	-2505
20	19	0	0	0	78324	31.2047	2457	172677	68.7953	-2457
21	20	0	0	0	80869	32.2186	2545	170132	67.7814	-2545
22	21	0	0	0	83252	33.1680	2383	167749	66.8320	-2383
23	22	0	0	0	85726	34.1536	2474	165275	65.8464	-2474
24	23	0	0	0	88106	35.1019	2380	162895	64.8981	-2380
25	24	0	0	0	90446	36.0341	2340	160555	63.9659	-2340
26	25	0	0	0	92722	36.9409	2276	158279	63.0591	-2276
27	26	0	0	0	94979	37.8401	2257	156022	62.1599	-2257
28	27	0	0	0	97206	38.7273	2227	153795	61.2727	-2227
29	28	0	0	0	99399	39.6010	2193	151602	60.3990	-2193
30	29	0	0	0	101553	40.4592	2154	149448	59.5408	-2154
31	30	0	0	0	103697	41.3134	2144	147304	58.6866	-2144
32	31	0	0	0	105803	42.1524	2106	145198	57.8476	-2106
33	32	0	0	0	107881	42.9803	2078	143120	57.0197	-2078
34	33	0	0	0	109899	43.7843	2018	141102	56.2157	-2018
35	34	0	0	0	111934	44.5950	2035	139067	55.4050	-2035
36	35	0	0	0	113915	45.3843	1981	137086	54.6157	-1981

Image 54. Top layer diagnostics per day.

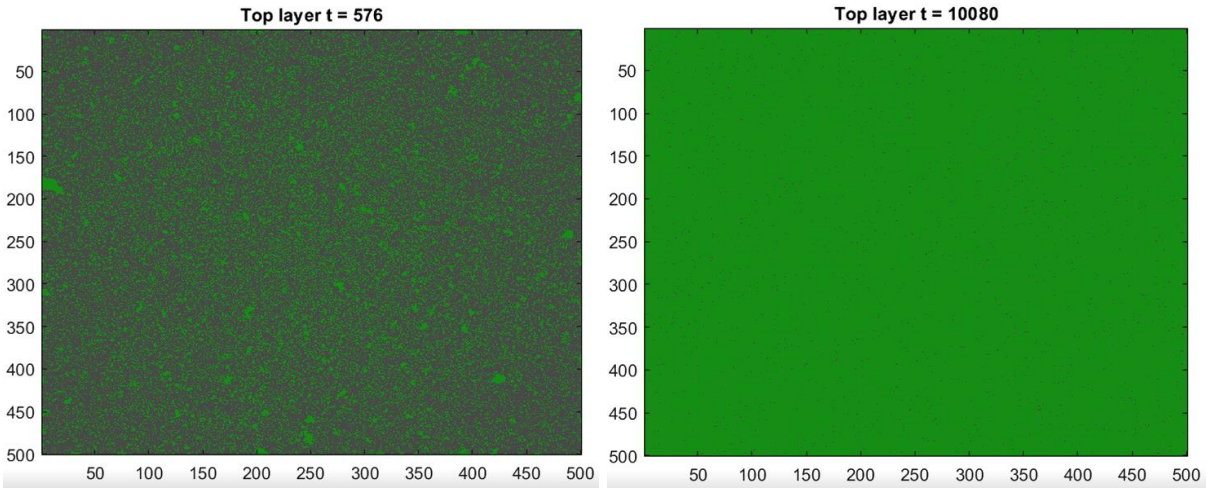

Image 55. Snapshots test run 22 P_{veg} = 5*-10^4.

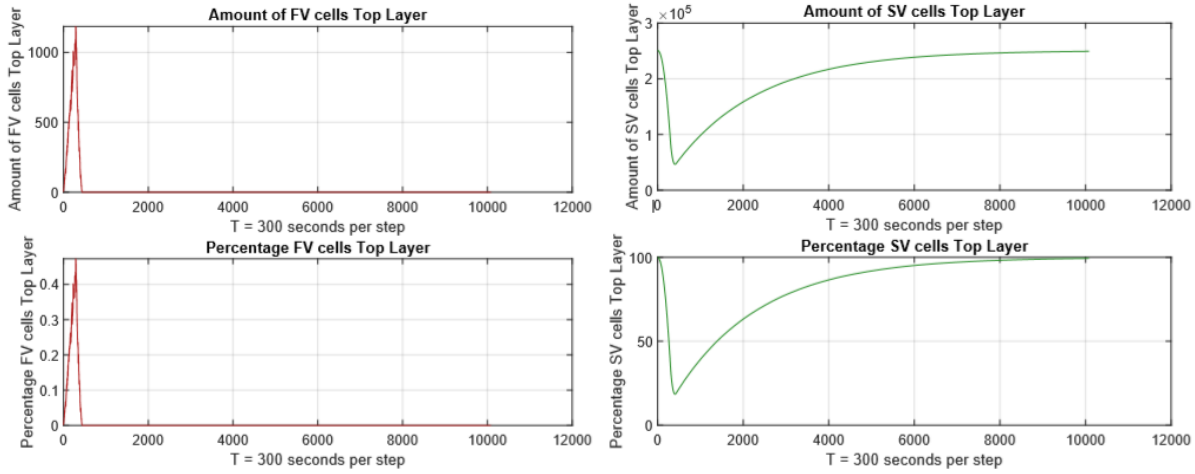

Image 56. Cell state diagnostics test run 22.

	Day	#FV	%FV	Δ#FV	#SV	%SV	Δ#SV	#EP	%EP	Δ#EP
1	0	1	0	0	251000	100	0	0	0	0
2	1	1186	0.4725	1186	101806	40.5600	101806	148009	58.9675	148009
3	2	0	0	-1186	61935	24.6752	-39871	189066	75.3248	41057
4	3	0	0	0	87567	34.8871	25632	163434	65.1129	-25632
5	4	0	0	0	109487	43.6201	21920	141514	56.3799	-21920
6	5	0	0	0	128703	51.2759	19216	122298	48.7241	-19216
7	6	0	0	0	145000	57.7687	16297	106001	42.2313	-16297
8	7	0	0	0	159343	63.4830	14343	91658	36.5170	-14343
9	8	0	0	0	171460	68.3105	12117	79541	31.6895	-12117
10	9	0	0	0	182164	72.5750	10704	68837	27.4250	-10704
11	10	0	0	0	191533	76.3077	9369	59468	23.6923	-9369
12	11	0	0	0	199411	79.4463	7878	51590	20.5537	-7878
13	12	0	0	0	206446	82.2491	7035	44555	17.7509	-7035
14	13	0	0	0	212428	84.6327	5983	38572	15.3673	-5983
15	14	0	0	0	217674	86.7224	5245	33327	13.2776	-5245
16	15	0	0	0	222237	88.5403	4563	28764	11.4597	-4563
17	16	0	0	0	226063	90.0646	3826	24938	9.9354	-3826
18	17	0	0	0	229437	91.4088	3374	21564	8.5912	-3374
19	18	0	0	0	232367	92.5761	2930	18634	7.4239	-2930
20	19	0	0	0	234891	93.5817	2524	16110	6.4183	-2524
21	20	0	0	0	237117	94.4685	2226	13884	5.5315	-2226
22	21	0	0	0	239017	95.2255	1900	11984	4.7745	-1900
23	22	0	0	0	240646	95.8745	1629	10355	4.1255	-1629
24	23	0	0	0	242034	96.4275	1388	8967	3.5725	-1388
25	24	0	0	0	243207	96.8948	1173	7794	3.1052	-1173
26	25	0	0	0	244254	97.3120	1047	6747	2.6880	-1047
27	26	0	0	0	245183	97.6821	929	5818	2.3179	-929
28	27	0	0	0	245945	97.9857	762	5056	2.0143	-762
29	28	0	0	0	246629	98.2582	684	4372	1.7418	-684
30	29	0	0	0	247200	98.4857	571	3801	1.5143	-571
31	30	0	0	0	247707	98.6877	507	3294	1.3123	-507
32	31	0	0	0	248137	98.8590	430	2864	1.1410	-430
33	32	0	0	0	248555	99.0255	418	2446	0.9745	-418
34	33	0	0	0	248864	99.1486	309	2137	0.8514	-309
35	34	0	0	0	249121	99.2510	257	1880	0.7490	-257
36	35	0	0	0	249370	99.3502	249	1631	0.6498	-249

Image 57. Top layer diagnostics per day.

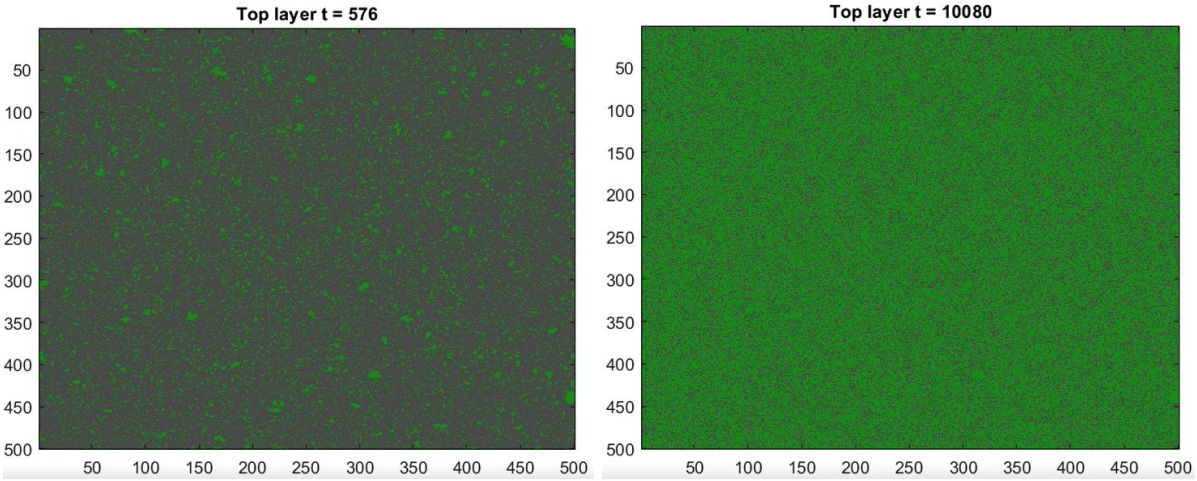

Image 58. Snapshots test run 23 P_{veg} = 1*-10^4.

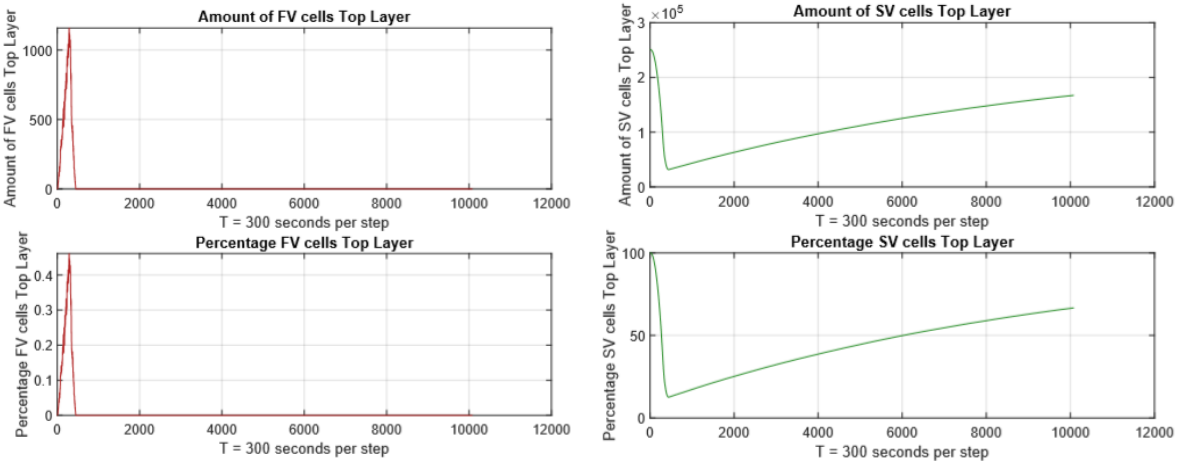

Image 59. Cell state diagnostics test run 23.

	Day	#FV	%FV	Δ#FV	#SV	%SV	Δ#SV	#EP	%EP	Δ#EP
1	0	1	0	0	251000	100	0	0	0	0
2	1	1152	0.4590	1152	109676	43.6954	109676	140173	55.8456	140173
3	2	0	0	-1152	34561	13.7693	-75115	216440	86.2307	76267
4	3	0	0	0	40567	16.1621	6006	210434	83.8379	-6006
5	4	0	0	0	46664	18.5912	6097	204337	81.4088	-6097
6	5	0	0	0	52506	20.9186	5842	198495	79.0814	-5842
7	6	0	0	0	58125	23.1573	5619	192876	76.8427	-5619
8	7	0	0	0	63538	25.3138	5413	187463	74.6862	-5413
9	8	0	0	0	68852	27.4310	5314	182149	72.5690	-5314
10	9	0	0	0	74029	29.4935	5177	176972	70.5065	-5177
11	10	0	0	0	79043	31.4911	5014	171958	68.5089	-5014
12	11	0	0	0	83917	33.4329	4874	167084	66.5671	-4874
13	12	0	0	0	88620	35.3066	4703	162381	64.6934	-4703
14	13	0	0	0	93167	37.1182	4547	157834	62.8818	-4547
15	14	0	0	0	97629	38.8959	4462	153372	61.1041	-4462
16	15	0	0	0	101968	40.6245	4339	149033	59.3755	-4339
17	16	0	0	0	106264	42.3361	4296	144737	57.6639	-4296
18	17	0	0	0	110312	43.9488	4048	140689	56.0512	-4048
19	18	0	0	0	114432	45.5903	4120	136569	54.4097	-4120
20	19	0	0	0	118345	47.1492	3913	132656	52.8508	-3913
21	20	0	0	0	122153	48.6663	3808	128848	51.3337	-3808
22	21	0	0	0	125907	50.1620	3754	125094	49.8380	-3754
23	22	0	0	0	129456	51.5759	3549	121545	48.4241	-3549
24	23	0	0	0	132840	52.9241	3384	118161	47.0759	-3384
25	24	0	0	0	136122	54.2317	3282	114879	45.7683	-3282
26	25	0	0	0	139378	55.5289	3256	111623	44.4711	-3256
27	26	0	0	0	142614	56.8181	3236	108387	43.1819	-3236
28	27	0	0	0	145631	58.0201	3017	105370	41.9799	-3017
29	28	0	0	0	148645	59.2209	3014	102356	40.7791	-3014
30	29	0	0	0	151583	60.3914	2938	99418	39.6086	-2938
31	30	0	0	0	154443	61.5308	2860	96558	38.4692	-2860
32	31	0	0	0	157200	62.6292	2757	93801	37.3708	-2757
33	32	0	0	0	159860	63.6890	2660	91141	36.3110	-2660
34	33	0	0	0	162463	64.7260	2603	88538	35.2740	-2603
35	34	0	0	0	164976	65.7272	2513	86025	34.2728	-2513
36	35	0	0	0	167341	66.6695	2365	83660	33.3305	-2365

Image 60. Top layer diagnostics per day.

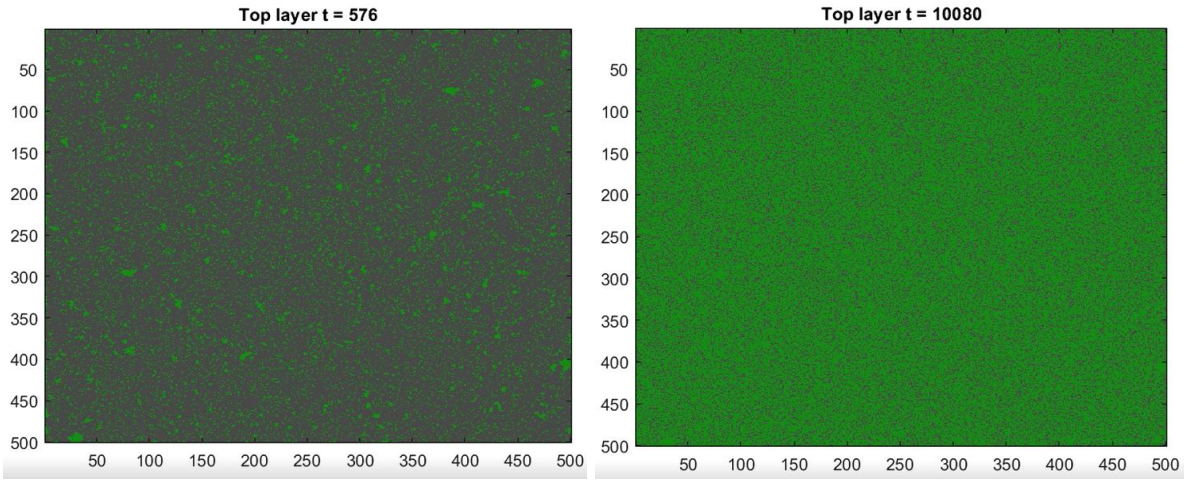

Image 61. Snapshots test run 24 P_{veg} = 1.25*-10^4.

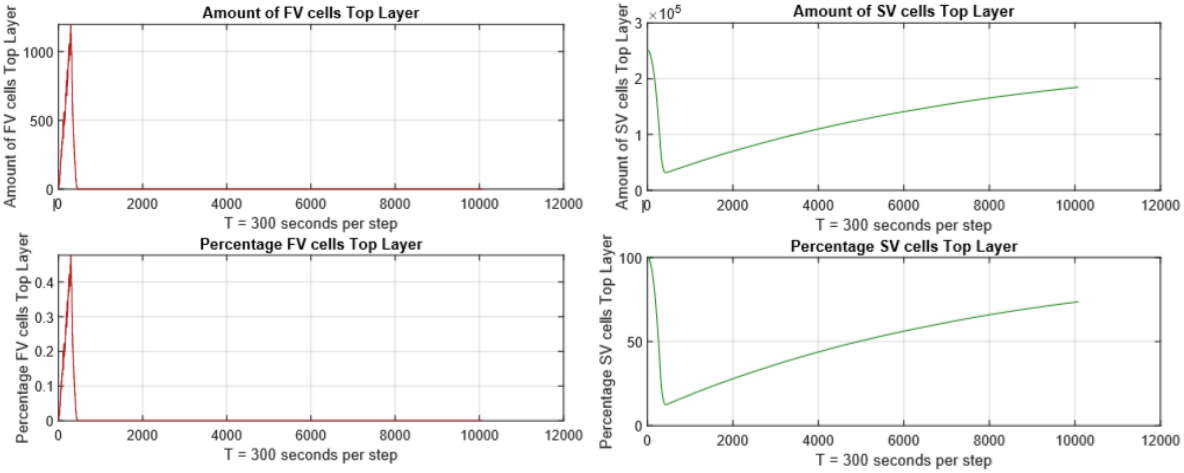

Image 62. Cell state diagnostics test run 24.

	Day	#FV	%FV	Δ#FV	#SV	%SV	Δ#SV	#EP	%EP	Δ#EP
1	0	1	0	0	251000	100	0	0	0	0
2	1	1123	0.4474	1123	98092	39.0803	98092	151786	60.4723	151786
3	2	0	0	-1123	35068	13.9713	-63024	215933	86.0287	64147
4	3	0	0	0	42660	16.9959	7592	208341	83.0041	-7592
5	4	0	0	0	50063	19.9453	7403	200938	80.0547	-7403
6	5	0	0	0	57098	22.7481	7035	193903	77.2519	-7035
7	6	0	0	0	63895	25.4561	6797	187106	74.5439	-6797
8	7	0	0	0	70476	28.0780	6581	180525	71.9220	-6581
9	8	0	0	0	76730	30.5696	6254	174271	69.4304	-6254
10	9	0	0	0	82821	32.9963	6091	168180	67.0037	-6091
11	10	0	0	0	88755	35.3604	5934	162246	64.6396	-5934
12	11	0	0	0	94608	37.6923	5853	156393	62.3077	-5853
13	12	0	0	0	100079	39.8720	5471	150922	60.1280	-5471
14	13	0	0	0	105448	42.0110	5369	145553	57.9890	-5369
15	14	0	0	0	110518	44.0309	5070	140483	55.9691	-5070
16	15	0	0	0	115552	46.0365	5034	135449	53.9635	-5034
17	16	0	0	0	120406	47.9703	4854	130595	52.0297	-4854
18	17	0	0	0	124923	49.7699	4517	126078	50.2301	-4517
19	18	0	0	0	129312	51.5185	4389	121689	48.4815	-4389
20	19	0	0	0	133680	53.2588	4368	117321	46.7412	-4368
21	20	0	0	0	137797	54.8990	4117	113204	45.1010	-4117
22	21	0	0	0	141708	56.4571	3911	109293	43.5429	-3911
23	22	0	0	0	145463	57.9532	3755	105538	42.0468	-3755
24	23	0	0	0	149189	59.4376	3726	101812	40.5624	-3726
25	24	0	0	0	152828	60.8874	3639	98173	39.1126	-3639
26	25	0	0	0	156435	62.3245	3607	94566	37.6755	-3607
27	26	0	0	0	159843	63.6822	3408	91158	36.3178	-3408
28	27	0	0	0	163101	64.9802	3258	87900	35.0198	-3258
29	28	0	0	0	166246	66.2332	3145	84755	33.7668	-3145
30	29	0	0	0	169208	67.4133	2962	81793	32.5867	-2962
31	30	0	0	0	172087	68.5603	2879	78914	31.4397	-2879
32	31	0	0	0	174816	69.6475	2729	76185	30.3525	-2729
33	32	0	0	0	177461	70.7013	2645	73540	29.2987	-2645
34	33	0	0	0	180076	71.7431	2615	70925	28.2569	-2615
35	34	0	0	0	182570	72.7368	2494	68431	27.2632	-2494
36	35	0	0	0	184926	73.6754	2356	66075	26.3246	-2356

Image 63. Top layer diagnostics per day.

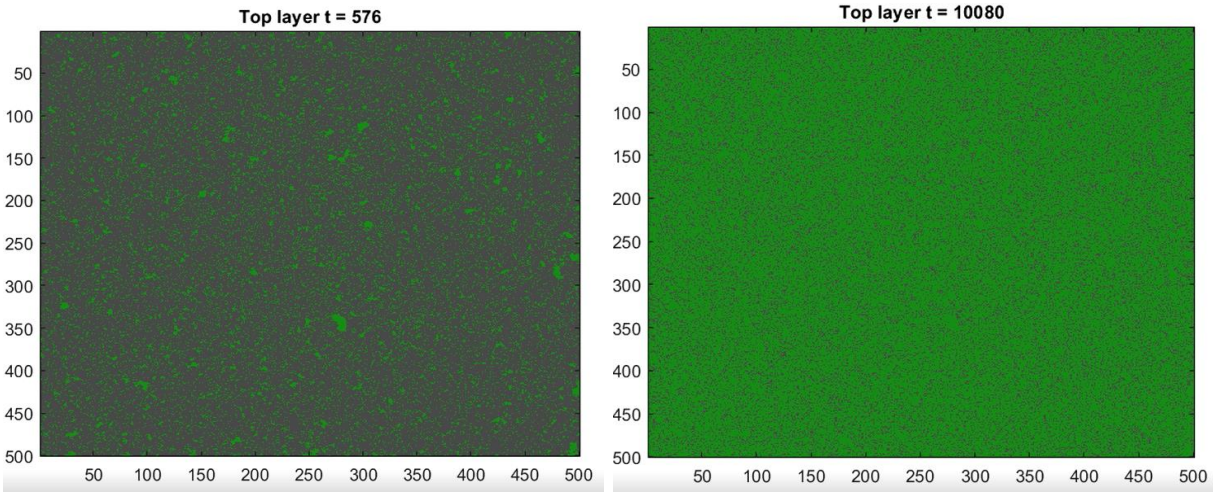

Image 64. Snapshots test run 25 P_{veg} = 1.5*-10^4.

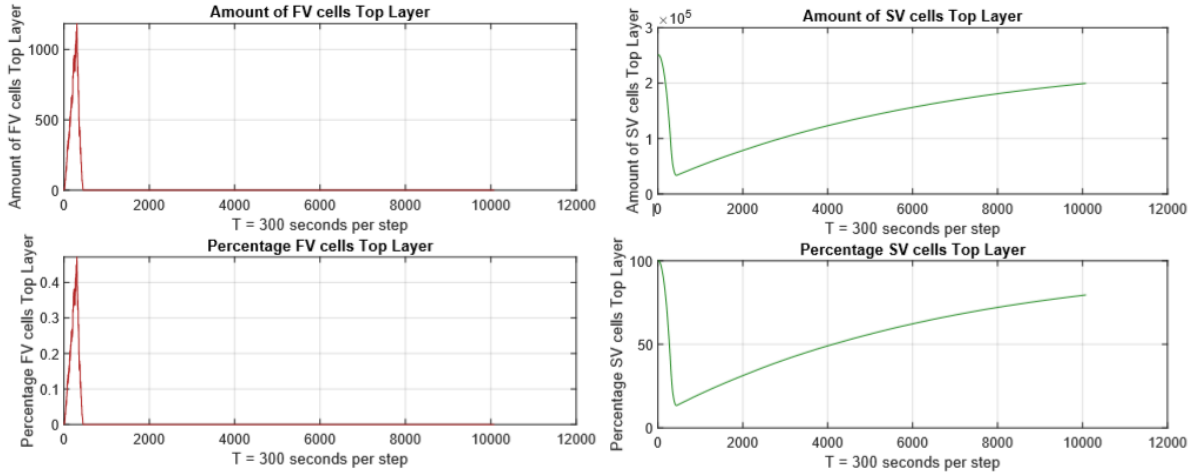

Image 65. Cell state diagnostics test run 25.

	Day	#FV	%FV	Δ#FV	#SV	%SV	Δ#SV	#EP	%EP	Δ#EP
1	0	1	0	0	251000	100	0	0	0	0
2	1	1127	0.4490	1127	109011	43.4305	109011	140863	56.1205	140863
3	2	0	0	-1127	37974	15.1290	-71037	213027	84.8710	72164
4	3	0	0	0	46953	18.7063	8979	204048	81.2937	-8979
5	4	0	0	0	55469	22.0991	8516	195532	77.9009	-8516
6	5	0	0	0	63619	25.3461	8150	187382	74.6539	-8150
7	6	0	0	0	71451	28.4664	7832	179550	71.5336	-7832
8	7	0	0	0	78954	31.4557	7503	172047	68.5443	-7503
9	8	0	0	0	86253	34.3636	7299	164748	65.6364	-7299
10	9	0	0	0	93299	37.1708	7046	157702	62.8292	-7046
11	10	0	0	0	99993	39.8377	6694	151008	60.1623	-6694
12	11	0	0	0	106404	42.3919	6411	144597	57.6081	-6411
13	12	0	0	0	112447	44.7994	6043	138554	55.2006	-6043
14	13	0	0	0	118307	47.1341	5860	132694	52.8659	-5860
15	14	0	0	0	123829	49.3341	5522	127172	50.6659	-5522
16	15	0	0	0	129075	51.4241	5246	121926	48.5759	-5246
17	16	0	0	0	134286	53.5002	5211	116715	46.4998	-5211
18	17	0	0	0	139187	55.4528	4901	111814	44.5472	-4901
19	18	0	0	0	143926	57.3408	4739	107075	42.6592	-4739
20	19	0	0	0	148488	59.1583	4562	102513	40.8417	-4562
21	20	0	0	0	152872	60.9049	4384	98129	39.0951	-4384
22	21	0	0	0	157010	62.5535	4138	93991	37.4465	-4138
23	22	0	0	0	160942	64.1201	3932	90059	35.8799	-3932
24	23	0	0	0	164867	65.6838	3925	86134	34.3162	-3925
25	24	0	0	0	168422	67.1001	3555	82579	32.8999	-3555
26	25	0	0	0	171980	68.5177	3558	79021	31.4823	-3558
27	26	0	0	0	175334	69.8539	3354	75667	30.1461	-3354
28	27	0	0	0	178557	71.1380	3223	72444	28.8620	-3223
29	28	0	0	0	181626	72.3607	3069	69375	27.6393	-3069
30	29	0	0	0	184493	73.5029	2867	66508	26.4971	-2867
31	30	0	0	0	187275	74.6113	2782	63726	25.3887	-2782
32	31	0	0	0	189966	75.6834	2691	61035	24.3166	-2691
33	32	0	0	0	192517	76.6997	2551	58484	23.3003	-2551
34	33	0	0	0	194981	77.6814	2464	56020	22.3186	-2464
35	34	0	0	0	197333	78.6184	2352	53668	21.3816	-2352
36	35	0	0	0	199610	79.5256	2277	51391	20.4744	-2277

Image 66. Top layer diagnostics per day.

As can be seen in the diagnostic data from the six test runs in the revegetation calibration phase, the FENIX framework is able to incorporate revegetation over a period of 35 days. Unfortunately, no previous work was found that considers the probability of revegetation on the field scale. Interpreting the results from the cell state diagnostics per day the end result percentage of surface vegetation cell are summarized below in image 67.

Test run	**P_{veg}**	**Final % Surface vegetation**
20	$5*\text{-}10^{6}$	14.9%
21	$5*\text{-}10^{5}$	45.4%
22	$5*\text{-}10^{4}$	99.4%
23	$1*\text{-}10^{4}$	66.7%
24	$1.25*\text{-}10^{4}$	73.7%
25	$1.5*\text{-}10^{4}$	79.5%

Image 67. Results percentage Surface Vegetation cells after 35 days.

Considering the diagnostic information the final probability for revegetation was set to be equal to the probability value of the last test run, $P_{veg} = 1.5*\text{-}10^{4}$.

Phase 4: Reignition probability calibration phase

Similar to the case of revegetation, the phenomenon of revegetation has not been considered in wildfire modeling before at the field scale. A previous study has been found that investigate the smoldering to flaming combustion transition but it did not provide a satisfying probability for the transition considering peat smoldering and revegetated surface fuel (Santoso et al., 2019). Five test runs were executed in order to test a range of probabilities between 0.001 and 0.0001. These values are derived from the probability transition of flaming to smoldering combustion and have been pushed down by an order of magnitude in order to account for the need of more ignition energy and higher temperatures based on the findings of Santoso et al. (2019). The relevant diagnostics for this calibration phase are considered to be a snapshot at the end of the test run (t=10080), a graph of amount and percentage flaming vegetation after the initial burning phase of 2 days (after t=588). The results of the reignition calibration phase are presented in images 68 until 72.

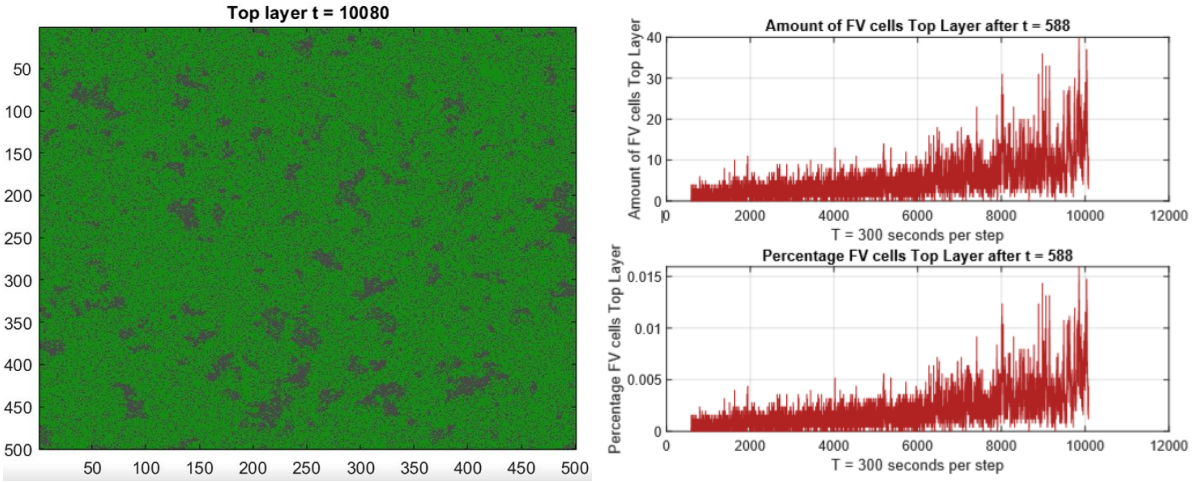

Image 68. Results test run 27 $P_{rei} = 0.001$.

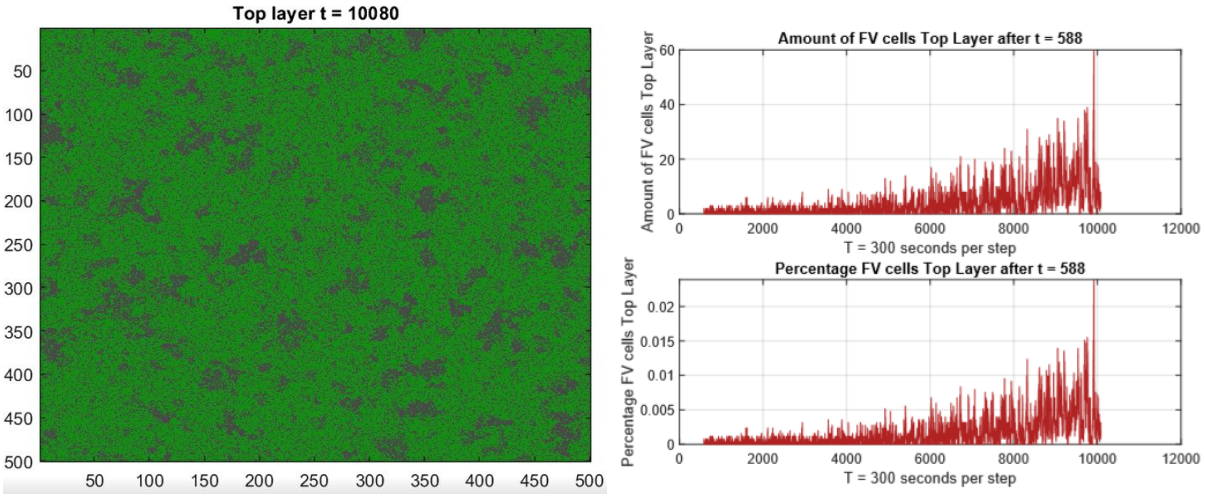

Image 69. Results test run 28 P_{rei} = 0.0025.

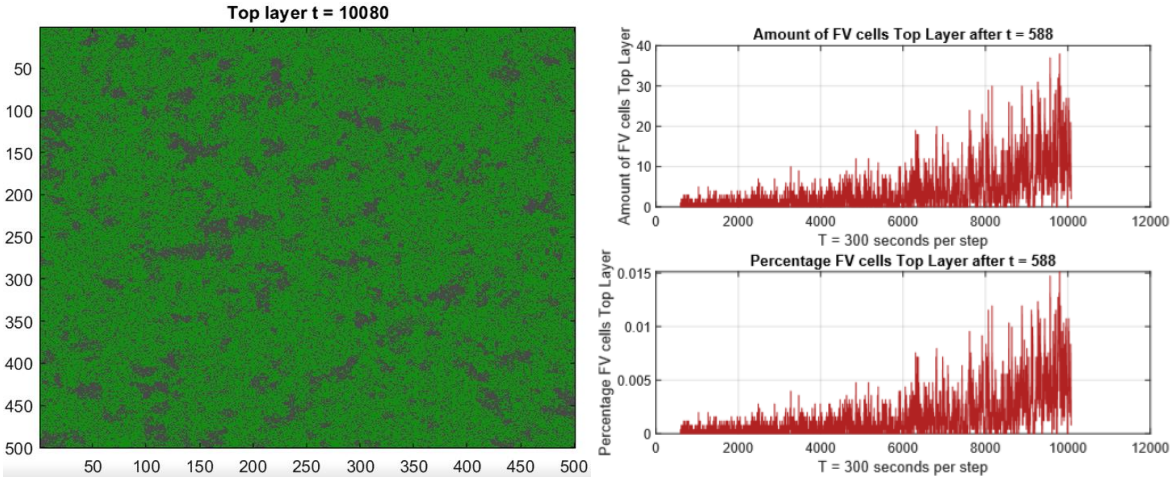

Image 70. Results test run 29 P_{rei} = 0.005.

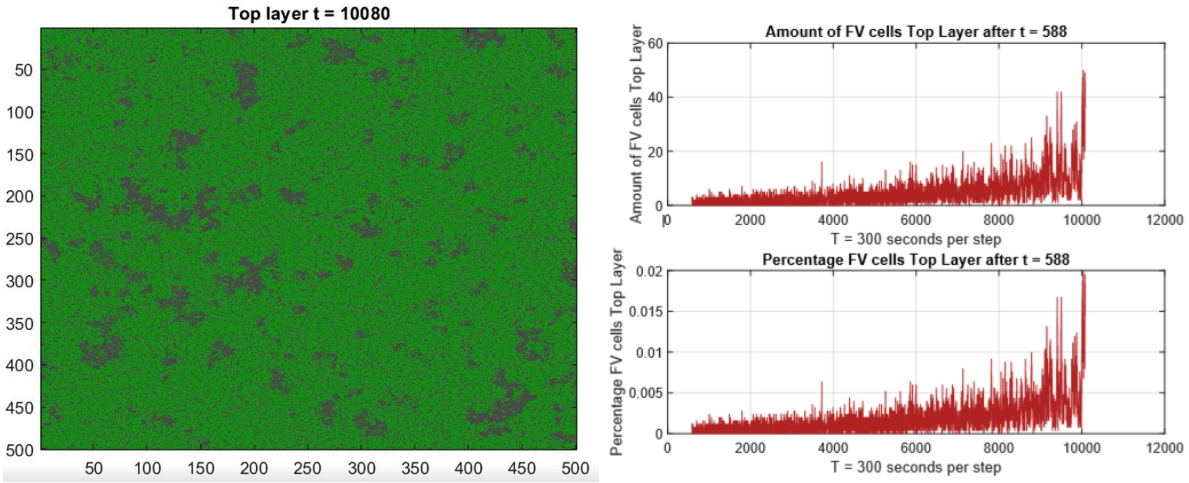

Image 71. Results Test run 30 P_{rei} = 0.0075.

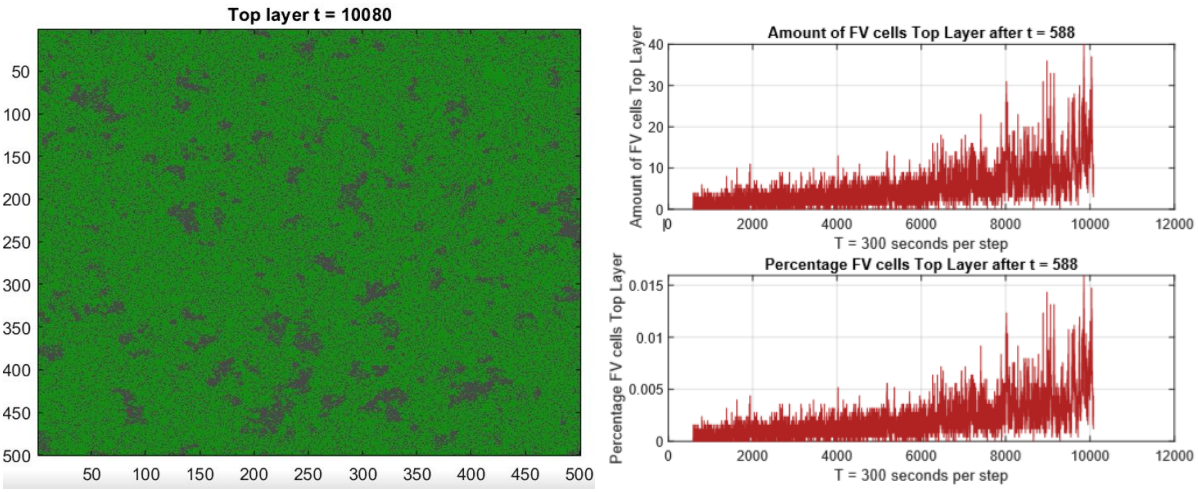

Image 72. Results test run 31 P_{rei} = 0.01.

Based on the results of the reignition probability calibration phase it can be stated that the FENIX wildfire spread model does not yield significantly different results when the probability for reignition is changed. The following section will address the final calibration for the FENIX framework as used for the aplication to model the Peel region wildfire from early 2020.

§8.3 Final calibration FENIX wildfire model framework

Following the results of previous calibration phase, a final calibration for the FENIX wildfire model can be configured. Considering the methodology and previous research the FENIX model follows the KAPAS structure as proposed by Purnomo et al. (2020) with the slight adaption of the flaming fire propagation probability. This value is set to be equal to P_R = 0.3, the theory behind this adaption is addressed in both the methodology and the calibration section of this thesis. With regards to the augmented wind parameter, the FENIX model incorporates the original equations as proposed by Alexandridis et al. (2004) but in essence, these equations are similar to the equation for wind influence as proposed by Purnomo et al. (2020). The probability for flaming to smoldering combustion is derived from the work of Frandsen (1997) and the probabilities for both smoldering combustion spread and smoldering combustion extinction are derived again from the work of Purnomo et al. (2020).

For the novelties in the FENIX wildfire model framework, reignition and revegetation, values were derived from the calibration phase. The probability of revegetation was set to be P_{veg} = 1.5*-10^4. The probability of reignition was set to be P_{rei} = 0.001. Both of these choices will be further discussed in the discussion chapter of this thesis.

§8.4 Application to the Peel region 2020 wildfire

With the calibration finalized the FENIX framework can be applied to a real world wildfire phenomenon. The selected case is the Peel region wildfire of early 2020, which is addressed extensively in earlier chapters. In order to make FENIX applicable to the case one extra cell state is added to the framework. This cell state of *incombustible area (IA)* can exist in both the soil and the top layer. In the top layer IA cells can represent cells inhabited for instance by water or buildings. In the soil layer IA cells represent non-organic soil types, which cannot facilitate smoldering combustion.

The transformation of the input data to make the FENIX model applicable was addressed in the data chapter of this thesis. Based on findings by Stoof et al. (2020) and the specialized team for wildfire research of the Dutch fire department the ignition point was located at cell (111, 569) in the top layer. This choice for the top layer is made because the specialized team only investigated the flaming fire phase of the wildfire event. Based on the timeline as presented by Stoof et al. (2020) the duration of the model run was set to be equal to 63 days (t=18144). Based on the extensive drought period of the period 2018-2020, the value for moisture content in the peat layer was set at 70%. Furthermore based on the interview as presented in appendix A. the P_R value was amplified to be equal to 0.35 to account for the death vegetation and extreme fire behavior as indicated by the interviewee. Results of the application are presented below. Snapshots will be included for four points in time. The situation after 2 days (t=576), the situation after 5 days (t=1440), the situation after 35 days (t=10080) and the final situation after 63 days (t=18144). First, the top layer will be addressed. After that, the results of the soil layer will be presented.

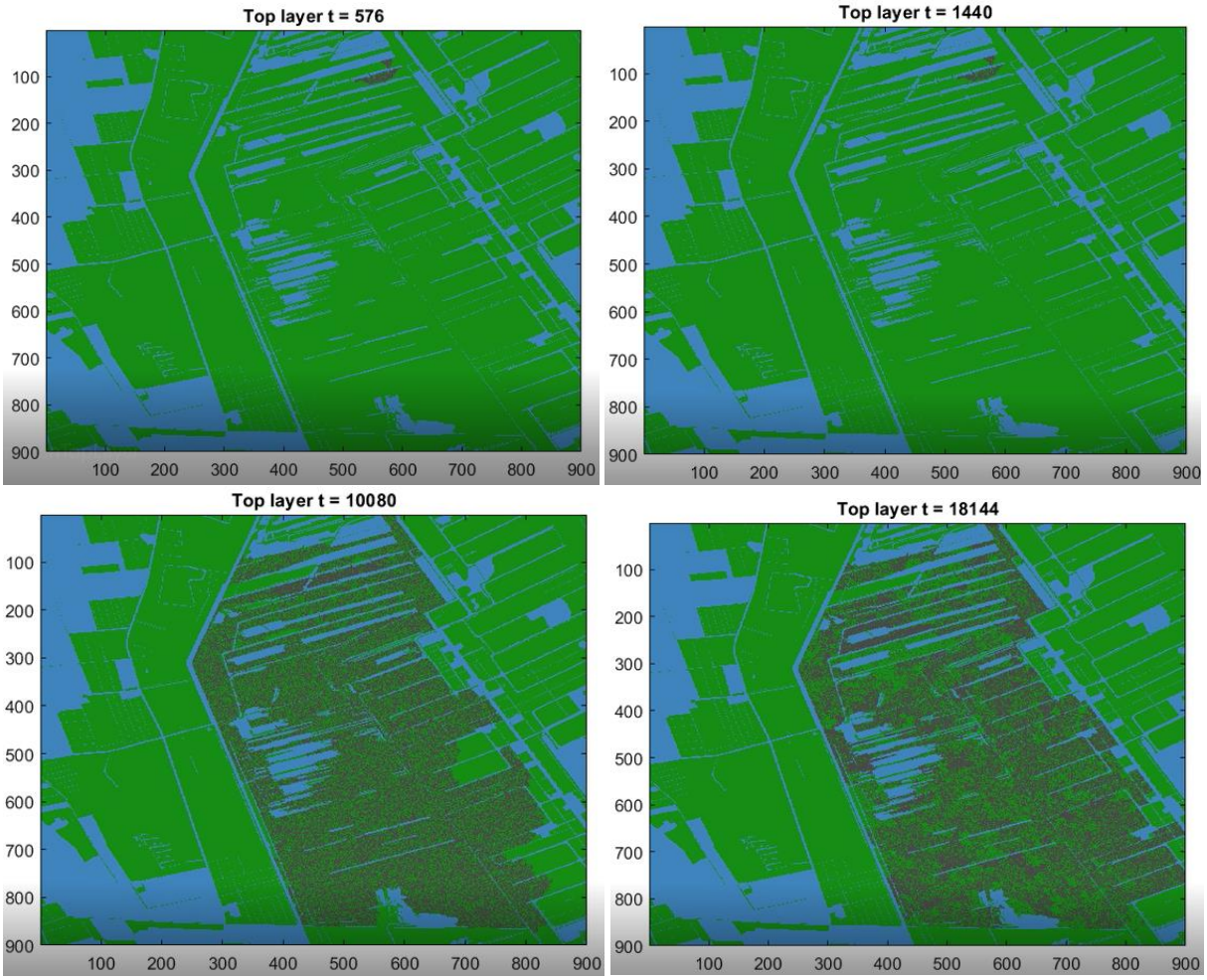

Image 73. Snapshots situation after time steps top layer.

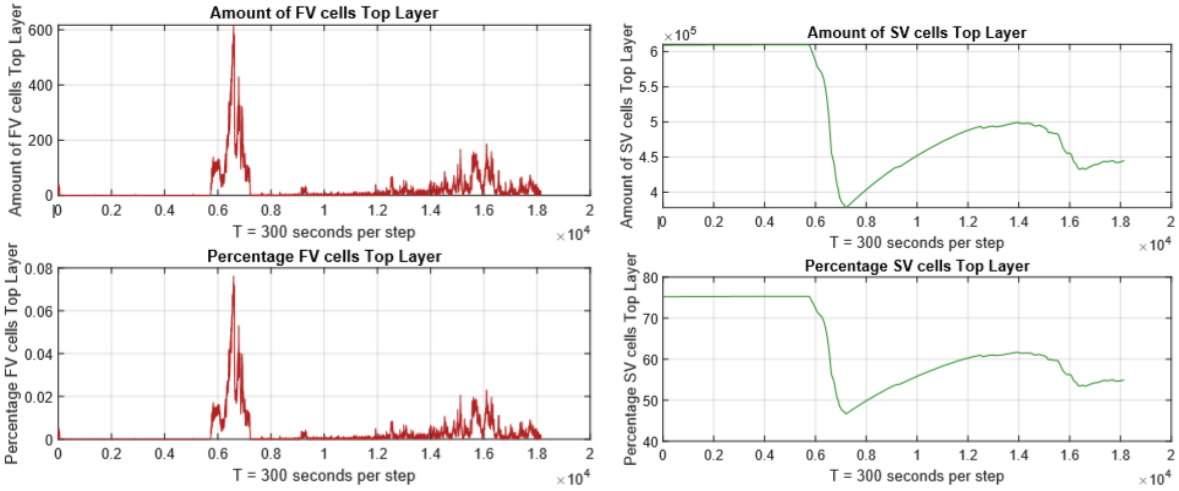

Image 74. Graphs cell states top layer.

From the snapshots presented in image 73 it can be seen that the initial burning period only affected a small portion of the study area. However a second burning period around the 6000th-8000th time step period mimics the destructivness of the wildfire event pretty well. This period is derived from the results presented in image 74. After that period a third period can be distinguished in which revegetation and reignition play a significant role in the amount of cells in flaming vegetation state.

	Day	#FV	%FV	Δ#FV	#SV	%SV	Δ#SV	#EP	%EP	Δ#EP
1	0	1	0	0	610395	0	0	0	0	0
2	1	0	0	0	609228	75.2133	609228	1167	0.1441	1167
3	2	0	0	0	609274	75.2190	46	1121	0.1384	-46
4	3	0	0	0	609325	75.2253	51	1070	0.1321	-51
5	4	0	0	0	609370	75.2309	45	1025	0.1265	-45
6	5	0	0	0	609421	75.2372	51	974	0.1202	-51
7	6	0	0	0	609458	75.2417	37	937	0.1157	-37
8	7	0	0	0	609502	75.2472	44	893	0.1102	-44
9	8	0	0	0	609535	75.2512	33	860	0.1062	-33
10	9	0	0	0	609577	75.2564	42	818	0.1010	-42
11	10	0	0	0	609616	75.2612	39	779	0.0962	-39
12	11	0	0	0	609628	75.2627	12	767	0.0947	-12
13	12	0	0	0	609654	75.2659	26	741	0.0915	-26
14	13	0	0	0	609683	75.2695	29	712	0.0879	-29
15	14	0	0	0	609720	75.2741	37	675	0.0833	-37
16	15	0	0	0	609754	75.2783	34	641	0.0791	-34
17	16	0	0	0	609777	75.2811	23	618	0.0763	-23
18	17	0	0	0	609808	75.2849	31	587	0.0725	-31
19	18	0	0	0	609812	75.2854	4	583	0.0720	-4
20	19	0	0	0	609833	75.2880	21	562	0.0694	-21
21	20	27	0.0033	27	608996	75.1847	-837	1372	0.1694	810
22	21	127	0.0157	100	581442	71.7830	-27554	28826	3.5588	27454
23	22	201	0.0248	74	559407	69.0626	-22035	50787	6.2700	21961
24	23	580	0.0716	379	458264	56.5758	-101143	151551	18.7100	100764
25	24	279	0.0344	-301	401542	49.5731	-56722	208574	25.7499	57023
26	25	65	0.0080	-214	378378	46.7133	-23164	231952	28.6360	23378
27	26	0	0	-65	387399	47.8270	9021	222996	27.5304	-8956
28	27	0	0	0	396758	48.9825	9359	213637	26.3749	-9359
29	28	1	1.2346e-04	1	405598	50.0738	8840	204796	25.2835	-8841
30	29	1	1.2346e-04	0	414152	51.1299	8554	196242	24.2274	-8554
31	30	0	0	-1	422077	52.1083	7925	188318	23.2491	-7924
32	31	1	1.2346e-04	1	429764	53.0573	7687	180630	22.3000	-7688
33	32	4	4.9383e-04	3	435755	53.7969	5991	174636	21.5600	-5994
34	33	2	2.4691e-04	-2	440688	54.4059	4933	169705	20.9512	-4931
35	34	1	1.2346e-04	-1	447390	55.2333	6702	163004	20.1240	-6701
36	35	1	1.2346e-04	0	453851	56.0310	6461	156543	19.3263	-6461

Image 75. Cell state diagnostic top layer first 35 days.

	Day	#FV	%FV	Δ#FV	#SV	%SV	Δ#SV	#EP	%EP	Δ#EP
1	36	2	2.4691e-04	1	459773	56.7621	5922	150620	18.5951	-5923
2	37	2	2.4691e-04	0	465463	57.4646	5690	144930	17.8926	-5690
3	38	0	0	-2	471109	58.1616	5646	139286	17.1958	-5644
4	39	6	7.4074e-04	6	476045	58.7710	4936	134344	16.5857	-4942
5	40	4	4.9383e-04	-2	480994	59.3820	4949	129397	15.9749	-4947
6	41	1	1.2346e-04	-3	485609	59.9517	4615	124785	15.4056	-4612
7	42	7	8.6420e-04	6	489288	60.4059	3679	121100	14.9506	-3685
8	43	15	0.0019	8	492676	60.8242	3388	117704	14.5314	-3396
9	44	11	0.0014	-4	491723	60.7065	-953	118661	14.6495	957
10	45	24	0.0030	13	493844	60.9684	2121	116527	14.3860	-2134
11	46	7	8.6420e-04	-17	494010	60.9889	166	116378	14.3677	-149
12	47	15	0.0019	8	496074	61.2437	2064	114306	14.1119	-2072
13	48	10	0.0012	-5	498485	61.5414	2411	111900	13.8148	-2406
14	49	27	0.0033	17	498119	61.4962	-366	112249	13.8579	349
15	50	36	0.0044	9	497958	61.4763	-161	112401	13.8767	152
16	51	5	6.1728e-04	-31	494346	61.0304	-3612	116044	14.3264	3643
17	52	33	0.0041	28	493110	60.8778	-1236	117252	14.4756	1208
18	53	26	0.0032	-7	485372	59.9225	-7738	124997	15.4317	7745
19	54	77	0.0095	51	482085	59.5167	-3287	128233	15.8312	3236
20	55	83	0.0102	6	457773	56.5152	-24312	152539	18.8320	24306
21	56	132	0.0163	49	446857	55.1675	-10916	163406	20.1736	10867
22	57	19	0.0023	-113	432855	53.4389	-14002	177521	21.9162	14115
23	58	4	4.9383e-04	-15	434418	53.6319	1563	175973	21.7251	-1548
24	59	6	7.4074e-04	2	439489	54.2579	5071	170900	21.0988	-5073
25	60	3	3.7037e-04	-3	443005	54.6920	3516	167387	20.6651	-3513
26	61	24	0.0030	21	444151	54.8335	1146	166220	20.5210	-1167
27	62	48	0.0059	24	442342	54.6101	-1809	168005	20.7414	1785
28	63	17	0.0021	-31	445368	54.9837	3026	165010	20.3716	-2995

Image 76. Cell state diagnostics top layer days 36-63.

Interpreting the diagnostic results per cell state per day as presented in images 75 and 76, it can be stated that the period of extreme fire spread happened around day 23 of the wildfire event, this is indicated by the significant increase of exposed peat cells in the top layer. The period after the extre flaming fire progression shows signs of revegetation and rekindling.

To interpret the results slightly more efficiently the final output of the model run was mapped back to the study area. This is shown in image 77. shows the same output but compares the situation to the fire extent from the actual wildfire event as defined by the EFFIS dataset.

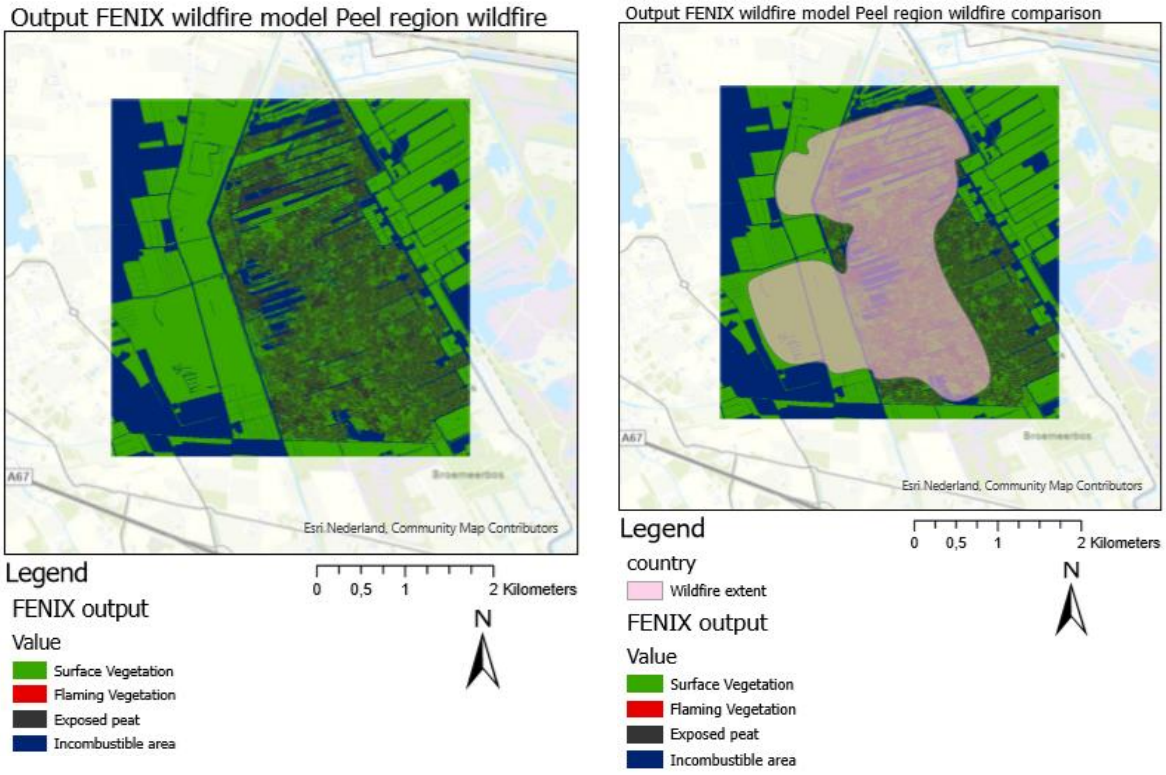

Image 77. final output mapped to study area and comparison with the final extent of the wildfire event.

Considering the comparison between the FENIX output of the flaming fire extent and the extent of the wildfire as defined by the EFFIS dataset it can be seen that the influence of the canal on the west side of the study area (het kanaal van Deurne) proves to have a great impact on the predicted extent. At least two flaming fronts formed on the west side of this canal according to the wildfire extent defined by EFFIS. This spread is due to spotting wildfire spread, this form of spread is not considered in the FENIX framework. Intrestingly the FENIX prediction considered the wildfire event to be more likely to progress slightly more eastward. This difference might be results of firefighting activities. The eastern edge of the study area situates multiple farms. Deployed firefighting activities to protect these farms is likely to be the influence for the difference in extents. The results of the soil layer will be presented below.

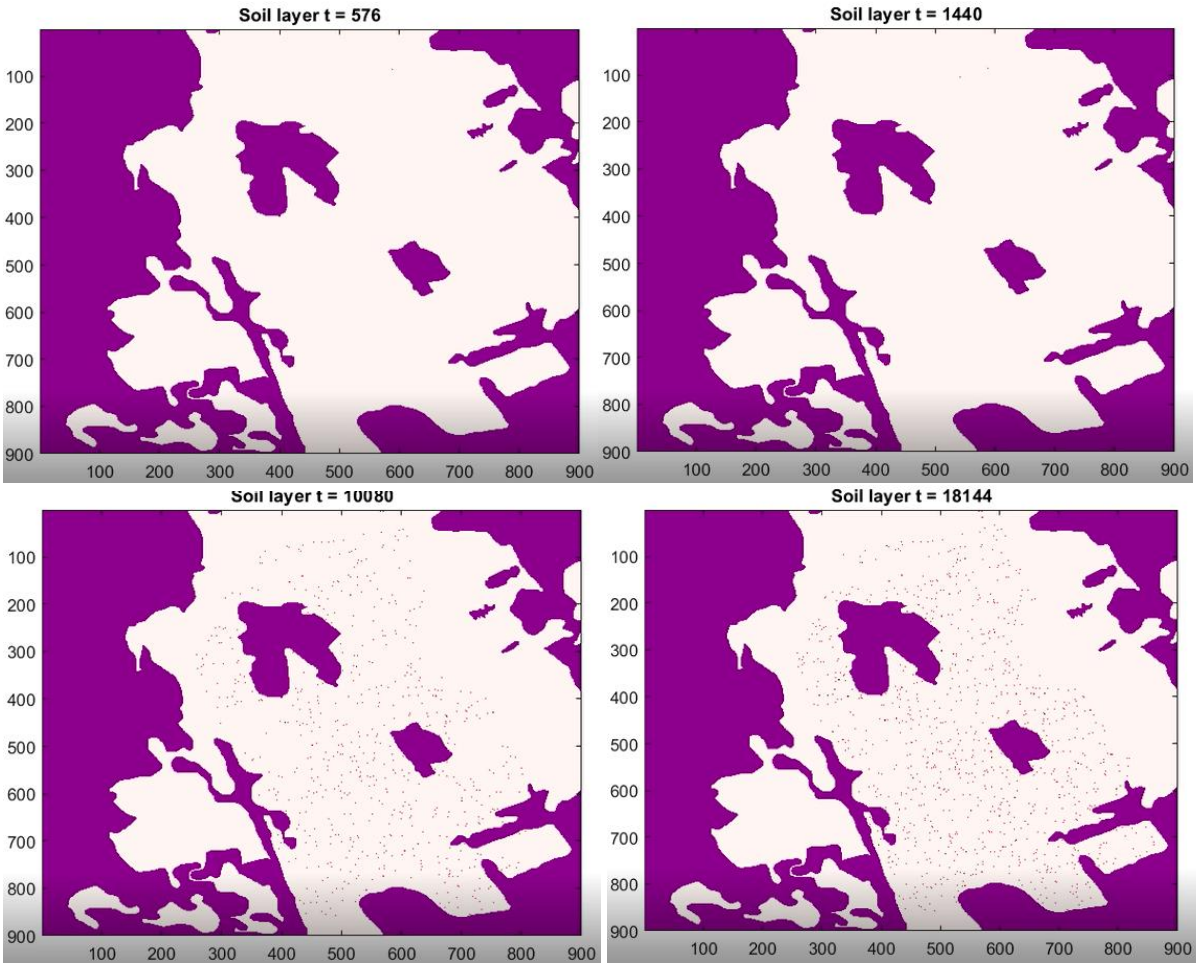

Image 78. Snapshots situation after time steps soil layer.

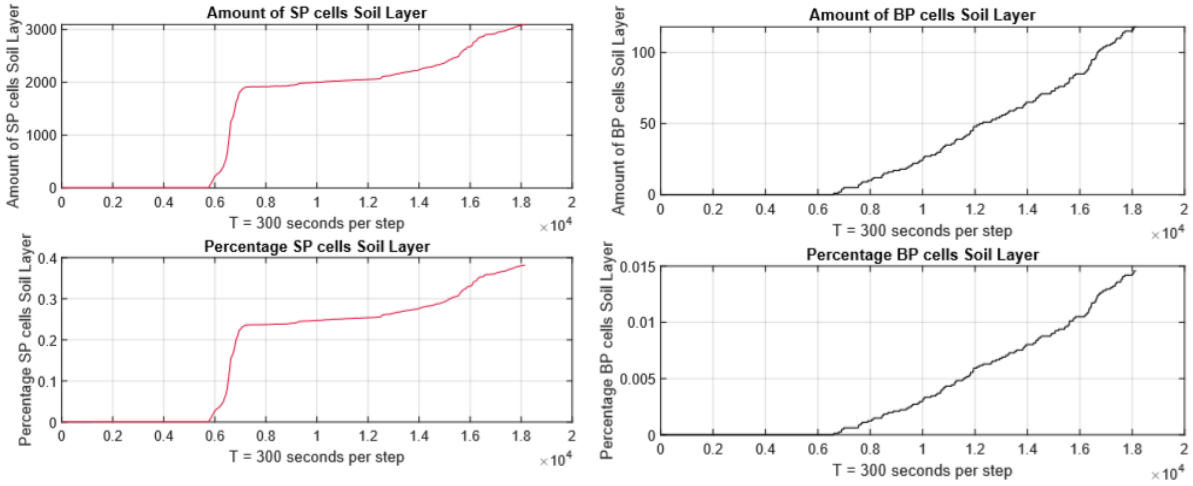

Image 79. Graphs cell states soil layer.

As can be seen in the snapshot the initial burning phase does not result in much smoldering peat, the patches are also to small to be seen in the first two snapshots presented in image 78. However, rekindling resulting from one of these smoledring peat cells rekindles the surface vegetation and results into a extreme fire phase. After this phase the smoldering peat cells can be seen easily and the amount grows over time as can be seen in the results presented in image 79. Furthermore, the amount of burned peat cells increases after this extreme flaming period. The tables with the diagnostic information are presented below in images. 80 and 81. From this table we can conclude that the smoldering combustion persisted during the first 20 days of the wildfire event and that rekindling is at the base of the extreme front fire spread period around day 23.

	Day	#EP	%EP	Δ#EP	#SP	%SP	Δ#SP	#BP	%BP	Δ#BP
1	0	488199	0	0	0	0	0	0	0	0
2	1	488192	60.2706	-6	7	8.6420e-04	7	0	0	0
3	2	488192	60.2706	0	7	8.6420e-04	0	0	0	0
4	3	488192	60.2706	0	7	8.6420e-04	0	0	0	0
5	4	488191	60.2705	-1	8	9.8765e-04	1	0	0	0
6	5	488190	60.2704	-1	9	0.0011	1	0	0	0
7	6	488190	60.2704	0	9	0.0011	0	0	0	0
8	7	488190	60.2704	0	9	0.0011	0	0	0	0
9	8	488190	60.2704	0	9	0.0011	0	0	0	0
10	9	488190	60.2704	0	9	0.0011	0	0	0	0
11	10	488190	60.2704	0	9	0.0011	0	0	0	0
12	11	488190	60.2704	0	9	0.0011	0	0	0	0
13	12	488190	60.2704	0	9	0.0011	0	0	0	0
14	13	488190	60.2704	0	9	0.0011	0	0	0	0
15	14	488190	60.2704	0	9	0.0011	0	0	0	0
16	15	488190	60.2704	0	9	0.0011	0	0	0	0
17	16	488190	60.2704	0	9	0.0011	0	0	0	0
18	17	488190	60.2704	0	9	0.0011	0	0	0	0
19	18	488190	60.2704	0	9	0.0011	0	0	0	0
20	19	488190	60.2704	0	9	0.0011	0	0	0	0
21	20	488185	60.2698	-5	14	0.0017	5	0	0	0
22	21	487958	60.2417	-227	241	0.0298	227	0	0	0
23	22	487799	60.2221	-159	400	0.0494	159	0	0	0
24	23	486952	60.1175	-847	1246	0.1538	846	1	1.2346e-04	1
25	24	486471	60.0581	-481	1725	0.2130	479	3	3.7037e-04	2
26	25	486283	60.0349	-188	1911	0.2359	186	5	6.1728e-04	2
27	26	486276	60.0341	-7	1918	0.2368	7	5	6.1728e-04	0
28	27	486274	60.0338	-2	1916	0.2365	-2	9	0.0011	4
29	28	486268	60.0331	-6	1920	0.2370	4	11	0.0014	2
30	29	486259	60.0320	-9	1928	0.2380	8	12	0.0015	1
31	30	486254	60.0314	-5	1930	0.2383	2	15	0.0019	3
32	31	486241	60.0298	-13	1941	0.2396	11	17	0.0021	2
33	32	486221	60.0273	-20	1960	0.2420	19	18	0.0022	1
34	33	486190	60.0235	-31	1989	0.2456	29	20	0.0025	2
35	34	486181	60.0223	-9	1996	0.2464	7	22	0.0027	2
36	35	486171	60.0211	-10	2001	0.2470	5	27	0.0033	5

Image 80. Cell state diagnostic soil layer first 35 days.

	Day	#EP	%EP	Δ#EP	#SP	%SP	Δ#SP	#BP	%BP	Δ#BP
1	36	486156	60.0193	-15	2015	0.2488	14	28	0.0035	1
2	37	486144	60.0178	-12	2025	0.2500	10	30	0.0037	2
3	38	486136	60.0168	-8	2028	0.2504	3	35	0.0043	5
4	39	486124	60.0153	-12	2037	0.2515	9	38	0.0047	3
5	40	486112	60.0138	-12	2048	0.2528	11	39	0.0048	1
6	41	486107	60.0132	-5	2049	0.2530	1	43	0.0053	4
7	42	486093	60.0115	-14	2057	0.2540	8	49	0.0060	6
8	43	486083	60.0102	-10	2065	0.2549	8	51	0.0063	2
9	44	486027	60.0033	-56	2119	0.2616	54	53	0.0065	2
10	45	486005	60.0006	-22	2139	0.2641	20	55	0.0068	2
11	46	485974	59.9968	-31	2168	0.2677	29	57	0.0070	2
12	47	485943	59.9930	-31	2196	0.2711	28	60	0.0074	3
13	48	485916	59.9896	-27	2222	0.2743	26	61	0.0075	1
14	49	485878	59.9849	-38	2256	0.2785	34	65	0.0080	4
15	50	485845	59.9809	-33	2286	0.2822	30	68	0.0084	3
16	51	485801	59.9754	-44	2327	0.2873	41	71	0.0088	3
17	52	485764	59.9709	-37	2362	0.2916	35	73	0.0090	2
18	53	485686	59.9612	-78	2437	0.3009	75	76	0.0094	3
19	54	485625	59.9537	-61	2495	0.3080	58	79	0.0098	3
20	55	485479	59.9357	-146	2635	0.3253	140	85	0.0105	6
21	56	485364	59.9215	-115	2750	0.3395	115	85	0.0105	0
22	57	485248	59.9072	-116	2859	0.3530	109	92	0.0114	7
23	58	485191	59.9001	-57	2908	0.3590	49	100	0.0123	8
24	59	485170	59.8975	-21	2925	0.3611	17	104	0.0128	4
25	60	485126	59.8921	-44	2966	0.3662	41	107	0.0132	3
26	61	485075	59.8858	-51	3013	0.3720	47	111	0.0137	4
27	62	485024	59.8795	-51	3060	0.3778	47	115	0.0142	4
28	63	484987	59.8749	-37	3094	0.3820	34	118	0.0146	3

Image 81. Cell state diagnostics soil layer days 36-63.

In accordance with the work of Purnomo et al. (2020), results for φ_b for each day will be presented below. Moreover to give a slightly more detailed insight into those results a graph is included that considers φ_b over time. From the results presented in images 82 and 83 it can be concluded that the percentage of affected peat cells by the wildfire remains low. Furthermore, only after the extreme wildfire phase, a sharp increase in affected peat can be observed.

	Day	#SP&BP	Δ#SP&BP	φb	Δφb
1	0	0	0	0	0
2	1	7	7	8.6420e-04	8.6420e-04
3	2	7	0	8.6420e-04	0
4	3	7	0	8.6420e-04	0
5	4	8	1	9.8765e-04	1.2346e-04
6	5	9	1	0.0011	1.2346e-04
7	6	9	0	0.0011	0
8	7	9	0	0.0011	0
9	8	9	0	0.0011	0
10	9	9	0	0.0011	0
11	10	9	0	0.0011	0
12	11	9	0	0.0011	0
13	12	9	0	0.0011	0
14	13	9	0	0.0011	0
15	14	9	0	0.0011	0
16	15	9	0	0.0011	0
17	16	9	0	0.0011	0
18	17	9	0	0.0011	0
19	18	9	0	0.0011	0
20	19	9	0	0.0011	0
21	20	14	5	0.0017	6.1728e-04
22	21	241	227	0.0298	0.0280
23	22	400	159	0.0494	0.0196
24	23	1247	847	0.1540	0.1046
25	24	1728	481	0.2133	0.0594
26	25	1916	188	0.2365	0.0232
27	26	1923	7	0.2374	8.6420e-04
28	27	1925	2	0.2377	2.4691e-04
29	28	1931	6	0.2384	7.4074e-04
30	29	1940	9	0.2395	0.0011
31	30	1945	5	0.2401	6.1728e-04
32	31	1958	13	0.2417	0.0016
33	32	1978	20	0.2442	0.0025
34	33	2009	31	0.2480	0.0038
35	34	2018	9	0.2491	0.0011
36	35	2028	10	0.2504	0.0012

	Day	#SP&BP	Δ#SP&BP	φb	Δφb
1	36	2043	15	0.2522	0.0019
2	37	2055	12	0.2537	0.0015
3	38	2063	8	0.2547	9.8765e-04
4	39	2075	12	0.2562	0.0015
5	40	2087	12	0.2577	0.0015
6	41	2092	5	0.2583	6.1728e-04
7	42	2106	14	0.2600	0.0017
8	43	2116	10	0.2612	0.0012
9	44	2172	56	0.2681	0.0069
10	45	2194	22	0.2709	0.0027
11	46	2225	31	0.2747	0.0038
12	47	2256	31	0.2785	0.0038
13	48	2283	27	0.2819	0.0033
14	49	2321	38	0.2865	0.0047
15	50	2354	33	0.2906	0.0041
16	51	2398	44	0.2960	0.0054
17	52	2435	37	0.3006	0.0046
18	53	2513	78	0.3102	0.0096
19	54	2574	61	0.3178	0.0075
20	55	2720	146	0.3358	0.0180
21	56	2835	115	0.3500	0.0142
22	57	2951	116	0.3643	0.0143
23	58	3008	57	0.3714	0.0070
24	59	3029	21	0.3740	0.0026
25	60	3073	44	0.3794	0.0054
26	61	3124	51	0.3857	0.0063
27	62	3175	51	0.3920	0.0063
28	63	3212	37	0.3965	0.0046

Image 82. Tables φ_b.

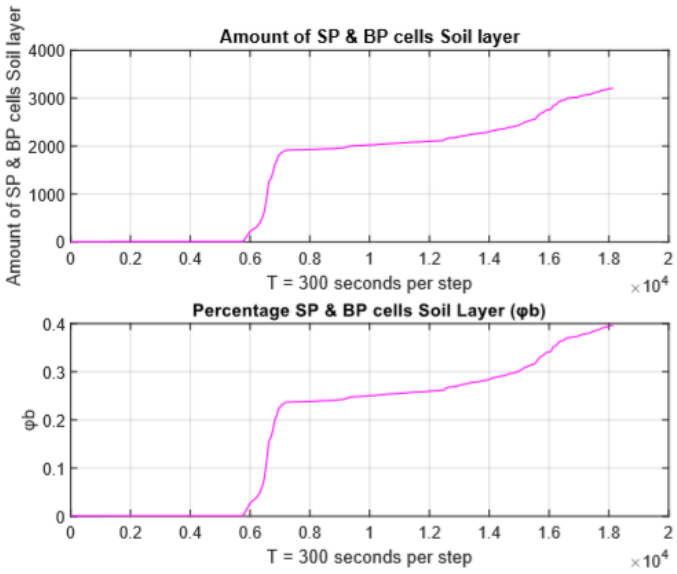

Image 83. Graphs φ_b over time.

Considering findings of the specialized team for wildfire research of the Dutch national fire department another hypothesis was tested. The specialized team concluded that no definite origin of the fire could be distinguished from their field research. They did however find a piece of glass but its angle towards the sun was not sufficient to start a flaming fire front (Brandweer, 2020). Based on the findings of Santoso et al. (2019) a hypothesis was formed that the piece of glass did indeed not start the flaming fire front but started smoldering combustion in the soil layer, a form of combustion that needs less energy and heat to ignite. Results for the top layer are presented below in images 84 untill 87.

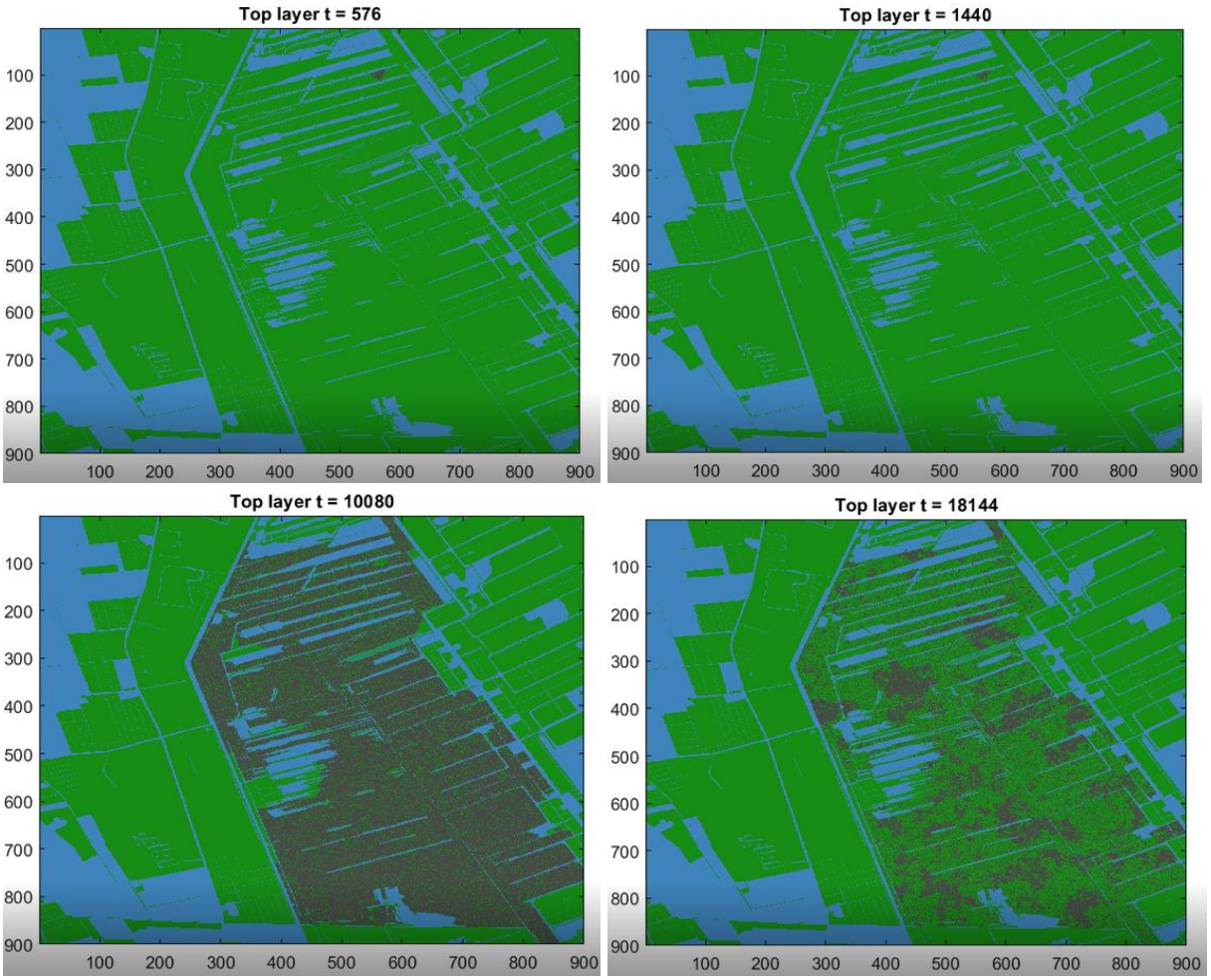

Image 84. Snapshots situation after time steps top layer.

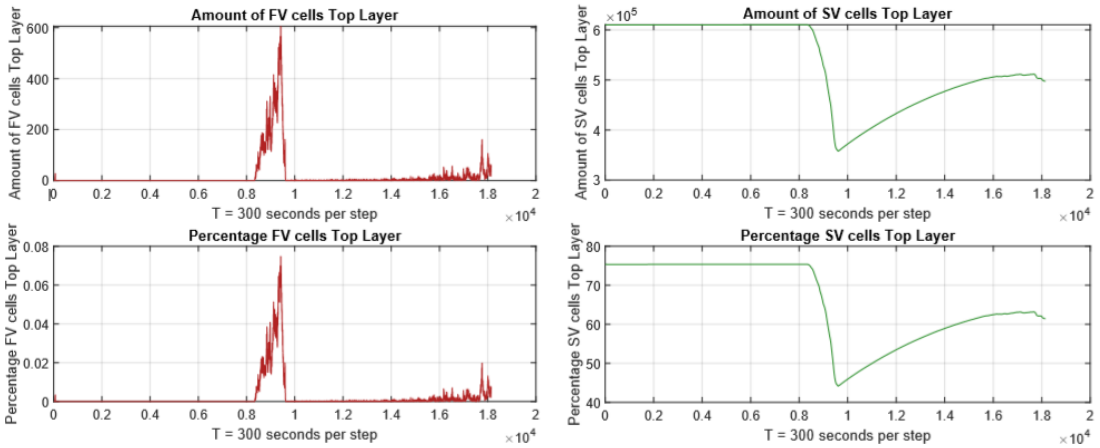

Image 85. Graphs cell states top layer.

	Day	#FV	%FV	Δ#FV	#SV	%SV	Δ#SV	#EP	%EP	Δ#EP
1	0	0	0	0	610395	0	0	0	0	0
2	1	0	0	0	610089	75.3196	610089	306	0.0378	306
3	2	0	0	0	610102	75.3212	13	293	0.0362	-13
4	3	0	0	0	610114	75.3227	12	281	0.0347	-12
5	4	0	0	0	610128	75.3244	14	267	0.0330	-14
6	5	0	0	0	610147	75.3268	19	248	0.0306	-19
7	6	0	0	0	610160	75.3284	13	235	0.0290	-13
8	7	0	0	0	610169	75.3295	9	226	0.0279	-9
9	8	0	0	0	610179	75.3307	10	216	0.0267	-10
10	9	0	0	0	610186	75.3316	7	209	0.0258	-7
11	10	0	0	0	610196	75.3328	10	199	0.0246	-10
12	11	0	0	0	610201	75.3335	5	194	0.0240	-5
13	12	0	0	0	610206	75.3341	5	189	0.0233	-5
14	13	0	0	0	610212	75.3348	6	183	0.0226	-6
15	14	0	0	0	610218	75.3356	6	177	0.0219	-6
16	15	0	0	0	610222	75.3360	4	173	0.0214	-4
17	16	0	0	0	610227	75.3367	5	168	0.0207	-5
18	17	0	0	0	610232	75.3373	5	163	0.0201	-5
19	18	0	0	0	610242	75.3385	10	153	0.0189	-10
20	19	0	0	0	610251	75.3396	9	144	0.0178	-9
21	20	0	0	0	610253	75.3399	2	142	0.0175	-2
22	21	0	0	0	610257	75.3404	4	138	0.0170	-4
23	22	0	0	0	610262	75.3410	5	133	0.0164	-5
24	23	0	0	0	610273	75.3423	11	122	0.0151	-11
25	24	0	0	0	610275	75.3426	2	120	0.0148	-2
26	25	0	0	0	610277	75.3428	2	118	0.0146	-2
27	26	0	0	0	610286	75.3440	9	109	0.0135	-9
28	27	0	0	0	610291	75.3446	5	104	0.0128	-5
29	28	0	0	0	610296	75.3452	5	99	0.0122	-5
30	29	14	0.0017	14	610226	75.3365	-70	155	0.0191	56
31	30	136	0.0168	122	588650	72.6728	-21576	21609	2.6678	21454
32	31	248	0.0306	112	543415	67.0883	-45235	66732	8.2385	45123
33	32	311	0.0384	63	473674	58.4783	-69741	136410	16.8407	69678
34	33	231	0.0285	-80	365978	45.1825	-107696	244186	30.1464	107776
35	34	0	0	-231	364609	45.0135	-1369	245786	30.3440	1600
36	35	0	0	0	374976	46.2933	10367	235419	29.0641	-10367

Image 86. Cell state diagnostic soil layer first 35 days.

	Day	#FV	%FV	Δ#FV	#SV	%SV	Δ#SV	#EP	%EP	Δ#EP
1	36	0	0	0	384888	47.5170	9912	225507	27.8404	-9912
2	37	1	1.2346e-04	1	394323	48.6819	9435	216071	26.6754	-9436
3	38	0	0	-1	403070	49.7617	8747	207325	25.5957	-8746
4	39	0	0	0	411782	50.8373	8712	198613	24.5201	-8712
5	40	0	0	0	420051	51.8581	8269	190344	23.4993	-8269
6	41	0	0	0	427968	52.8356	7917	182427	22.5219	-7917
7	42	0	0	0	435626	53.7810	7658	174769	21.5764	-7658
8	43	0	0	0	442835	54.6710	7209	167560	20.6864	-7209
9	44	1	1.2346e-04	1	449676	55.5156	6841	160718	19.8417	-6842
10	45	0	0	-1	456201	56.3211	6525	154194	19.0363	-6524
11	46	0	0	0	462443	57.0917	6242	147952	18.2657	-6242
12	47	0	0	0	468498	57.8393	6055	141897	17.5181	-6055
13	48	4	4.9383e-04	4	474069	58.5270	5571	136322	16.8299	-5575
14	49	5	6.1728e-04	1	479442	59.1904	5373	130948	16.1664	-5374
15	50	1	1.2346e-04	-4	484541	59.8199	5099	125853	15.5374	-5095
16	51	2	2.4691e-04	1	489213	60.3967	4672	121180	14.9605	-4673
17	52	3	3.7037e-04	1	493604	60.9388	4391	116788	14.4183	-4392
18	53	2	2.4691e-04	-1	497710	61.4457	4106	112683	13.9115	-4105
19	54	0	0	-2	501832	61.9546	4122	108563	13.4028	-4120
20	55	7	8.6420e-04	7	504311	62.2606	2479	106077	13.0959	-2486
21	56	3	3.7037e-04	-4	507074	62.6017	2763	103318	12.7553	-2759
22	57	9	0.0011	6	507502	62.6546	428	102884	12.7017	-434
23	58	7	8.6420e-04	-2	508606	62.7909	1104	101782	12.5657	-1102
24	59	34	0.0042	27	510872	63.0706	2266	99489	12.2826	-2293
25	60	12	0.0015	-22	509476	62.8983	-1396	100907	12.4577	1418
26	61	21	0.0026	9	511328	63.1269	1852	99046	12.2279	-1861
27	62	25	0.0031	4	503225	62.1265	-8103	107145	13.2278	8099
28	63	54	0.0067	29	497110	61.3716	-6115	113231	13.9791	6086

Image 87. Cell state diagnostic soil layer first 35 days.

Similar to the results of the FENIX output where the ignition point was set to be at the top layer, three periods can be distinguished from the results as presented in image 85. The first period only affects a small portion of the study area but results in some, minor, smoldering area the extent of this initial phase can be seen in image 84. A second period of extreme flaming wildfire progression follows, this time slightly later in the period t=8000-10000. The third period shows the effects of reignition between the soil and top layer. From the tables presented in images 86 and 87 it can be derrived that the extreme flaming fire progression period happened around day 30. Below the comparion with the actual extent of the wildfire as defined by EFFIS is made again.

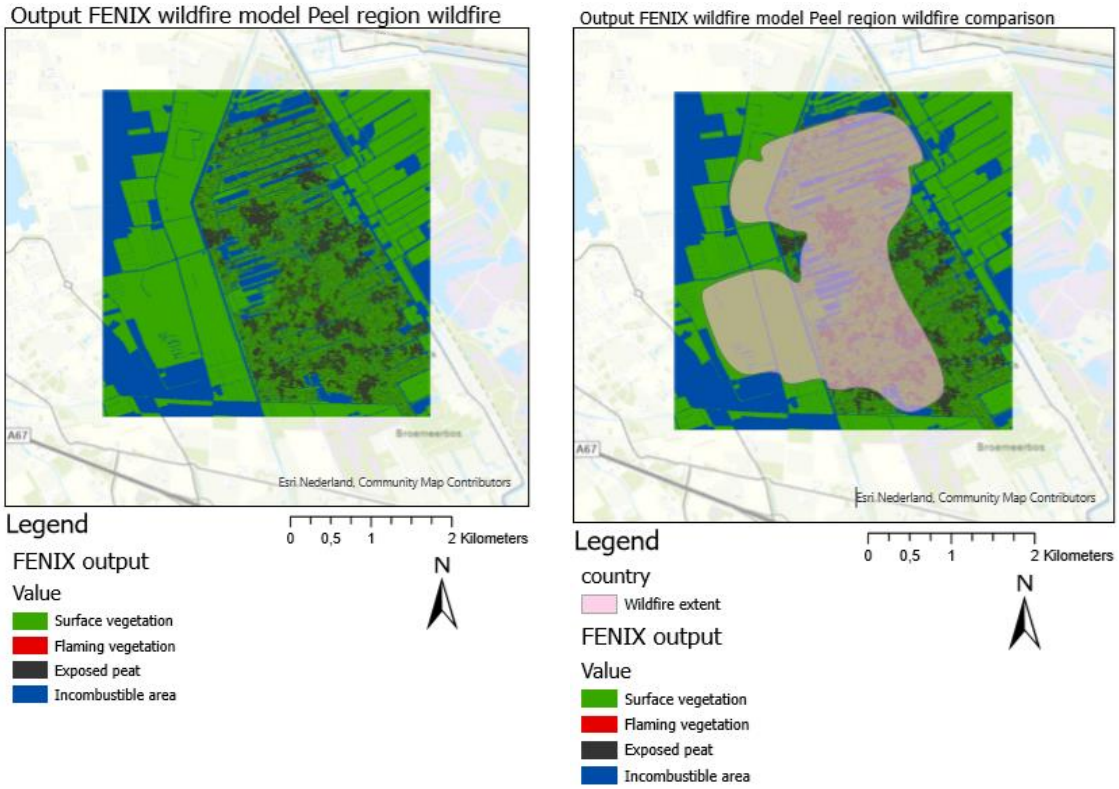

Image 88. Comparison FENIX output and wildfire extent.

Again considering the comparison as presented in image 88 it can be seen that the output of the FENIX framework does not incorporate the flaming fire fronts at the west side of the canal. This issue will be addressed later in the discussion chapter of this thesis. In line with the first prediction the extent of the wildfire as predicted by the FENIX framework does not differ significantly with respect to its final outcome. The same more eastward spread can be seen, the only significant different is the period of extreme flaming front formation. Below the results of the soil layer will be presented in images 89 until 94.

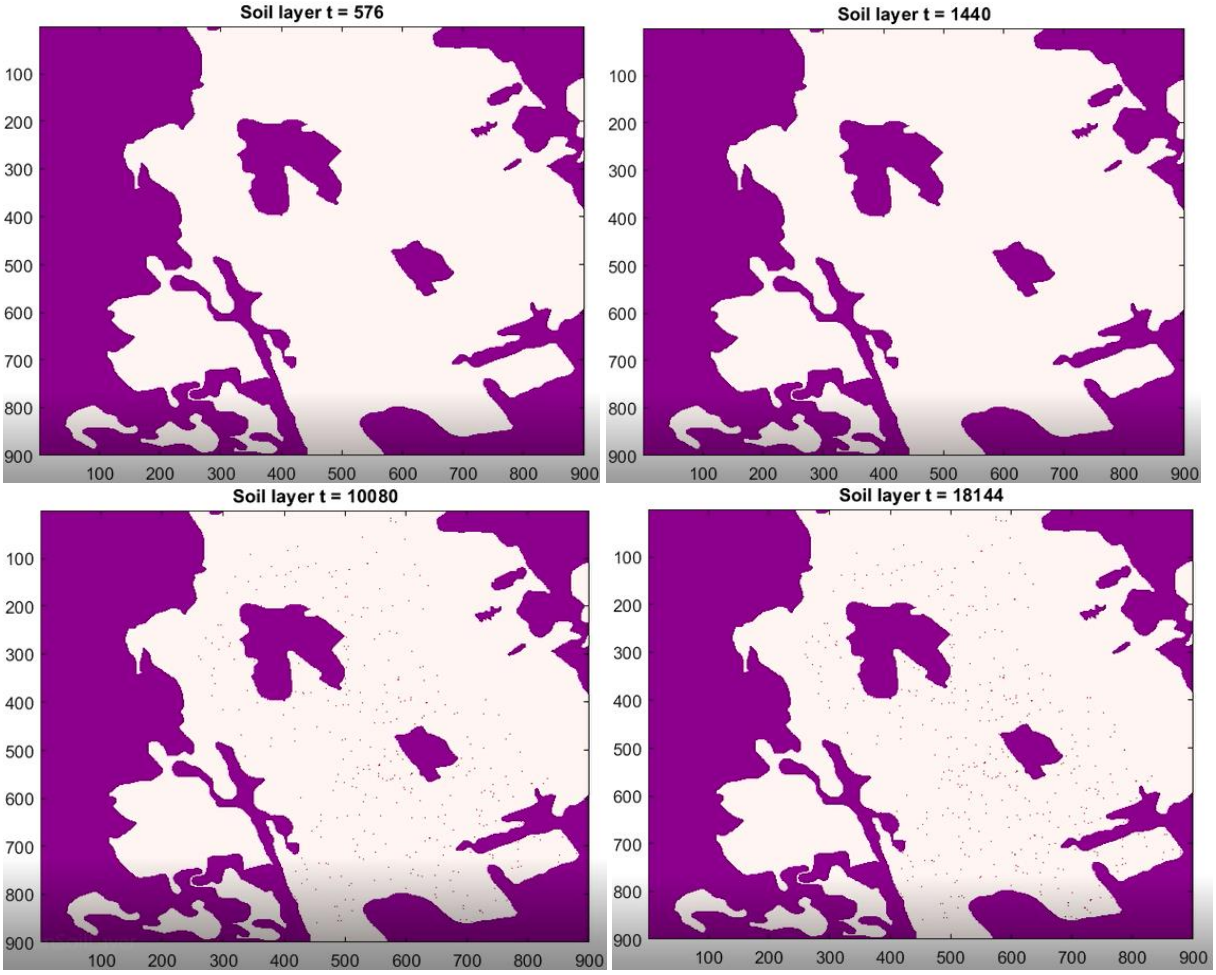

Image 89. Snapshots situation after time steps soil layer.

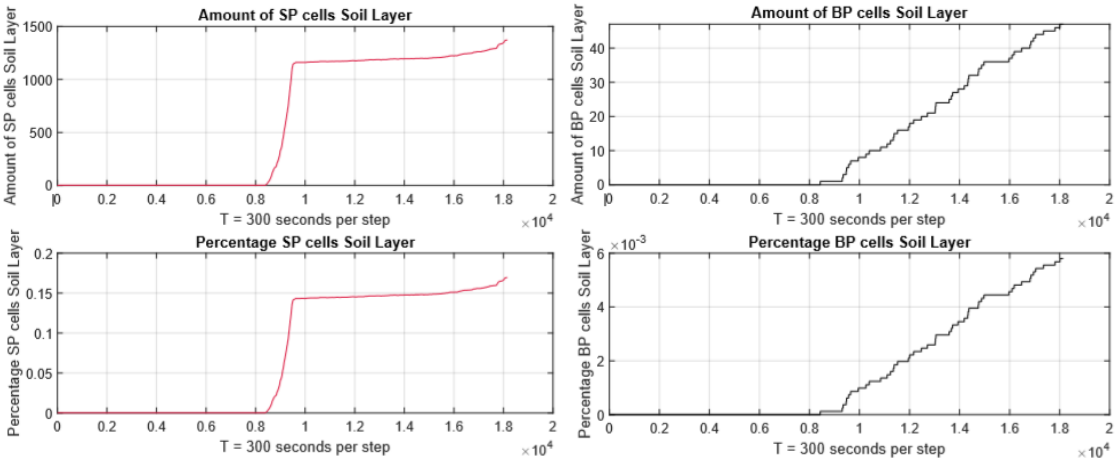

Image 90. Graphs cell states soil layer.

As can be seen in the snapshot the results as presented in image 89 between the predictions are similar. The initial burning phase does not result in much smoldering peat, the patches are also to small to be seen in the first two snapshots. However rekindling resulting from one of these smoledring peat cells rekindles the surface vegetation and results into a extreme fire phase.

After this phase the smoldering peat cells can be seen easily and the amount grows over time as can be seen in image 90. Furthermore, the amount of burned peat cells increases after this extreme flaming period. The tables with the diagnostic information are presented below in images 91 and 92.

	Day	#EP	%EP	Δ#EP	#SP	%SP	Δ#SP	#BP	%BP	Δ#BP
1	0	488198	0	0	1	0	0	0	0	0
2	1	488197	60.2712	-1	2	2.4691e-04	2	0	0	0
3	2	488197	60.2712	0	2	2.4691e-04	0	0	0	0
4	3	488197	60.2712	0	2	2.4691e-04	0	0	0	0
5	4	488197	60.2712	0	2	2.4691e-04	0	0	0	0
6	5	488197	60.2712	0	2	2.4691e-04	0	0	0	0
7	6	488197	60.2712	0	2	2.4691e-04	0	0	0	0
8	7	488197	60.2712	0	2	2.4691e-04	0	0	0	0
9	8	488197	60.2712	0	2	2.4691e-04	0	0	0	0
10	9	488197	60.2712	0	2	2.4691e-04	0	0	0	0
11	10	488197	60.2712	0	2	2.4691e-04	0	0	0	0
12	11	488197	60.2712	0	2	2.4691e-04	0	0	0	0
13	12	488197	60.2712	0	2	2.4691e-04	0	0	0	0
14	13	488197	60.2712	0	2	2.4691e-04	0	0	0	0
15	14	488197	60.2712	0	2	2.4691e-04	0	0	0	0
16	15	488197	60.2712	0	2	2.4691e-04	0	0	0	0
17	16	488197	60.2712	0	2	2.4691e-04	0	0	0	0
18	17	488197	60.2712	0	2	2.4691e-04	0	0	0	0
19	18	488197	60.2712	0	2	2.4691e-04	0	0	0	0
20	19	488197	60.2712	0	2	2.4691e-04	0	0	0	0
21	20	488197	60.2712	0	2	2.4691e-04	0	0	0	0
22	21	488197	60.2712	0	2	2.4691e-04	0	0	0	0
23	22	488197	60.2712	0	2	2.4691e-04	0	0	0	0
24	23	488197	60.2712	0	2	2.4691e-04	0	0	0	0
25	24	488197	60.2712	0	2	2.4691e-04	0	0	0	0
26	25	488197	60.2712	0	2	2.4691e-04	0	0	0	0
27	26	488197	60.2712	0	2	2.4691e-04	0	0	0	0
28	27	488197	60.2712	0	2	2.4691e-04	0	0	0	0
29	28	488197	60.2712	0	2	2.4691e-04	0	0	0	0
30	29	488197	60.2712	0	2	2.4691e-04	0	0	0	0
31	30	488109	60.2604	-88	89	0.0110	87	1	1.2346e-04	1
32	31	487947	60.2404	-162	251	0.0310	162	1	1.2346e-04	0
33	32	487600	60.1975	-347	598	0.0738	347	1	1.2346e-04	0
34	33	487055	60.1302	-545	1139	0.1406	541	5	6.1728e-04	4
35	34	487032	60.1274	-23	1160	0.1432	21	7	8.6420e-04	2
36	35	487028	60.1269	-4	1163	0.1436	3	8	9.8765e-04	1

Image 91. Cell state diagnostic soil layer first 35 days.

	Day	#EP	%EP	Δ#EP	#SP	%SP	Δ#SP	#BP	%BP	Δ#BP
1	36	487024	60.1264	-4	1166	0.1440	3	9	0.0011	1
2	37	487019	60.1258	-5	1170	0.1444	4	10	0.0012	1
3	38	487019	60.1258	0	1169	0.1443	-1	11	0.0014	1
4	39	487016	60.1254	-3	1171	0.1446	2	12	0.0015	1
5	40	487011	60.1248	-5	1173	0.1448	2	15	0.0019	3
6	41	487007	60.1243	-4	1176	0.1452	3	16	0.0020	1
7	42	487004	60.1240	-3	1177	0.1453	1	18	0.0022	2
8	43	487001	60.1236	-3	1179	0.1456	2	19	0.0023	1
9	44	486993	60.1226	-8	1186	0.1464	7	20	0.0025	1
10	45	486991	60.1223	-2	1187	0.1465	1	21	0.0026	1
11	46	486987	60.1219	-4	1188	0.1467	1	24	0.0030	3
12	47	486982	60.1212	-5	1193	0.1473	5	24	0.0030	0
13	48	486977	60.1206	-5	1195	0.1475	2	27	0.0033	3
14	49	486975	60.1204	-2	1196	0.1477	1	28	0.0035	1
15	50	486971	60.1199	-4	1196	0.1477	0	32	0.0040	4
16	51	486967	60.1194	-4	1200	0.1481	4	32	0.0040	0
17	52	486964	60.1190	-3	1199	0.1480	-1	36	0.0044	4
18	53	486958	60.1183	-6	1205	0.1488	6	36	0.0044	0
19	54	486953	60.1177	-5	1210	0.1494	5	36	0.0044	0
20	55	486940	60.1160	-13	1223	0.1510	13	36	0.0044	0
21	56	486937	60.1157	-3	1224	0.1511	1	38	0.0047	2
22	57	486918	60.1133	-19	1242	0.1533	18	39	0.0048	1
23	58	486911	60.1125	-7	1248	0.1541	6	40	0.0049	1
24	59	486895	60.1105	-16	1261	0.1557	13	43	0.0053	3
25	60	486883	60.1090	-12	1272	0.1570	11	44	0.0054	1
26	61	486866	60.1069	-17	1288	0.1590	16	45	0.0056	1
27	62	486820	60.1012	-46	1333	0.1646	45	46	0.0057	1
28	63	486779	60.0962	-41	1373	0.1695	40	47	0.0058	1

Image 92. Cell state diagnostic soil layer first 35 days.

In accordance with the work of Purnomo et al. (2020), results for φ_b for each day will be presented below in image 93. Moreover to give a slightly more detailed insight into those results a graph is included that considers φ_b over time. This graph is presented in image 94.

From the results as presented in images 93 and 94 it can be concluded that the percentage of affected peat cells by the wildfire remains low. Furthermore, only after the extreme wildfire phase, a sharp increase in affected peat can be observed

Before drawing conclusions based on the presented results the next chapter will first present an informed discussion about the thesis itself. In this discussion possible avenues of further research will be distinguished and a thorough reflection on the FENIX framework will be presented.

	Day	#SP&BP	Δ#SP&BP	φb	Δφb
1	0	0	0	0	0
2	1	2	2	2.4691e-04	2.4691e-04
3	2	2	0	2.4691e-04	0
4	3	2	0	2.4691e-04	0
5	4	2	0	2.4691e-04	0
6	5	2	0	2.4691e-04	0
7	6	2	0	2.4691e-04	0
8	7	2	0	2.4691e-04	0
9	8	2	0	2.4691e-04	0
10	9	2	0	2.4691e-04	0
11	10	2	0	2.4691e-04	0
12	11	2	0	2.4691e-04	0
13	12	2	0	2.4691e-04	0
14	13	2	0	2.4691e-04	0
15	14	2	0	2.4691e-04	0
16	15	2	0	2.4691e-04	0
17	16	2	0	2.4691e-04	0
18	17	2	0	2.4691e-04	0
19	18	2	0	2.4691e-04	0
20	19	2	0	2.4691e-04	0
21	20	2	0	2.4691e-04	0
22	21	2	0	2.4691e-04	0
23	22	2	0	2.4691e-04	0
24	23	2	0	2.4691e-04	0
25	24	2	0	2.4691e-04	0
26	25	2	0	2.4691e-04	0
27	26	2	0	2.4691e-04	0
28	27	2	0	2.4691e-04	0
29	28	2	0	2.4691e-04	0
30	29	2	0	2.4691e-04	0
31	30	90	88	0.0111	0.0109
32	31	252	162	0.0311	0.0200
33	32	599	347	0.0740	0.0428
34	33	1144	545	0.1412	0.0673
35	34	1167	23	0.1441	0.0028
36	35	1171	4	0.1446	4.9383e-04

	Day	#SP&BP	Δ#SP&BP	φb	Δφb
1	36	1175	4	0.1451	4.9383e-04
2	37	1180	5	0.1457	6.1728e-04
3	38	1180	0	0.1457	0
4	39	1183	3	0.1460	3.7037e-04
5	40	1188	5	0.1467	6.1728e-04
6	41	1192	4	0.1472	4.9383e-04
7	42	1195	3	0.1475	3.7037e-04
8	43	1198	3	0.1479	3.7037e-04
9	44	1206	8	0.1489	9.8765e-04
10	45	1208	2	0.1491	2.4691e-04
11	46	1212	4	0.1496	4.9383e-04
12	47	1217	5	0.1502	6.1728e-04
13	48	1222	5	0.1509	6.1728e-04
14	49	1224	2	0.1511	2.4691e-04
15	50	1228	4	0.1516	4.9383e-04
16	51	1232	4	0.1521	4.9383e-04
17	52	1235	3	0.1525	3.7037e-04
18	53	1241	6	0.1532	7.4074e-04
19	54	1246	5	0.1538	6.1728e-04
20	55	1259	13	0.1554	0.0016
21	56	1262	3	0.1558	3.7037e-04
22	57	1281	19	0.1581	0.0023
23	58	1288	7	0.1590	8.6420e-04
24	59	1304	16	0.1610	0.0020
25	60	1316	12	0.1625	0.0015
26	61	1333	17	0.1646	0.0021
27	62	1379	46	0.1702	0.0057
28	63	1420	41	0.1753	0.0051

Image 93. Tables φ_b.

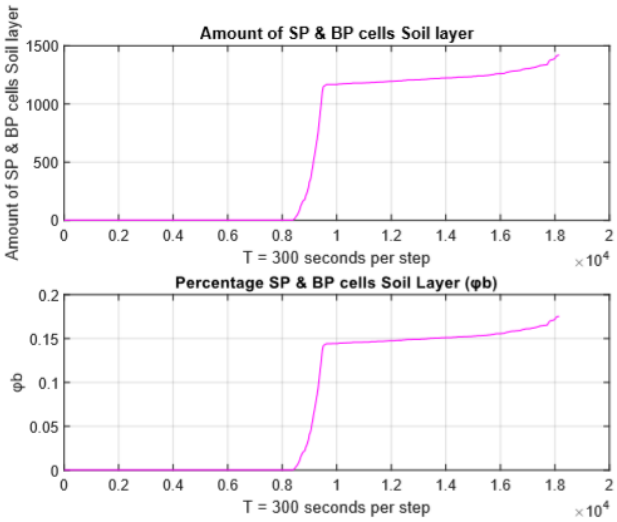

Image 94. Graphs φ_b over time.

§9. Discussion

This thesis set out to end the mosaic like division of knowledge about wildfires that was found in contemporary academic literature. While many topics in fire science and modelling theory were combined with one another, a vast majority of relevant knowledge about wildfire phenomena remain untouched. Topics including but not limited to, the role of hydrology and biology remain mostly unaddressed in this work. From the literature, it is known that these very important fields of knowledge play a crucial role in how wildfires behave, especially when focusing on wildfires situated on organic soil layers such as peat.

Furthermore, a crucial omission in this work are the effects that result from wildfires. The influence of wildfires on the emission of greenhouse gasses is named but not researched in depth. However, it was found that continuously smoldering wildfires can add a vast share to the annual worldwide emissions of greenhouse gasses. Therefore understanding wildfires and how these phenomena interplay with emissions is of crucial importance in the contemporary struggle to limit the emission of these greenhouse gasses annually. The role wildfire phenomena play in endangering the urban-nature interface was not addressed. However, in the literature it was found that wildfires play an active role in endangering not only flora and fauna but also directly humankind. Next to the immediate threat of death, smoke produced by these wildfires forms a danger to traffic, and can influence air quality over large areas (Burgess et al., 2020; Stoof et al., 2020). Furthermore, wildfires heavily affect the mental health of nearby inhabitants under pressure of possible loss of homes, businesses, places with emotional value and sudden evacuations (Taufik et al., 2019). Finding ways to better predict how wildfire complexes will behave will help to limit all of these severe dangers to the world around us.

The data that was used for the application of the FENIX wildfire model framework proved to be of high quality. However, to make the data applicable in the framework vast simplifications had to be made. This severely influenced the predictions of the framework. This fact is, as stated, not due to limiting factors of the underlying datasets but due to limiting factors of the framework. A further development of the framework to incorporate more flaming fire spread probabilities for different types of vegetation is necessary to improve the framework. Furthermore, it should be emphasized that data collection for wildfire is up to this point still in its infancy in the Netherlands. More aspects of wildfire phenomenon should be considered to be collected (Appendix A). At the very least, data collection should incorporate the spatial extent of the wildfire events and the deployment of firefighting material. Struggles with issues concerning privacy should be reconsidered to facilitate this registration and the automated coupling with emergency room systems and the newly created wildfire registration should be completed.

It should be stated that the Netherlands has a solid wildfire spread model (NBVM). This model is based on the vector approach as explained in chapter three of this thesis. In the future, it will be improved with more fuel models for different kinds of vegetation (Appendix B; Oswald et al., 2017). In relation to smoldering fires, this model will be computationally too expensive to run over the course of a long time period at the field scale. The FENIX framework as proposed in this work can be a starting point for a complementary wildfire spread model for the Dutch context. With the ability to run for longer time periods without the need for extensive computing power such a model can help in predicting the behavior of

wildfire events based on an organic soil layer. Furthermore, such a model can be used for educational purposes or to raise awareness for the impact of smoldering combustion in wildfire events.

With respect to the framework, it is important to note that multiple important aspects of wildfire spread remain unconsidered. The influence of elevation was omitted due to the relative flat character of the Peel region, however from accounts it was found that the combination between elevation and hydrology heavily impacted where smoldering combustion took place in the actual wildfire even of early 2020 (Stoof et al., 2020). Furthermore, the influence of spotting fires were not considered in the FENIX framework. The effects of this spread phenomenon proved very influential in the actual Peel region wildfire (Stoof et al., 2020). Based on the work of Alexandridis et al. (2004) it is possible to incorporate this spread phenomenon in a cellular automate based wildfire spread model such as the FENIX framework. Other limiting factors are the first order Moore neighborhood, while this neighborhood proves to facilitate the modelling of the identified framework it might be an improvement to incorporate a second order Moore neighborhood, this neighborhood considers the 5*5 grid around the central cell, to allow modelled flaming fire to spread over small obstacles such as ditches.

Considering the probabilities of transitions between cell states the probabilities for extinction (P_e), the probability of revegetation P_{veg} and the probability for reignition P_{rei} are to this moment still somewhat arbitrary values. Following probabilistic theory, it is assumable that probabilities can mimic the uncertainty of the events. However, slightly more specified formulas for the calculations of these probabilities must be considered to model the current understanding of wildfire spread phenomena.

For the probability of reignition, the work of Santoso et al. (2019) can be considered a starting point into the formulation of a formula that can incorporate influencing aspects for revegetation between certain smoldering soils and certain types of vegetation. However, to specify such a formula would require more research and data collection into this specific aspect of smoldering to flaming combustion transition.

For the probability of revegetation insights from literature show that the speed of revegetation can be increased due to the green flush effect (Greene et al., 2012). This green flux states that the increased availability of nutrients such as nitrogen speed up the growth process for certain vegetation types. Furthermore, a change of cell states between exposed peat and surface vegetation can be facilitated by leftover fuel that remains in a cell after the initial burning period (Stoof et al., 2020). Based on these findings a formula is formulated in order to incorporate these aspects with regards to revegetation. This formula is given below in equation 11.

$$P_{veg} = 1/(1+ e^{-(c5*L+c6*N)}) \quad \text{(eq. 11)}$$

In this formula c5 and c6 are constants that are to be defined. L indicates the amount of leftover fuel in cubic meters and N indicates the percentage of nitrogen in the air of a given cell. The way the formula is composed leaves P_{veg} with a sigmoid relationship with respect to the identified variables. A combined team of biologists and mechanical engineers should focus on the precise formulation of this formula based on empirical results and a broader theoretical understanding of the underlying processes. Moreover, it should be indicated that a

revegetated cell would not be likely to have the same burning characteristics as a surface vegetation cell as considered in the initial state of the model. A specified fire front propagation probability constant should be considered based on the work of Rothermel (1972).

Considering the definition of cellular automate modelling, the state of a model in one generation can only be a result of a previous generation (Inoue, 2005; Wolfram, 2002). However, the process of revegetation can be considered a process where the probability of change between cell states increases when more time for vegetation to regrow has passed. Incorporating an updating probability for revegetation for each time step a cell is in the state of exposed peat to mimic this time function would be against the definition of cellular automate modelling. However, cellular automate based models are often diversifying from the original definition. The incorporation of time has been successfully considered before in other cellular automate based models (Couclelis, 1997).

With regards to the probability of extinction it would be logically consistent with the probability of flaming to smoldering transition and smoldering spread probability to incorporate the influencing aspects of peat that govern these probabilities. These aspects are bulk density, percentage of inorganic content and the percentage of moisture content (Frandsen, 1997; Purnomo et al., 2020). A possible formulation based on the work of Frandsen (1997) could be the formula as presented below in equation 12.

$$P_e = 1/(1+ e^{-(c7*ash+c8*rho+c9*MC)}) \quad \text{(eq. 12)}$$

In this equation c7, c8 and c9 are constants that need to be determined. Ash indicates the percentage inorganic content, rho indicates the bulk density and MC indicates the percentage moisture content. The way the formula is composed leaves P_e with a sigmoid relationship with respect to the identified variables. Both the proposed formulas should be validated by extensive empirical research.

As stated many times before, wildfires prove to be a highly multidisciplinary phenomenon and therefore they should be addressed as such. This thesis tried to end the mosaic like distribution of knowledge from different fields and combine them in one work. This, as expected, proved to be infeasible and only the surface of fire science and modelling theory concerning wildfires was addressed. With this being said, it should be emphasized that the multidisciplinarity should be embraced. Studies, conferences and advisory boards concerning wildfires should consider to contain academics for a wide variety of fields. These fields can be biology, mechanical engineering, physics, hydrology, geography and math. Moreover, the social impact of wildfires should be considered more in future research.

Finally, it should be stated that fire is part of nature and that we should focus on understanding and management of the phenomenon rather than preventing the process to take place. Prescribed burnings when the peat layers have a high moisture content percentage can limit the extent of the wildfires (Davies et al., 2016; Purnomo et al., 2020). Furthermore, preparing the peatland areas in the way that they become more accessible might help with the success rate of initial response by the emergency services. Peatlands and their management can become a crucial phenomenon to manage and mitigate Climate Change since the areas prove to be a natural CO_2 sink (Rein, 2016; Wösten et al., 2020). Therefore, understanding the phenomenon of wildfires on organic soil is of crucial importance for our future.

§10. Conclusion

To answer the main research question of this thesis, first each sub-question will be answered. The basis for these answers lie in findings that were presented in previous chapters of this thesis. Below the main research question will be presented. Subsequently the answer to the sub-questions are addressed. Finally, the final answer to the main research question will be presented.

To what extend can a smoldering and flaming peatland based wildfire spread be simulated from the real world into a data driven cellular automate model?

Broken down into six sub-questions:

1. *What are the influencing variables and characteristics with relation to wildfire fire front progression in smoldering and flaming combustion?*

Considering the theory on fire science as presented in chapter two of this thesis multiple important characteristics concerning fire front progression can be identified. First of all, wildfires based on organic soils are characterized by two main forms of combustion. Smoldering combustion is combustion that happens in the organic soil. This form of combustion proves to be very persistent and can take place over extensive time periods. A second form of combustion for wildfires based on organic soils is flaming combustion. This form of combustion is more widely researched as opposed to smoldering combustion and takes place in the vegetation of an area affected by a wildfire event. Both combustion processes are result of the same underlying chemical process of pyrolysis. This shared base reaction allows for both types of combustion to transfer from one to the other. Meaning that a flaming combustion can transfer to a smoldering combustion and the other way around.

Fuel is the most important factor with regards to these forms of combustion. As stated, flaming combustion happens in the vegetation. The kind of vegetation defines how a flaming combustion process behaves and spreads. Furthermore, smoldering combustion happens in the organic soil. Characteristics of this soil, such as inorganic content, bulk density and moisture content play a key role in how the combustion behaves and spreads.

Meteorological conditions influence the way fire spreads. Most important is the influence of wind. Other meteorological conditions such as temperature and rain play a key role in the emergence and progression of a wildfire. Furthermore, topology influences the way a fire spreads. Slope governs fire spread speed and is addressed in chapter two of this thesis. Moreover, elevation plays a key role with regards to the hydrological characteristics of an area. Unfortunately, exploring this interplay between elevation and hydrology was out of scope in this thesis.

In lengthy wildfire phenomena, such as wildfires that take place in an area with organic soils, the perseverance of smoldering combustion can take such a long time that vegetation starts to grow back. This phenomenon of revegetation combined with leftover fuel from the initial flaming phase can lead to a new availability of fuel to allow for a combustion transfer from smoldering to flaming combustion.

2. *What modelling theories are deployed in contemporary wildfire spread models?*

Two main types of wildfire spread models are deployed in current wildfire modelling. First, vector models, based on partial differential equations are used. These models prove to be highly efficient in predicting the spread of flaming fire fronts for shorter amounts of time. The biggest drawback of this modelling approach is the demanded computational power to solve the underlying partial differential equations. Often these models require too much computing power to allow for real time applications, this means that the prediction is slower than the actual wildfire spread. Another drawback concerning computational demands is that when considering wildfire events that inhabit both smoldering and flaming combustion, these vector based models are not useable at the field scale.

A second main modelling approach lies in grid-based approaches such as through cellular automate modelling. Though this form of modelling inherently leads to more simplifications as opposed to the vector approach, it proves to be computationally light. Thereby, this grid-based approach overcomes the issues with computational power as addressed above. Cellular automate based wildfire spread models can be used to model both smoldering and flaming combustion processes in wildfire events successfully although this is insight is a recent development.

3. *What are the specific characteristics of the Peel region 2020 wildfire?*

The Peel region wildfire is the biggest wildfire ever recorded in the Netherlands, burning over 700 hectares. The initial flaming phase of the wildfire event lasted for about four days. However, smoldering combustion and rekindling lasted for 63 days. The wildfire also spread through the form of spotting fire spread and could via this form of spread, overcome natural borders such as the Deurnese Kanaal. The rapidly progressing flaming fire front led to evacuations of nearby houses. Furthermore, smoke resulting from both types of combustion proved to be a direct and indirect danger to the health of people in the region.

The Peel region wildfire event proves to be a good example of a wildfire that is characterized by both smoldering and flaming combustion phenomena. Even with the deployment of extensive firefighting material, water bombings by army helicopters and other spread reducing activities, the event still lasted for over two months.

4. *What is the current state of modelling and data collection for wildfires in the Netherlands?*

At the time of writing, a new database for wildfire data collection is developed by the Dutch Institute for Physical Safety. This database has the goal to better investigate the impact wildfire events have in the Netherlands. As of 2018, data for wildfire events are presented in the annual fire reports of the European Forest Fire Information Systems (EFFIS) institute of the European Union. From the interviews it was found that the Dutch Institute for Physical Safety aims to improve data collection with regards to wildfires that affect smaller areas.

Furthermore, since a few years a wildfire spread model is deployed in the Netherlands. This NBVM model is based on a vector approach and proves to be a solid tool in wildfire management and prediction. With combined input of different parties, a useable front end was developed to make the model easy to deploy. The model focusses on the prediction of surface fire spread. This model will be further improved with the addition of more fuel models. Moreover, a more detailed vegetation map of the Netherlands is created in order to improve the predictions made by the Dutch wildfire spread model.

5. *To what extend can processes in smoldering and flaming wildfires be simulated to model wildfire front fire spread over a hypothetical field?*

Based on results of the earlier presented sub-questions a new wildfire spread modelling framework is proposed in this thesis. The proposed wildfire-modelling framework FENIX is based on a cellular automate approach. This approach allowed for the incorporation of the most influential aspects of wildfires based on organic soils. As identified in sub-question one, these aspects are most prominently the spread of both smoldering and flaming combustion fronts. Other influencing aspects such as wind are also considered in the framework. The FENIX framework is the first wildfire model ever presented to incorporate the phenomena of revegetation and smoldering to flaming combustion transitions at the field scale.

Although not incorporated in the FENIX framework, cellular automate based approaches have proven to be able to incorporate spotting wildfire spread. Further development of the framework might focus on this spread phenomenon. More research is needed in order to further strengthen understanding of smoldering to flaming combustion transitions to be better incorporated in future wildfire modelling frameworks. However, the FENIX framework proves to be able to incorporate the identified aspects to predict the spread of both smoldering and flaming combustion over a hypothetical field. Furthermore, the FENIX model proves to be computationally light, which gives the model considerable advantages when compared to vector based approaches such as the NBVM.

6. *To what extend can a cellular automate based model be used to explain the spread of the 2020 Peel region wildfire in the Netherlands?*

Considering no data on firefighting activities was available, no precise prediction for the Peel region wildfire could be made. However, by incorporating and simplifying data of the regions soil, vegetation and weather for the period of the wildfire event the FENIX framework proved to be able to predict wildfire spread. Based on findings from earlier sub-questions a new hypothesis was tested and predicted where the wildfire event started as a smoldering combustion. Both of the predictions showed a phase of extreme flaming front fire propagation similar to the actual situation during the first five days after April 20th, 2020. However, both predictions failed in predicting this extreme flaming front fire progression phase at the right time. Both predictions showed a phase of rekindling in the region similar to the behavior of the actual wildfire event. However, due to a lack of data there is no way to validate if the location and the extent of this rekindling was modelled correctly.

Considering the answers to the six presented sub-questions an answer to the main research question can be formulated. Below, the main research question is repeated and subsequently the answer to the main research is presented.

To what extend can a smoldering and flaming peatland based wildfire spread be simulated from the real world into a data driven cellular automate model?

This extensive work started out by presenting the fundamental characteristics of smoldering and flaming combustion. Identifying the most influential aspects with respect to spread of both combustion phenomena. These phenomena are, vegetation, wind, revegetation, flaming to smoldering and smoldering to flaming combustion transfers. After addressing contemporary wildfire modelling approaches a grid based cellular automate wildfire spread modelling framework was proposed called FENIX. The FENIX framework incorporates the earlier stated important aspects of wildfire spread based on organic soils. The FENIX wildfire spread modelling framework is the second wildfire spread model to incorporate both smoldering and flaming combustion. Moreover, FENIX is the first ever wildfire model to successfully incorporate the phenomena of revegetation and smoldering to flaming combustion transfers at the field scale.

The Dutch case of wildfire modelling and wildfire data collection were addressed in order to understand data availability and contemporary developments in the Netherlands. Findings from this part of the thesis were subsequently used in data selection for modelling the selected case of the Peel region wildfire of early 2020. This is at the time of writing, the biggest wildfire ever recorded in the Netherlands.

After extensive testing of the framework over a hypothetical field, selected data was prepared and the FENIX framework was used to simulate the Peel region wildfire of 2020. While the framework did not correctly predict the time of the extreme flaming front fire propagation, this behavior was shown in the simulation. The subsequent rekindling phase of the wildfire event was also simulated by the proposed framework. Data limitations with respect to firefighting deployment did not allow the incorporation of these activities in the framework. Therefore, the extent of the simulation and the extent of the actual wildfire event differed. Furthermore, the actual wildfire event also spread through the spotting phenomenon, by flying embers through the air. This kind of spread phenomenon was not considered in the proposed framework.

Though the extent of the prediction and the extent of the actual wildfire event differed, the most important spread phenomena and governing aspects were successfully incorporated in the framework. Earlier studies show that the effects of spotting fire spread can be successfully modelled by cellular automate modelling approaches.

Further research should aim to improve cellular automate modelling approaches with respect to wildfires based on organic soils. As stated in this work, understanding the role of smoldering combustion in wildfires is key in the contemporary struggle to manage greenhouse gas emissions. Since wildfires are a highly multidisciplinary phenomenon future studies should aim to integrate knowledge that is already available in order to grow new insights.

Literature

Alexander, M. E., & Cruz, M. G. (2006). Evaluating a model for predicting active crown fire rate of spread using wildfire observations. *Canadian Journal of Forest Research, 36*(11), 3015-3028.

Alexandridis, A., Vakalis, D., Siettos, C. I., & Bafas, G. V. (2008). A cellular automata model for forest fire spread prediction: The case of the wildfire that swept through Spetses Island in 1990. *Applied Mathematics and Computation, 204*(1), 191-201.

Amin, H. M., Hu, Y., & Rein, G. (2020). Spatially resolved horizontal spread in smouldering peat combining infrared and visual diagnostics. *Combustion and Flame, 220*, 328-336.

Arienti, M. C., Cumming, S. G., & Boutin, S. (2006). Empirical models of forest fire initial attack success probabilities: the effects of fuels, anthropogenic linear features, fire weather, and management. *Canadian Journal of Forest Research, 36*(12), 3155-3166.

Bakhshaii, A., & Johnson, E. A. (2019). A review of a new generation of wildfire–atmosphere modelling. *Canadian Journal of Forest Research, 49*(6), 565-574.

Brabants Dagblad (2020, 5, October). Geopark Peelhorst en Maasvallei i.o. heeft er twee steungemeenten bij
Retrieved from: https://www.bd.nl/uden-veghel-e-o/geopark-peelhorst-en-maasvallei-i-o-heeft-er-twee-steungemeenten bij~abfb075a/?referrer=https%3A%2F%2Fwww.google.nl%2F

Brandweer (2020). Team Natuurbrandonderzoeken *Natuurbrandonderzoek Deurnese Peel*.

Brandweeracademie (2019). Grootschalig brandweeroptreden 2016-2018. Arnhem: Instituut Fysieke Veiligheid.

Bowd, E. J., Banks, S. C., Strong, C. L., & Lindenmayer, D. B. (2019). Long-term impacts of wildfire and logging on forest soils. *Nature Geoscience, 12*(2), 113-118.

Box, G. E. P.,& Draper, N. R. (1987), *Empirical Model-Building and Response Surfaces.* John Wiley & Sons.

Broadbent, S. R., & Hammersley, J. M. (1957). Percolation processes: I. Crystals and mazes. *Mathematical Proceedings of the Cambridge Philosophical Society, 53*(3), 629-641. Cambridge University Press.

Bryman, A. (2016). *Social research methods*. Oxford university press.

Burgess, T. Burgmann, JR. Hall, S. Holmes, D. and Turner, E. (2020) Black Summer: Australian newspaper reporting on the nation's worst bushfire season. Melbourne: Monash Climate Change Communication Research Hub, Monash University,

Cardil, A., Lorente, M., Boucher, D., Boucher, J., & Gauthier, S. (2019). Factors influencing fire suppression success in the province of Quebec (Canada). *Canadian Journal of Forest Research, 49*(5), 531-542.

CalFire (2020), California Statewide Fire Summary October 6 2020
Retrieved from: https://www.fire.ca.gov/daily-wildfire-report/

Christensen, E. G., Fernandez-Anez, N., & Rein, G. (2020a). Influence of soil conditions on the multidimensional spread of smouldering combustion in shallow layers. *Combustion and Flame, 214*, 361-370.

Christensen, E. G., Hu, Y., Purnomo, D. M., & Rein, G. (2020b). Influence of wind and slope on multidimensional smouldering peat fires. *Proceedings of the Combustion Institute*.

Chuvieco, E., Cocero, D., Riano, D., Martin, P., Martınez-Vega, J., de la Riva, J., & Pérez, F. (2004). Combining NDVI and surface temperature for the estimation of live fuel moisture content in forest fire danger rating. *Remote Sensing of Environment, 92*(3), 322-331.

Couclelis, H. (1997). From cellular automata to urban models: new principles for model development and implementation. *Environment and planning B: Planning and design, 24*(2), 165-174.

Davies, G. M., Kettridge, N., Stoof, C. R., Gray, A., Ascoli, D., Fernandes, P. M., ... & McMorrow, J. (2016). The role of fire in UK peatland and moorland management: the need for informed, unbiased debate. *Philosophical Transactions of the Royal Society B: Biological Sciences, 371*(1696).

Devillers, R., & Jeansoulin, R. (2007). *Fundamentals of spatial data quality*. London: ISTE.

Drysdale, D. (2011). *An introduction to fire dynamics*. John Wiley & Sons.

Encinas, A. H., Encinas, L. H., White, S. H., Del Rey, A. M., & Sánchez, G. R. (2007a). Simulation of forest fire fronts using cellular automata. *Advances in Engineering Software, 38*(6), 372-378.

Encinas, L. H., White, S. H., Del Rey, A. M., & Sánchez, G. R. (2007b). Modelling forest fire spread using hexagonal cellular automata. *Applied mathematical modelling*, 31(6), 1213-1227.

European Forest Fire Information Systems Wildfire Database (2020) (Data request granted on 10-10-2020)

Favier, C. (2004). Percolation model of fire dynamic. *Physics Letters A, 330*(5), 396-401.

Fernandez-Anez, N., Christensen, K., Frette, V., & Rein, G. (2019). Simulation of fingering behavior in smoldering combustion using a cellular automaton. *Physical Review E, 99*(2).

Frandsen, W. H. (1997). Ignition probability of organic soils. *Canadian Journal of Forest Research, 27*(9), 1471-1477.

Fotheringham, A. S., Brundson, C., & Charlton, M. (2002). *Geographically weighted regression: The analysis of spatially varying relationships*. Chichester, West Sussex , England: Wiley.

Fortin, M. (2020). Updating plots to improve the precision of small-area estimates: the example of the Lorraine region, France. *Canadian Journal of Forest Research, 50*(7).

Gazmeh, H., Alesheikh, A. A., Karimi, M., & Chehreghan, A. (2013). Spatio Temporal Forest Fire Spread Modelling Using Cellular Automata Honey Bee Foraging and GIS. *Environ. Pharmacol. Life Science*, 3, 201-214.

Greene, L., Hebblewhite, M., & Stephenson, T. R. (2012). Short-term vegetation response to wildfire in the eastern Sierra Nevada: implications for recovering an endangered ungulate. *Journal of Arid Environments*, *87*, 118-128

Grishin, A. M., Yakimov, A. S., Rein, G., & Simeoni, A. (2009). On physical and mathematical modelling of the initiation and propagation of peat fires. *Journal of Engineering Physics and Thermophysics*, *82*(6), 1235-1243.

Haider, W., Knowler, D., Trenholm, R., Moore, J., Bradshaw, P., & Lertzman, K. (2019). Climate change, increasing forest fire incidence, and the value of visibility: evidence from British Columbia, Canada. *Canadian Journal of Forest Research*, *49*(10), 1242-1255.

Halofsky, J. E., Peterson, D. L., & Harvey, B. J. (2020). Changing wildfire, changing forests: the effects of climate change on fire regimes and vegetation in the Pacific Northwest, USA. *Fire Ecology*, *16*(1).

Heywood, I., Cornelius, S., & Carver, S. (2011). *An introduction to geographical information systems*. Essex

Huang, X., & Rein, G. (2015). Computational study of critical moisture and depth of burn in peat fires. *International Journal of Wildland Fire*, *24*(6), 798-808.

Huang, X., & Rein, G. (2017). Downward spread of smouldering peat fire: the role of moisture, density and oxygen supply. *International Journal of Wildland Fire*, *26*(11), 907-918.

Huang, X., & Rein, G. (2019). Upward-and-downward spread of smoldering peat fire. *Proceedings of the Combustion Institute*, 37(3), 4025-4033.

Inoue, J. I. (2005). *Modeling Reality: How Computers Mirror Life*.

Instituut Fysieke Veiligheid (IFV) (2016) Natuurbrandverspreidingsmodel

Karafyllidis, I., & Thanailakis, A. (1997). A model for predicting forest fire spreading using cellular automata. *Ecological Modelling*, *99*(1), 87-97.

Kok, E., Stoof, C., (2020). Country report for the Netherlands in San-Miguel-Ayanz et al., (EDS), Forest Fires in Europe, Middle East and North Africa 2019. EUR 30402. EN. Publications Office of the European Union, Luxembourg.

Kötz, B., Schaepman, M., Morsdorf, F., Bowyer, P., Itten, K., & Allgöwer, B. (2004). Radiative transfer modelling within a heterogeneous canopy for estimation of forest fire fuel properties. *Remote Sensing of Environment*, *92*(3), 332-344.

Lin, S., Sun, P., & Huang, X. (2019). Can peat soil support a flaming wildfire?. *International Journal of Wildland Fire*, *28*(8), 601-613.

Longley, P. A., Goodchild, M. F., Maguire, D. J., & Rhind, D. W. (2005). *Geographic information systems and science*. John Wiley & Sons.

Malamud, B. D., & Turcotte, D. L. (2000). Cellular-automata models applied to natural hazards. *Computing in Science & Engineering, 2*(3), 42-51.

McClave, J. T., Benson, P. G., & Sincich, T. (2008). *Statistics for business and economics*. Pearson Education.

McDermott, R. J., & Rein, G. (2016). Special issue on fire model validation. *Fire Technology, 52*. DOI: 10.1007/s10694-015-0559-x.

Mutthulakshmi, K., Wee, M. R. E., Wong, Y. C. K., Lai, J. W., Koh, J. M., Acharya, U. R., & Cheong, K. H. (2020). Simulating forest fire spread and fire-fighting using cellular automata. *Chinese Journal of Physics*.

Nusantara, R. W., Hazriani, R., & Suryadi, U. E. (2018). Water-table Depth and Peat Subsidence Due to Land-use Change of Peatlands. *IOP Conference Series: Earth and Environmental Science* 145(1). IOP Publishing.

Omroep Brabant (2020) Brand Deurnese Peel nog lang niet geblust, tientallen omwonenden brengen nacht ergens anders door Retrieved from: https://www.omroepbrabant.nl/nieuws/3192554/brand-deurnese-peel-nog-lang-niet-geblust-tientallen-omwonenden-brengen-nacht-ergens-anders-door

Oswald, B. P., Brouwer, N., & Willemsen, E. (2017). Initial development of surface fuel models for the Netherlands.

Prat-Guitart, N., Rein, G., Hadden, R. M., Belcher, C. M., & Yearsley, J. M. (2016). Effects of spatial heterogeneity in moisture content on the horizontal spread of peat fires. *Science of The Total Environment, 572*, 1422-1430.

Purnomo, D. M., Bonner, M., Moafi, S., & Rein, G. (2020). Using cellular automata to simulate field-scale flaming and smouldering wildfires in tropical peatlands. *Proceedings of the Combustion Institute.*

Rein, G., Cleaver, N., Ashton, C., Pironi, P., & Torero, J. L. (2008a). The severity of smouldering peat fires and damage to the forest soil. *Catena, 74*(3), 304-309.

Rein, G., Garcia, J., Simeoni, A., Tihay, V., & Ferrat, L. (2008b). Smouldering natural fires: comparison of burning dynamics in boreal peat and Mediterranean humus. *WIT Transactions on Ecology and the Environment, 119*, 183-192.

Rein, G. (2009). *Smouldering combustion phenomena in science and technology*.

Rein, G., & Belcher, C. M. (2013). Smouldering fires and natural fuels. *Fire phenomena and the Earth system: an interdisciplinary guide to fire science*, (1984), 15-33.

Rein, G. (2016). Smoldering combustion. In *SFPE Handbook of Fire Protection Engineering*. 581-603. Springer, New York, NY.

Rothermel, R. C. (1972). *A mathematical model for predicting fire spread in wildland fuels*. Intermountain Forest & Range Experiment Station, Forest Service, US Department of Agriculture.

Restuccia, F., Huang, X., & Rein, G. (2017). Self-ignition of natural fuels: can wildfires of carbon-rich soil start by self-heating?. *Fire Safety Journal, 91*, 828-834.

Sabokbar, H. F., Roodposhti, M. S., & Tazik, E. (2014). Landslide susceptibility mapping using geographically-weighted principal component analysis. *Geomorphology*, *226*, 15-24.

Santoso, M. A., Christensen, E., Yang, J., & Rein, G. (2019). Review of the transition from smouldering to flaming combustion in wildfires. *Frontiers in Mechanical Engineering*.

San-Miguel-Ayanz, Tracy Durrant, Roberto Boca, Giorgio Libertà, Alfredo Branco, Daniele de Rigo, Davide Ferrari, Pieralberto Maianti, Tomàs Artés Vivancos, Duarte Oom, Hans Pfeiffer, Daniel Nuijten, Thaïs Leray; *Forest Fires in Europe, Middle East and North Africa 2018*. EUR 29856 EN, ISBN 978-9276-11234-1, doi:10.2760/1128

Smulders, H. & Bossenbroek, P. (2016). *De Groote Peel in vogelvlucht.*

Stoof, C. R., Tavia, V. M., Marcotte, A. L., Stoorvogel, J. J., & Ribau, M. C. (2020). *Relatie tussen natuurbeheer en brandveiligheid in de Deurnese Peel: onderzoek naar aanleiding van de brand in de Deurnese Peel van 20 april 2020.*

Takama, T. (2005). *Stochastic agent-based modelling for reality* (Doctoral dissertation, Oxford University, UK).

Takama, T., & Preston, J. (2008). Forecasting the effects of road user charge by stochastic agent-based modelling. *Transportation Research Part A: Policy and Practice*, *42*(4), 738-749.

Taufik, M., Veldhuizen, A. A., Wösten, J. H. M., & van Lanen, H. A. J. (2019). Exploration of the importance of physical properties of Indonesian peatlands to assess critical groundwater table depths, associated drought and fire hazard. *Geoderma*, *347*, 160-169.

Tobler, W. R. (1970). A computer movie simulating urban growth in the Detroit region. *Economic geography*, *46*(1), 234-240.

Trunfio, G. A. (2004). Predicting wildfire spreading through a hexagonal cellular automata model. *International Conference on Cellular Automata*. (pp. 385-394). Springer, Berlin, Heidelberg.

Turetsky, M. R., Benscoter, B., Page, S., Rein, G., Van Der Werf, G. R., & Watts, A. (2015). Global vulnerability of peatlands to fire and carbon loss. *Nature Geoscience*, *8*(1), 11 14.

Van de Kam, J. van de (2020). *De Peel in vier seizoenen.*

Wang, R. Y., & Strong, D. M. (1996). Beyond accuracy: What data quality means to data consumers. *Journal of management information systems*, *12*(4), 5-33.

Wolfram, S. (2002). *A new kind of science*.

WolframMathworld (2021) Retrieved from: https://mathworld.wolfram.com/ElementaryCellularAutomaton.html

Wösten, H., Brouwer, F., & Veraart, J. (2020). *Kansenkaart voor bescherming van koolstofvoorraad en CO2-emissiereductie in natte natuur en multifunctionele klimaatbuffers: Technische achtergrondmemo* (No. 3003). Wageningen Environmental Research.

Yassemi, S., Dragićević, S., & Schmidt, M. (2008). Design and implementation of an integrated GIS-based cellular automata model to characterize forest fire behaviour. *ecological modelling*, *210*(1-2), 71-84.

Appendix A. Interview Dutch wildfire database

NOTE: The interview was held in Dutch, the transcript is translated by the researcher.

Question 1:

What are the direct motivations for the creation of the current Dutch wildfire database?

Interviewee:

The direct motivations are multiple. In 2010 there has been a relatively big wildfire at the Strabrechtse Heide (Noord-Brabant, the Netherlands red.). From the resulting study from *de inspectie openbare orde en veiligheid* (public order and safety inspection) one of the resulting suggestions was to start registering the extent and amount of wildfires in the Netherlands. The study was the indirect motivation for the Dutch fire department to start a full flight project on wildfire management, called the project large scale and specialized fire fight deployment. Within the specialism of wildfires this project consists of 18 sub-projects of which the wildfire spread model and the database are few examples. The aim of these projects is to strengthen the information position of the Dutch fire department on the one hand, on the other hand a couple of specialized teams have been trained or rescaled to the national level. Furthermore the collection of statistics on forest fires have been stopped in 1995 or 1996 before these were collected by the Dutch institute of forest management *(Staatsbosbeheer)* but they quit this project because of declining frequency of wildfires, smaller extent of wildfires and due to collection costs reasons. This lack of information does not allow us to draw any conclusions on the changing patterns of wildfires over the last 20 years. The last motivation was the European database on wildfires from the European Forest Fire Information System (EFFIS) institute. The Netherlands started their contribution to the database in 2017, before this information was not collected, partly because it is not mandatory to do so.

The most obvious motivations to start with the database was to get a better understanding of patterns in wildfire frequency and extent in the Netherlands, but there is also a motivation to collect this data and information to get the attention of the board (Fire department board red.) to show urgency. Without any quantitative foundation it's hard to say something sensible about these patterns.

Interviewer:

You shortly introduced EFFIS. From their documentation and annual reports I've seen that the Netherlands is only incorporated in the report on the 2018 wildfire season. EFFIS started these annual reports in 2000, the Netherlands has therefore been missing for a period of almost 18 years. Was this due to the study of the public order and safety inspection?

Interviewee:

Absolutely, we have been collecting data about wildfires since 2017. Back then we were not included with the expert group on forest fires which is a sub-department of EFFIS. Before this relation was management by representatives of the ministry of safety and justice, but they did not really contribute to the expert group. So when we started collecting the data on wildfires we took the decision to contribute to the expert group. We have been delivering data and information starting from 2018, they also have the crude data of 2017. But this is not yet included in the annual wildfire documentation. This will be included in the report on the 2019 wildfire report, which is to be published in the incoming weeks. This report will have paragraphs on the Dutch wildfire seasons of 2017, 2018 and 2019.

Question 2:

Which stakeholders are involved in the development of the database?

Interviewee:

At this moment the database is not more than an excel-spreadsheet in which the data is registered about how many wildfires there are and at which location. This is due to the fact that there is no good filtering from the control room system in which the emergency services work. So at this moment we collect data which is publicly available. A way is being developed to automate the connection between the control room system of the emergency services and the database. The control system allows for several reporting classifications for instance, forest fire, grassland fire or dune fire. It is our goal to automate the transfer of these classifications into the database. Technically speaking this is possible, however there are two problems. First, not all fires receive the right classification. For instance a car that caught fire in the verge next to a highway can receive the classification *vehicle fire*, where actually the fire progresses into an adjacent forest area, therefore actually being also a forest fire. Secondly, combining incidents forms a problem. Every report from a control room creates a new incident identification. Wildfires tend to be so big that multiple departments have to work together in order to fight the fire. This can easily increase into around ten different incident identifications whereas it is actually one big incident. Coupling these identifications has to be done manually in order to make sure that data on a fire is collected righteous.

Furthermore there is a problem with privacy issues due to the direct coupling with the control room system. This raises the issue of what can be published. Normally I would say we're not working with personal information because we address wildfires, not fires in homes where an address would be coupled. This is not the fact with wildfires, but with current regulations on personal data we cannot collect data on how many vehicles are deployed during the fire fight because it might be traced back which vehicles are deployed. I personally think this is far fetched but it forms a problem. With this in mind there are some issues that hinder the automated transfer between the control room system and the database.

This is what we do at *het insituut fysieke veiligheid* (the institute of physical safety) ourselves. However we enrich this data with local knowledge and media reporting. We normally don't know what kind of vegetation burned and what the extent of the fire was. This qualitative data we can't get from the control room system due to the fact that we can only collect this data when someone is deployed into the field to track down this information. So we are currently working on a data warehouse in which on the one hand input is formed through the direct coupling of the control room system, but also weather data. On the other hand a warehouse in which we can enrich the data with findings of the team wildfire research and regional researches.

Interviewer:

You named the impact of the GDPR, I personally did not expect this to play a role in a database on wildfires. What issues does this raise?

Interviewee:

Actually it forms issues on everything that can be traced back to locations. Our mission was to couple the control room system with the database, which is possible. However we're faced with restrictions on data collection. Normally the control rooms system always registers an address. There is a regional agreement that this data cannot be used due to the fact that they can be traced back to individuals, unless you can defend that you're not investigating this personal data. However, the location of a fire is not traceable to any kind of individual but because of this agreement we cannot use this location data. This means that we have to look for a work around to show that we do not use that personal data. Furthermore the fact that the database and regulations are relatively young we're still looking into how these issues play together.

Interviewer:

I've read that the police and fire department both collect data on wildfires however the nature of their data collection differs. Is this both incorporated into the database?

Interviewee:

Yes this data is incorporated into the database. What you're describing is the work process of the regular team on fire research. There is also a specialized team on wildfires. They have received further training to map and investigate wildfires. Their unique component is that they consist of both police men and fire fighters. This means that they can collect both kinds of data in a combined way.

We see that wildfires often occur due to human action. Therefore, the cause of the fire is an important aspect of the research. However, we are also interested progression of the fire. These aspects of wildfires along with validation of the wildfire spread model are also investigated by the specialized team. With regards to the Peel region fire, where I was myself for two days, I have seen the aggressive fire behavior. This was due to a thick layer of death fern vegetation. We have to investigate these driving factors behind what makes a wildfire so destructive. In this case it was due to weather impact but also due to a lot of potential fuel in the region. This kind of data is collected by the specialized team on wildfires if they are deployed into the field. This year they did two investigations, the Peel region fire and the Meinweg region fire (Limburg red). Starting next year we aim to investigate a lot more small wildfires. At this moment we do not much information on small wildfires because nobody is sent to investigate.

Interviewer:

The Peel region fire was characterized by a peat fire. This can result in an underground fire progression which can last for weeks. What is the role of *Staatsbosbeheer* (National Forest Management Agency) in the data collection of this aspect of the fire, or is the specialized team on wildfires only deployed after the fire is completely in the past?

Interviewee:

No, the specialized team was deployed before the complete fire was out. They also have been deployed in the fire period where the fire progressed underground. They primarily aim to map and investigate progression and learning points for fire fighting deployment. We know that these kind of wildfires progress underground, however it would be almost fundamental research to investigate what processes are driving this aspect. For these kind of things we use our international networks. The specialized team is not capable of doing this fundamental research. However, we did organize a meeting together with experts from the fire department and *Staatsbosbeheer* to see how we approach this stage the fire.

For this we asked input of Guillermo Rein (professor at the Imperial College in London red.) who specializes in ground fires. We evaluated his suggestions on how we could fight this fire, however all were either too costly or destructive to the ecology of the area. But to show, we make a differentiation between what the specialized team is capable of investigating and for what things we have to reach out to out international and academic network.

Question 3:

Will the database be openly accessible?

Interviewer:

We discussed this subject partially and we can conclude that the full database will not become openly accessible. But to rephrase the question. Will the database be shared for research purposes?

Interviewee:

Yes we have this ambition. However, we aim to keep a sight on what is done with the data and what data is shared. For instance we want to protect for the situation where media couple phenomena and conclude in a too straightforward way. A recent example is the coupling of soil drought and wildfires by a Dutch media collective where they concluded that if a soil moisture percentage goes below 10 percent there is a steep increase in wildfires. This conclusion got a lot of attention in the media. However, we know that drought is an impacting factor, yet this phenomenon might be more complex. So we like to keep an eye on how the data is interpreted before conclusions are drawn. Of course we do this without any form of censuring research. With this in mind we aim to share data from the database as long as there is a clear intention for the research.

Question 4:

What data is collected and are there any requirements for spatial and temporal accuracy?

Interviewee:

Accuracy is by far our biggest challenge. I've been working closely with Cathelijne (Stoof, dr.ir at WUR) to index the challenges with data and accuracy. For instance in the current situation the data gets collected through the common emergency room system. This system requires an address for every record, this address has to be a recognized street address in the Netherlands. Now you can imagine that if a fire starts in the middle of a vast nature area it's hard to couple it to a nearby street address. The emergency room has to pinpoint the place where they think that the call is made, however this can be kilometers away from the actual place of the fire. Therefore, we always have an address but it comes with a potentially huge error margin. With bigger fires we often know exact locations because of the investigation and the composition of a footprint. However, at this moment satellite technology is not far enough developed to locate small wildfires. EFFIS uses a threshold of 20 to 25 hectares to map. We're investigating if we can improve this resolution, this seems to become a hard challenge. So exact locations are now mostly known if the special team on forest fire research has investigated the fire.

We're relatively sure about the temporal accuracy of the data. especially in the Netherlands the time of discovery and the actual ignition time are close due to a closely related human nature relationship. We're also pretty sure about how many firefighters are deployed at a fire. And further we collect data from media to enhance our understanding of the vegetation and extent of the smaller fires. Currently we often estimate the extent of a wildfire from news articles.

Another challenge is to know the cause of a fire. Because we use the European system we can use five grades. Ranging from we know hardly anything (1) to we're sure (5). So we are trying to use this to investigate human caused fires, for instance If one nature reserve suffers from fires more often than another similar nature reserve. But we cannot conclude this without in-depth research.

Question 5:

To what standards have the collected data be conformed?

Interviewee:

Right now our data collection and archiving happens through the use of Excel. We're working on a automated database based on a python-powered environment. But without going into too much technical detail the data will be easily shareable. I'm personally not sure how the technical personal tackles this question. But interoperability is promised. However a pressing issue is that even with an automated database a lot of man-hours are required for validations purposes.

Question 6:

What are direct plans for further development of the wildfire database? Let's say over the period of the next three years.

Interviewee:

For now we want to focus on the automated input. So a coupling with the emergency room system is of top priority. Further we have to see what developments will be. I would personally be interested in the use of coordinate locations. Also the coupling with the vegetation map is an interesting development. We could couple these data to investigate for instance what kind of fuel burned during a given fire. This is technically feasible if we have quality footprints of the wildfires.

Further I would like to see that the safety regions will also start to contribute to the knowledge of wildfires by doing investigation work themselves. With this development we can compare certain wildfires and therefore learn from experience and different settings.

Interviewer:

Sure, are you also interested in enhancing the resolution of the data?

Interviewee:

No, this is not currently a priority. We are however enhancing the wildfire spread model with respect to the fuel models used in the model. From a fire fighting perspective it would also be only a relevant development for bigger wildfires.

Question 7:

We just talked about direct further developments of the database. What are the projected developments a bit further on the horizon?

Interviewee:

There are a few different things we have in mind. Firstly we want to analyze more the data that we collect. Therefore looking into longitudinal trends in extent and frequency of wildfires. Furthermore we would like to investigate the coupling with meteorological data to investigate more the impact of these variables on wildfire spread. We also want to investigate wildfire trends of the last 40 years in collaboration with the data of EFFIS. This way we can investigate why wildfires reach a beyond control extent.

Further we want to get attention from the board of the fire department and the ministries to show that wildfires are a growing challenge, this can only be achieved with a fact-based and data driven research.

Appendix B. Interview Dutch wildfire spread model (NBVM)

NOTE: The interview was held in Dutch, the transcript is translated by the researcher.

Question 1:

What are the direct causes for the development of the Dutch wildfire spread model?

Interviewee:

For that we have to go back in time a little bit. First steps were made in 2008. After a couple of incidents we saw that we knew a lot about building fires and other incidents but less about the spread of wildfires. There we dived into what knowledge we could find from other places such as academia and experience of other countries. We also looked into contemporary spread models. At first the developments were for incident management, during the wildfire itself. How does it spread and how can a model help with the decision-making were the central questions at the start of the developments of the model.

Interviewer:

A short time ago I spoke with your colleague, he told me the wildfire database is developed later.

Interviewee:

Yes that's true but these are two things. So the wildfire spread model really aims to look into how a fire progresses. The database is aimed at registering what fires we have and what their characteristics are. This information can be used for validation of the spreadmodel

Question 2:

What are the involved parties in the development of the wildfire spread model?

Interviewee:

Going back in time again a lot of partners have been involved. The wildfire spread model is developed together with safety regions, the end-users. Besides them Universities, partners and Universities.

input for the the model, the fuel models, are developed in collaboration with the Stephen F. Austin State University in Texas, United States. They helped with research in vegetation and fuel studies with focus on the Netherlands. Every vegetation type has its own properties. With the findings of multiple years of study we generated our own models. Furthermore, Dutch safety regions were involved. With them we really focused on the end users of the model. So we tried to combine academia knowledge with people who will have to use it. This is essential to develop a model that will and can be used in the field.

Question 3:

we talked a little bit about input data already, for what specific vegetation types have you developed fuel types? And are there plans to develop more fuel models?

Interviewee:

At this moment we have developed 20 fuel models. These break down into subcategories as well, for example we have four different models on heath vegetation types. We do this because the properties of similar vegetation types can already differ with a huge amount with respect to their behavior. Therefore we have models on a wide variety of vegetation types such as grassland, dune areas and forests. The model currently uses this as input for the modelling of surface fires.

Interviewer:

What other input data is used in the model?

Interviewee:

Meteorological data mostly. For example temperatures and humidity,. the model use this information to make an assessment of the draught. This of course influences the spread of a wildfire. But also data during the day itself, one of these important characteristics is wind speed and wind direction.

Interviewer:

Okay, and are characteristics like elevation also involved?

Interviewee:

Not at this moment. We used this in the past but realized that the influence of elevation differences in the Netherlands in combination with the measurement accuracy of that time was not impacting the prediction. But of course elevation data have been improved in the last year and in the future we want to look into how we can include height data again into the spread model.

Question 4:

What modelling theory is the wildfire spread model based on?

Interviewee:

The model is a vector based model, the underlying theory is based on Rothermel seminar work. .

Question 5:

How do you assess the accuracy of the model?

Interviewee:

All larger wildfires are evaluated and validated for the model. We always look into the vegetation at the location, the model behavior and the actual situation. We always improve our model with new insights and experience, we receive from studying the actual events. For example, the model simulates surface fires, one of the things we would like to include in the future is spotfire With this in mind we also train our end users to understand what the model does and what it tries to predict. They shouldn't see it as the truth of what will happen but rather a tool to help in the firefighting process or risk management. Using the model is one thing, understanding the model is something else.

We also use the findings of the special team on wildfire research as validation for the model. They trace back the full progression of the wildfire and the deployment of firefighters. In the aftermath we also ask for feedback with the safety regions to see how the model was used during the event itself.

Question 6:

From experience, when is the wildfire spread model actually used. Is this while the fire is still small or is it at the moment where we understand that a fire has a potential to affect an extensive area?

Interviewee:

This is mainly used with bigger fires. The initial response in smaller fires is often worth the most, when the fire is already in control after this initial response the model is not needed . However if a fire is big the model is often applied to support with further response. The model is also during the years more and more used for risk management, to assess what measures could be taken to prevent a wildfire can become a large wildfire and to raise awareness of these fires.

Question 7:

We talked a little bit about future developments for the wildfire spread model, what other developments are planned?

Interviewee:

The most important development is the enhancement of vegetation and fuel models. Based on satellite data we try to improve our understanding of the vegetation spread in the Netherlands based on a newly created more accurate vegetation map. This satellite map gives us more accurate information on the vegetation. This map is now validated and will be updated every year. The challenge we face now is to load and use it inside the model. We also try to asses wildfire risk, this is also projected to be done using satellite data. The use of satellite data will be one of the big developments with regards to the model.

Appendix C. FENIX wildfire framework code

```
%% FENIX WILDFIRE SPREAD MODEL
clc, clear, close all
% Cell states:
% Surface Vegetation (SV) = 0 (Top matrix (A))
% Flaming Vegetation (FV) = 1 (Top matrix (A))
% Exposed Peat       (EP) = 2 (Top matrix (A) & Soil
matrix (B))
% Smoldering Peat    (SP) = 3 (Soil matrix (B))
% Burned Peat        (BP) = 4 (Soil matrix (B))

%application to Peel region wildfire one extra state
%incombustible area (IA) = 6 (Both matrices)

%% Setup
%Probabilities
format long
MC = 70;
Pf  = 0.35;   % 0 -> 1 (in Top Layer)
Pt  = (1./(1+(exp(1).^(9.85+0.057*(MC))))); % 2 -> 3 (in
Soil Layer)
Ps  = (1./(1+exp(-(-19.8198+(-
0.1169*(MC))+(1.0414*3.7)+(0.0782*222))))));  % 1 -> 3
(tussen Top en Soil)
Pe  = 5e-7; % 3 -> 4 (in Soil Layer)
Vt = 15e-5;  % 2 -> 0 (in Top Layer)
Prei  = 0.001; % 3 -> 1 (tussen Top en Soil)

%inladen data Peel
A = dlmread('tlg.txt'); %Load top layer raster file
B = dlmread('slg.txt'); %Load soil layer raster file
%A(111,569) = 1; %Ignition top layer
B(111,569) = 3;  %Ignition soil layer
a = 900; %Lenght array

%Create environment hypothetical plane
%A = zeros(501); %Create Top Layer matrix
%A(251,251)=1; %Ignite center Top Layer matrix
%a=501; %Define array length
%B = 2 * ones(501); %Create Soil Layer matrix

%Neighbourhood Definition (Moore Neighbourhood)
spread=[-1 1; 0 1; 1 1; 1 0; 1 -1; 0 -1; -1 -1; -1 0];

%Initial fire occurs at timestep 0
ta=0;
tb=0;
```

```
%Wind matrix
Wi = [135, 180, 225
      90, 0, 270
      45, 360, 315];

%Wind parameters
vhalf = readtable('WV.csv'); %Load wind speed data
V = table2array(vhalf); %create array for wind speed data
implementation
yhalf = readtable('WDTGG.txt'); %Load wind direction data
y = table2array(yhalf,1); %Create array for wind direction
data implementation

%Variables wind speed and direction if set to be constant
%V=0;
%y=0;

%Wind calculations
%t1 = Wi -y;
%FT = exp(V*0.131*(cosd (t1)-1));
%pw = exp(0.045*V)*FT;

%% SETUP Visual frames
%Colour schemes
colourA=[0.1328, 0.5430, 0.1328; 0.6953, 0.1328, 0.1328;
0.3102, 0.3102, 0.3102; 1,1,1; 1,1,1; 1, 1,1; 0.2734,
0.5078, 0.7031];
colourB=[1, 0.8906, 0.8789; 0.8594 0.0781 0.2344; 0 0 0;
0.5429, 0, 0.5429];

%Create figures
f1 = figure;
f2 = figure;
%Define videoimage Top Layer
obj= VideoWriter ('AnimationTopLayer.avi');
obj.Quality = 100;
obj.FrameRate = 20;
open(obj);

%Define video image Soil Layer
obj1= VideoWriter ('AnimationSoilLayer.avi');
obj1.Quality = 100;
obj1.FrameRate = 20;
open(obj1);

%% FENIX FRAMEWORK & DATA COLLECTION
```

```
for ii = 0:18144
    t1 = Wi -y(ii+1);
    FT = exp(V(ii+1)*0.131*(cosd (t1)-1));
    pw = exp(0.045*V(ii+1))*FT;
    [i,j]=find(A==1); %Coordinates of the fire
    for x=1:length(i) %For each fire
        for M=1:8 %Checking each spreading option
            try %Makes it so off grid checks don't cause
an error
                if A(i(x)+spread(M),j(x)+spread(M+8))==0
%Checking for SV in Moore Neighbourhood
                    try
                    W = pw((2-(j(x)+spread(M+8)-
j(x))),(2+(i(x)+spread(M)-i(x)))); %Wind Influence
                    SW = Pf.*W;
                    end
                        if rand<= SW %Chance SV will
ignite

A((i(x)+spread(M)),(j(x)+spread(M+8)))=1; %Fire spreads to
found SV
                        end
                end
            end
            A(i(x),j(x))=2; %SV has been burned
            try
                if A(i(x)+spread(M),j(x)+spread(M+8))==1
%If cell state is FV
                    if B(i(x),j(x)) == 2
                        if rand <= Ps %Chance of
transition to Smoldering combustion
                        B(i(x),j(x))=3; %Cell state
changes to SP
                        end
                    end
                end
            end
        end
    end
    [i,j]=find(B==3);
    for x=1:length(i) %For each SP
        for M=1:8 %Checking each spreading option
            try %Makes it so off grid checks don't cause
an error
                if B(i(x)+spread(M),j(x)+spread(M+8))==2
%Checking for EP
                    if rand <= Pt %Chance EP will ignite
```

```
                    B(i(x)+spread(M),j(x)+spread(M+8))=3;
%Smoldering spreads to found EP
                    end
                end
            end
            try
                if B(i(x),j(x))==3 %If cell state is EP
                    if rand <= Pe %Chance of transition to
BP
                    B(i(x),j(x))=4; %Cell state becomes BP
                    end
                end
            end
        end
    end
    [i,j]=find(A==2);
    for x=1:length(i) %For each EP in Top Layer
        if A(i(x),j(x))==2 %Checking for EP
            if rand <= Vt %Chance for revegetation
            A(i(x),j(x))=0; %Cell state becomes SV
            end
        end
    end
    [i,j]=find(B==3);
    for x=1:length(i) %For every SP
        for M=1:8 %Checking each spreading option
            try %Makes it so off grid checks don't cause
an error
                if A(i(x),j(x))==0 %If cell state above is
SV
                    if rand <=Prei %Probability of
reignition
                    A(i(x),j(x))=1; %Cell state becomes FV
                    end
                end
            end
        end
    end

%Draw Top Layer matrix
figure(f1);
imagesc(A); %The updated environment
colormap(colourA); %Apply colors
title(['Top layer t = ' num2str(ta)]) %Time since start of
fire to be seen on the plot
ta=ta+1; %Timesteps spent burning
```

```
%Draw Soil Layer matrix
figure(f2);
imagesc(B); %The updated environment
colormap(colourB); %Apply colors
title(['Soil layer t = ' num2str(tb)]) %Time since start
of fire to be seen on the plot
tb=tb+1; %Timesteps spent burning

%Time vector definition for data collection
T_Step(ii+1)= ta;

%Total Burned cells in Top layer
TotEPTL = sum(A(:) ==2);
VECTEPTLA(ii+1)=TotEPTL;

%Percentage burned cells in Top Layer
EPTLP = (sum(A(:) == 2)/(a*a))*100;
VECTEPTLP(ii+1)=EPTLP;

%Total Burning cells in Top Layer
TotFVTL = sum(A(:) == 1);
VECTFVA(ii+1)=TotFVTL;

%Percentage Burning cells in Top Layer
FVTLP = (sum(A(:) ==1)/(a*a))*100;
VECTFVP(ii+1)=FVTLP;

%Total Smoldering and burned cells soil layer
TotSPBPSL = ((sum(B(:) == 3) + sum(B(:) == 4)));
VECTSPBPA(ii+1)=TotSPBPSL;

%Percentage Smoldering and burned cells Soil Layer
SPBPSLP = ((sum(B(:) == 3) + sum(B(:) == 4))/ (a*a))*100 ;
VECTSPBPP(ii+1)=SPBPSLP;

%Total number of SV cells
TotSVTL = sum(A(:) == 0);
VECTSVA(ii+1) = TotSVTL;

%Percentage SV cells Top Layer
SVTLP = (sum(A(:) == 0)/ (a*a))*100;
VECTSVP(ii+1) = SVTLP;

%Total amount of EP cells SL
TotEPSL = sum(B(:) == 2);
VECTEPA(ii+1) = TotEPSL;

%Percentage EP cells SL
```

```
EPSLP = (sum(B(:) == 2)/(a*a))*100;
VECTEPP(ii+1) = EPSLP;

%Total amount of SP cells SL
TotSPSL = sum(B(:) == 3);
VECTSPA(ii+1) = TotSPSL;

%percentage SP cells SL
SPSLP = (sum(B(:) == 3)/(a*a))*100;
VECTSPP(ii+1) = SPSLP;

%Total amount of BP cells SL
TotBPSL = sum(B(:) == 4);
VECTBPA(ii+1) = TotBPSL;

%Percentage BP cells SL
BPSLP = (sum(B(:) == 4)/(a*a))*100;
VECTBPP(ii+1) = BPSLP;

%VideoFrame Top Layer
vf= getframe(f1);
writeVideo(obj,vf);

%VideoFrame Soil Layer
vf1= getframe(f2);
writeVideo(obj1,vf1);

end

%% END VIDEO
%Close VideoFrames
obj.close();
obj1.close();

%% DIAGNOSTICS
%Figure amount FV Top Layer
FigFV = figure;
subplot(2,1,1)
plot(T_Step,VECTFVA, 'color', [0.6953, 0.1328, 0.1328])
xlabel('T = 300 seconds per step')
ylabel('Amount of FV cells Top Layer')
grid on
title('Amount of FV cells Top Layer')

subplot(2,1,2)
plot(T_Step,VECTFVP, 'color', [0.6953, 0.1328, 0.1328])
xlabel('T = 300 seconds per step')
ylabel('Percentage FV cells Top Layer')
```

```
grid on
title('Percentage FV cells Top Layer')
saveas(FigFV, 'FVDTL.pdf')

%Figure EP cells amount Top Layer
FigBCD = figure;
subplot(2,1,1)
plot(T_Step,VECTEPTLA, 'color', [0.3102, 0.3102, 0.3102])
xlabel('T = 300 seconds per step')
ylabel('Amount of EP cells Top Layer')
grid on
title('Amount of EP cells Top Layer')

subplot(2,1,2)
plot(T_Step,VECTEPTLP, 'color', [0.3102, 0.3102, 0.3102])
xlabel('T = 300 seconds per step')
ylabel('Percentage EP cells Top Layer')
grid on
title('Percentage EP cells Top Layer')
saveas(FigBCD, 'BCDTL.pdf')

%Creating plots SPBPSL
FigSBSL = figure;
subplot(2,1,1)
plot(T_Step, VECTSPBPA,'m')
xlabel('T = 300 seconds per step')
ylabel('Amount of SP & BP cells Soil layer')
grid on
title('Amount of SP & BP cells Soil layer')

subplot(2,1,2)
plot(T_Step, VECTSPBPP, 'm')
xlabel('T = 300 seconds per step')
ylabel('?b')
grid on
title('Percentage SP & BP cells Soil Layer (?b)')
saveas(FigSBSL, 'SBSLD.pdf')

%creating plots SV
FigSV = figure;
subplot(2, 1, 1)
plot(T_Step, VECTSVA, 'color', [0.1328, 0.5430, 0.1328])
xlabel('T = 300 seconds per step')
ylabel('Amount of SV cells Top Layer')
grid on
title('Amount of SV cells Top Layer')

subplot(2, 1, 2)
```

```
plot(T_Step, VECTSVP, 'color', [0.1328, 0.5430, 0.1328])
xlabel('T = 300 seconds per step')
ylabel('Percentage SV cells Top Layer')
grid on
title('Percentage SV cells Top Layer')
saveas(FigSV, 'SVD.pdf')

%Figure EP cell amount Soil Layer
FigEP = figure;
subplot(2,1,1)
plot(T_Step,VECTEPA, 'color', [0.9542, 0.6406, 0.3750])
xlabel('T = 300 seconds per step')
ylabel('Amount of EP cells Soil Layer')
grid on
title('Amount of EP cells Soil Layer')

subplot(2,1,2)
plot(T_Step,VECTEPP, 'color', [0.9542, 0.6406, 0.3750])
xlabel('T = 300 seconds per step')
ylabel('Percentage EP cells Soil Layer')
grid on
title('Percentage EP cells Soil Layer')
saveas(FigEP, 'EPDSL.pdf')

%Figures SP in Soil layer
FigSP = figure;
subplot(2,1,1)
plot(T_Step,VECTSPA, 'color', [0.8594, 0.0781, 0.2344])
xlabel('T = 300 seconds per step')
ylabel('Amount of SP cells Soil Layer')
grid on
title('Amount of SP cells Soil Layer')

subplot(2,1,2)
plot(T_Step,VECTSPP, 'color', [0.8594, 0.0781, 0.2344])
xlabel('T = 300 seconds per step')
ylabel('Percentage SP cells Soil Layer')
grid on
title('Percentage SP cells Soil Layer')
saveas(FigSP, 'SPDSL.pdf')

%Figures BP in Soil layer
FigBP = figure;
subplot(2,1,1)
plot(T_Step,VECTBPA,'k')
xlabel('T = 300 seconds per step')
ylabel('Amount of BP cells Soil Layer')
```

```
grid on
title('Amount of BP cells Soil Layer')

subplot(2,1,2)
plot(T_Step,VECTBPP ,'k')
xlabel('T = 300 seconds per step')
ylabel('Percentage BP cells Soil Layer')
grid on
title('Percentage BP cells Soil Layer')
saveas(FigBP, 'BPDSL.pdf')

%Figure amount FV Top Layer after 2d
FigFV2d = figure;
subplot(2,1,1)
plot(T_Step(1728:end),VECTFVA(1728:end), 'color', [0.6953,
0.1328, 0.1328])
xlabel('T = 300 seconds per step')
ylabel('Amount of FV cells Top Layer')
grid on
title('Amount of FV cells Top Layer after t = 588')

subplot(2,1,2)
plot(T_Step(1728:end),VECTFVP(1728:end), 'color', [0.6953,
0.1328, 0.1328])
xlabel('T = 300 seconds per step')
ylabel('Percentage FV cells Top Layer')
grid on
title('Percentage FV cells Top Layer after t = 588')
saveas(FigFV2d, 'FVDTL2d.pdf')

%Grafiek percentages en aantallen Top Layer
col = {'Day' , '#FV', '%FV', '?#FV', '#SV', '%SV', '?#SV',
'#EP', '%EP', '?#EP'};

dat = {0,0,0,0,610395,0.0,0,0,0,0;
       1,VECTFVA(1,288),VECTFVP(1,288),(VECTFVA(1,288)-0),
VECTSVA(1,288),VECTSVP(1,288),(VECTSVA(1,288)-
0),VECTEPTLA(1,288),VECTEPTLP(1,288),(VECTEPTLA(1,288)-0);
       2,VECTFVA(1,576),VECTFVP(1,576),(VECTFVA(1,576)-
VECTFVA(1,288)),VECTSVA(1,576),VECTSVP(1,576),(VECTSVA(1,5
76)-
VECTSVA(1,288)),VECTEPTLA(1,576),VECTEPTLP(1,576),(VECTEPT
LA(1,576)-VECTEPTLA(1,288));
       3,VECTFVA(1,864),VECTFVP(1,864),(VECTFVA(1,864)-
VECTFVA(1,576)),VECTSVA(1,864),VECTSVP(1,864),(VECTSVA(1,8
64)-
```

```
VECTSVA(1,576)),VECTEPTLA(1,864),VECTEPTLP(1,864),(VECTEPT
LA(1,864)-VECTEPTLA(1,576));
       4,VECTFVA(1,1152),VECTFVP(1,1152),(VECTFVA(1,1152)-
VECTFVA(1,864)),VECTSVA(1,1152),VECTSVP(1,1152),(VECTSVA(1
,1152)-
VECTSVA(1,864)),VECTEPTLA(1,1152),VECTEPTLP(1,1152),(VECTE
PTLA(1,1152)-VECTEPTLA(1,864));
       5,VECTFVA(1,1440),VECTFVP(1,1440),(VECTFVA(1,1440)-
VECTFVA(1,1152)),VECTSVA(1,1440),VECTSVP(1,1440),(VECTSVA(
1,1440)-
VECTSVA(1,1152)),VECTEPTLA(1,1440),VECTEPTLP(1,1440),(VECT
EPTLA(1,1440)-VECTEPTLA(1,1152));
       6,VECTFVA(1,1728),VECTFVP(1,1728),(VECTFVA(1,1728)-
VECTFVA(1,1440)),VECTSVA(1,1728),VECTSVP(1,1728),(VECTSVA(
1,1728)-
VECTSVA(1,1440)),VECTEPTLA(1,1728),VECTEPTLP(1,1728),(VECT
EPTLA(1,1728)-VECTEPTLA(1,1440));
       7,VECTFVA(1,2016),VECTFVP(1,2016),(VECTFVA(1,2016)-
VECTFVA(1,1728)),VECTSVA(1,2016),VECTSVP(1,2016),(VECTSVA(
1,2016)-
VECTSVA(1,1728)),VECTEPTLA(1,2016),VECTEPTLP(1,2016),(VECT
EPTLA(1,2016)-VECTEPTLA(1,1728));
       8,VECTFVA(1,2304),VECTFVP(1,2304),(VECTFVA(1,2304)-
VECTFVA(1,2016)),VECTSVA(1,2304),VECTSVP(1,2304),(VECTSVA(
1,2304)-
VECTSVA(1,2016)),VECTEPTLA(1,2304),VECTEPTLP(1,2304),(VECT
EPTLA(1,2304)-VECTEPTLA(1,2016));
       9,VECTFVA(1,2592),VECTFVP(1,2592),(VECTFVA(1,2592)-
VECTFVA(1,2304)),VECTSVA(1,2592),VECTSVP(1,2592),(VECTSVA(
1,2592)-
VECTSVA(1,2304)),VECTEPTLA(1,2592),VECTEPTLP(1,2592),(VECT
EPTLA(1,2592)-VECTEPTLA(1,2304));

10,VECTFVA(1,2880),VECTFVP(1,2880),(VECTFVA(1,2880)-
VECTFVA(1,2592)),VECTSVA(1,2880),VECTSVP(1,2880),(VECTSVA(
1,2880)-
VECTSVA(1,2592)),VECTEPTLA(1,2880),VECTEPTLP(1,2880),(VECT
EPTLA(1,2880)-VECTEPTLA(1,2592));

11,VECTFVA(1,3168),VECTFVP(1,3168),(VECTFVA(1,3168)-
VECTFVA(1,2880)),VECTSVA(1,3168),VECTSVP(1,3168),(VECTSVA(
1,3168)-
VECTSVA(1,2880)),VECTEPTLA(1,3168),VECTEPTLP(1,3168),(VECT
EPTLA(1,3168)-VECTEPTLA(1,2880));

12,VECTFVA(1,3456),VECTFVP(1,3456),(VECTFVA(1,3456)-
VECTFVA(1,3168)),VECTSVA(1,3456),VECTSVP(1,3456),(VECTSVA(
```

```
1,3456)-
VECTSVA(1,3168)),VECTEPTLA(1,3456),VECTEPTLP(1,3456),(VECT
EPTLA(1,3456)-VECTEPTLA(1,3168));

13,VECTFVA(1,3744),VECTFVP(1,3744),(VECTFVA(1,3744)-
VECTFVA(1,3456)),VECTSVA(1,3744),VECTSVP(1,3744),(VECTSVA(
1,3744)-
VECTSVA(1,3456)),VECTEPTLA(1,3744),VECTEPTLP(1,3744),(VECT
EPTLA(1,3744)-VECTEPTLA(1,3456));

14,VECTFVA(1,4032),VECTFVP(1,4032),(VECTFVA(1,4032)-
VECTFVA(1,3744)),VECTSVA(1,4032),VECTSVP(1,4032),(VECTSVA(
1,4032)-
VECTSVA(1,3744)),VECTEPTLA(1,4032),VECTEPTLP(1,4032),(VECT
EPTLA(1,4032)-VECTEPTLA(1,3744));

15,VECTFVA(1,4320),VECTFVP(1,4320),(VECTFVA(1,4320)-
VECTFVA(1,4032)),VECTSVA(1,4320),VECTSVP(1,4320),(VECTSVA(
1,4320)-
VECTSVA(1,4032)),VECTEPTLA(1,4320),VECTEPTLP(1,4320),(VECT
EPTLA(1,4320)-VECTEPTLA(1,4032));

16,VECTFVA(1,4608),VECTFVP(1,4608),(VECTFVA(1,4608)-
VECTFVA(1,4320)),VECTSVA(1,4608),VECTSVP(1,4608),(VECTSVA(
1,4608)-
VECTSVA(1,4320)),VECTEPTLA(1,4608),VECTEPTLP(1,4608),(VECT
EPTLA(1,4608)-VECTEPTLA(1,4320));

17,VECTFVA(1,4896),VECTFVP(1,4896),(VECTFVA(1,4896)-
VECTFVA(1,4608)),VECTSVA(1,4896),VECTSVP(1,4896),(VECTSVA(
1,4896)-
VECTSVA(1,4608)),VECTEPTLA(1,4896),VECTEPTLP(1,4896),(VECT
EPTLA(1,4896)-VECTEPTLA(1,4608));

18,VECTFVA(1,5184),VECTFVP(1,5184),(VECTFVA(1,5184)-
VECTFVA(1,4896)),VECTSVA(1,5184),VECTSVP(1,5184),(VECTSVA(
1,5184)-
VECTSVA(1,4896)),VECTEPTLA(1,5184),VECTEPTLP(1,5184),(VECT
EPTLA(1,5184)-VECTEPTLA(1,4896));

19,VECTFVA(1,5472),VECTFVP(1,5472),(VECTFVA(1,5472)-
VECTFVA(1,5184)),VECTSVA(1,5472),VECTSVP(1,5472),(VECTSVA(
1,5472)-
VECTSVA(1,5184)),VECTEPTLA(1,5472),VECTEPTLP(1,5472),(VECT
EPTLA(1,5472)-VECTEPTLA(1,5184));

20,VECTFVA(1,5760),VECTFVP(1,5760),(VECTFVA(1,5760)-
```

```
VECTFVA(1,5472)),VECTSVA(1,5760),VECTSVP(1,5760),(VECTSVA(
1,5760)-
VECTSVA(1,5472)),VECTEPTLA(1,5760),VECTEPTLP(1,5760),(VECT
EPTLA(1,5760)-VECTEPTLA(1,5472));

21,VECTFVA(1,6048),VECTFVP(1,6048),(VECTFVA(1,6048)-
VECTFVA(1,5760)),VECTSVA(1,6048),VECTSVP(1,6048),(VECTSVA(
1,6048)-
VECTSVA(1,5760)),VECTEPTLA(1,6048),VECTEPTLP(1,6048),(VECT
EPTLA(1,6048)-VECTEPTLA(1,5760));

22,VECTFVA(1,6336),VECTFVP(1,6336),(VECTFVA(1,6336)-
VECTFVA(1,6048)),VECTSVA(1,6336),VECTSVP(1,6336),(VECTSVA(
1,6336)-
VECTSVA(1,6048)),VECTEPTLA(1,6336),VECTEPTLP(1,6336),(VECT
EPTLA(1,6336)-VECTEPTLA(1,6048));

23,VECTFVA(1,6624),VECTFVP(1,6624),(VECTFVA(1,6624)-
VECTFVA(1,6336)),VECTSVA(1,6624),VECTSVP(1,6624),(VECTSVA(
1,6624)-
VECTSVA(1,6336)),VECTEPTLA(1,6624),VECTEPTLP(1,6624),(VECT
EPTLA(1,6624)-VECTEPTLA(1,6336));

24,VECTFVA(1,6912),VECTFVP(1,6912),(VECTFVA(1,6912)-
VECTFVA(1,6624)),VECTSVA(1,6912),VECTSVP(1,6912),(VECTSVA(
1,6912)-
VECTSVA(1,6624)),VECTEPTLA(1,6912),VECTEPTLP(1,6912),(VECT
EPTLA(1,6912)-VECTEPTLA(1,6624));

25,VECTFVA(1,7200),VECTFVP(1,7200),(VECTFVA(1,7200)-
VECTFVA(1,6912)),VECTSVA(1,7200),VECTSVP(1,7200),(VECTSVA(
1,7200)-
VECTSVA(1,6912)),VECTEPTLA(1,7200),VECTEPTLP(1,7200),(VECT
EPTLA(1,7200)-VECTEPTLA(1,6912));

26,VECTFVA(1,7488),VECTFVP(1,7488),(VECTFVA(1,7488)-
VECTFVA(1,7200)),VECTSVA(1,7488),VECTSVP(1,7488),(VECTSVA(
1,7488)-
VECTSVA(1,7200)),VECTEPTLA(1,7488),VECTEPTLP(1,7488),(VECT
EPTLA(1,7488)-VECTEPTLA(1,7200));

27,VECTFVA(1,7776),VECTFVP(1,7776),(VECTFVA(1,7776)-
VECTFVA(1,7488)),VECTSVA(1,7776),VECTSVP(1,7776),(VECTSVA(
1,7776)-
VECTSVA(1,7488)),VECTEPTLA(1,7776),VECTEPTLP(1,7776),(VECT
EPTLA(1,7776)-VECTEPTLA(1,7488));
```

```
28,VECTFVA(1,8064),VECTFVP(1,8064),(VECTFVA(1,8064)-
VECTFVA(1,7776)),VECTSVA(1,8064),VECTSVP(1,8064),(VECTSVA(
1,8064)-
VECTSVA(1,7776)),VECTEPTLA(1,8064),VECTEPTLP(1,8064),(VECT
EPTLA(1,8064)-VECTEPTLA(1,7776));

29,VECTFVA(1,8352),VECTFVP(1,8352),(VECTFVA(1,8352)-
VECTFVA(1,8064)),VECTSVA(1,8352),VECTSVP(1,8352),(VECTSVA(
1,8352)-
VECTSVA(1,8064)),VECTEPTLA(1,8352),VECTEPTLP(1,8352),(VECT
EPTLA(1,8352)-VECTEPTLA(1,8064));

30,VECTFVA(1,8640),VECTFVP(1,8640),(VECTFVA(1,8640)-
VECTFVA(1,8352)),VECTSVA(1,8640),VECTSVP(1,8640),(VECTSVA(
1,8640)-
VECTSVA(1,8352)),VECTEPTLA(1,8640),VECTEPTLP(1,8640),(VECT
EPTLA(1,8640)-VECTEPTLA(1,8352));

31,VECTFVA(1,8928),VECTFVP(1,8928),(VECTFVA(1,8928)-
VECTFVA(1,8640)),VECTSVA(1,8928),VECTSVP(1,8928),(VECTSVA(
1,8928)-
VECTSVA(1,8640)),VECTEPTLA(1,8928),VECTEPTLP(1,8928),(VECT
EPTLA(1,8928)-VECTEPTLA(1,8640));

32,VECTFVA(1,9216),VECTFVP(1,9216),(VECTFVA(1,9216)-
VECTFVA(1,8928)),VECTSVA(1,9216),VECTSVP(1,9216),(VECTSVA(
1,9216)-
VECTSVA(1,8928)),VECTEPTLA(1,9216),VECTEPTLP(1,9216),(VECT
EPTLA(1,9216)-VECTEPTLA(1,8928));

33,VECTFVA(1,9504),VECTFVP(1,9504),(VECTFVA(1,9504)-
VECTFVA(1,9216)),VECTSVA(1,9504),VECTSVP(1,9504),(VECTSVA(
1,9504)-
VECTSVA(1,9216)),VECTEPTLA(1,9504),VECTEPTLP(1,9504),(VECT
EPTLA(1,9504)-VECTEPTLA(1,9216));

34,VECTFVA(1,9792),VECTFVP(1,9792),(VECTFVA(1,9792)-
VECTFVA(1,9504)),VECTSVA(1,9792),VECTSVP(1,9792),(VECTSVA(
1,9792)-
VECTSVA(1,9504)),VECTEPTLA(1,9792),VECTEPTLP(1,9792),(VECT
EPTLA(1,9792)-VECTEPTLA(1,9504));

35,VECTFVA(1,10080),VECTFVP(1,10080),(VECTFVA(1,10080)-
VECTFVA(1,9792)),VECTSVA(1,10080),VECTSVP(1,10080),(VECTSV
A(1,10080)-
```

```
VECTSVA(1,9792)),VECTEPTLA(1,10080),VECTEPTLP(1,10080),(VE
CTEPTLA(1,10080)-VECTEPTLA(1,9792));};

ftop= figure('name' , 'Top Layer Diagnostics');
atab = uitable('columnname', col, 'data', dat);
table_extent = get(atab,'Extent');
set(atab,'Position',[1 -25 table_extent(3)
table_extent(4)+40]);
figure_size = get(ftop,'outerposition');
desired_fig_size = [(figure_size(1)+150)
(figure_size(2)+150) (table_extent(3)+155)
(table_extent(4)+100)];
set(ftop,'outerposition', desired_fig_size);
saveas(atab, 'DIAGTop1.pdf')

dat2 =
{36,VECTFVA(1,10368),VECTFVP(1,10368),(VECTFVA(1,10368)-
VECTFVA(1,10080)),VECTSVA(1,10368),VECTSVP(1,10368),(VECTS
VA(1,10368)-
VECTSVA(1,10080)),VECTEPTLA(1,10368),VECTEPTLP(1,10368),(V
ECTEPTLA(1,10368)-VECTEPTLA(1,10080));

37,VECTFVA(1,10658),VECTFVP(1,10658),(VECTFVA(1,10658)-
VECTFVA(1,10368)),VECTSVA(1,10658),VECTSVP(1,10658),(VECTS
VA(1,10658)-
VECTSVA(1,10368)),VECTEPTLA(1,10658),VECTEPTLP(1,10658),(V
ECTEPTLA(1,10658)-VECTEPTLA(1,10368));

38,VECTFVA(1,10944),VECTFVP(1,10944),(VECTFVA(1,10944)-
VECTFVA(1,10658)),VECTSVA(1,10944),VECTSVP(1,10944),(VECTS
VA(1,10944)-
VECTSVA(1,10658)),VECTEPTLA(1,10944),VECTEPTLP(1,10944),(V
ECTEPTLA(1,10944)-VECTEPTLA(1,10658));

39,VECTFVA(1,11232),VECTFVP(1,11232),(VECTFVA(1,11232)-
VECTFVA(1,10944)),VECTSVA(1,11232),VECTSVP(1,11232),(VECTS
VA(1,11232)-
VECTSVA(1,10944)),VECTEPTLA(1,11232),VECTEPTLP(1,11232),(V
ECTEPTLA(1,11232)-VECTEPTLA(1,10944));

40,VECTFVA(1,11520),VECTFVP(1,11520),(VECTFVA(1,11520)-
VECTFVA(1,11232)),VECTSVA(1,11520),VECTSVP(1,11520),(VECTS
VA(1,11520)-
VECTSVA(1,11232)),VECTEPTLA(1,11520),VECTEPTLP(1,11520),(V
ECTEPTLA(1,11520)-VECTEPTLA(1,11232));

41,VECTFVA(1,11808),VECTFVP(1,11808),(VECTFVA(1,11808)-
```

```
VECTFVA(1,11520)),VECTSVA(1,11808),VECTSVP(1,11808),(VECTS
VA(1,11808)-
VECTSVA(1,11520)),VECTEPTLA(1,11808),VECTEPTLP(1,11808),(V
ECTEPTLA(1,11808)-VECTEPTLA(1,11520));

42,VECTFVA(1,12096),VECTFVP(1,12096),(VECTFVA(1,12096)-
VECTFVA(1,11808)),VECTSVA(1,12096),VECTSVP(1,12096),(VECTS
VA(1,12096)-
VECTSVA(1,11808)),VECTEPTLA(1,12096),VECTEPTLP(1,12096),(V
ECTEPTLA(1,12096)-VECTEPTLA(1,11808));

43,VECTFVA(1,12384),VECTFVP(1,12384),(VECTFVA(1,12384)-
VECTFVA(1,12096)),VECTSVA(1,12384),VECTSVP(1,12384),(VECTS
VA(1,12384)-
VECTSVA(1,12096)),VECTEPTLA(1,12384),VECTEPTLP(1,12384),(V
ECTEPTLA(1,12384)-VECTEPTLA(1,12096));

44,VECTFVA(1,12672),VECTFVP(1,12672),(VECTFVA(1,12672)-
VECTFVA(1,12384)),VECTSVA(1,12672),VECTSVP(1,12672),(VECTS
VA(1,12672)-
VECTSVA(1,12384)),VECTEPTLA(1,12672),VECTEPTLP(1,12672),(V
ECTEPTLA(1,12672)-VECTEPTLA(1,12384));

45,VECTFVA(1,12960),VECTFVP(1,12960),(VECTFVA(1,12960)-
VECTFVA(1,12672)),VECTSVA(1,12960),VECTSVP(1,12960),(VECTS
VA(1,12960)-
VECTSVA(1,12672)),VECTEPTLA(1,12960),VECTEPTLP(1,12960),(V
ECTEPTLA(1,12960)-VECTEPTLA(1,12672));

46,VECTFVA(1,13248),VECTFVP(1,13248),(VECTFVA(1,13248)-
VECTFVA(1,12960)),VECTSVA(1,13248),VECTSVP(1,13248),(VECTS
VA(1,13248)-
VECTSVA(1,12960)),VECTEPTLA(1,13248),VECTEPTLP(1,13248),(V
ECTEPTLA(1,13248)-VECTEPTLA(1,12960));

47,VECTFVA(1,13536),VECTFVP(1,13536),(VECTFVA(1,13536)-
VECTFVA(1,13248)),VECTSVA(1,13536),VECTSVP(1,13536),(VECTS
VA(1,13536)-
VECTSVA(1,13248)),VECTEPTLA(1,13536),VECTEPTLP(1,13536),(V
ECTEPTLA(1,13536)-VECTEPTLA(1,13248));

48,VECTFVA(1,13824),VECTFVP(1,13824),(VECTFVA(1,13824)-
VECTFVA(1,13536)),VECTSVA(1,13824),VECTSVP(1,13824),(VECTS
VA(1,13824)-
VECTSVA(1,13536)),VECTEPTLA(1,13824),VECTEPTLP(1,13824),(V
ECTEPTLA(1,13824)-VECTEPTLA(1,13536));
```

```
49,VECTFVA(1,14112),VECTFVP(1,14112),(VECTFVA(1,14112)-
VECTFVA(1,13824)),VECTSVA(1,14112),VECTSVP(1,14112),(VECTS
VA(1,14112)-
VECTSVA(1,13824)),VECTEPTLA(1,14112),VECTEPTLP(1,14112),(V
ECTEPTLA(1,14112)-VECTEPTLA(1,13824));

50,VECTFVA(1,14400),VECTFVP(1,14400),(VECTFVA(1,14400)-
VECTFVA(1,14112)),VECTSVA(1,14400),VECTSVP(1,14400),(VECTS
VA(1,14400)-
VECTSVA(1,14112)),VECTEPTLA(1,14400),VECTEPTLP(1,14400),(V
ECTEPTLA(1,14400)-VECTEPTLA(1,14112));

51,VECTFVA(1,14688),VECTFVP(1,14688),(VECTFVA(1,14688)-
VECTFVA(1,14400)),VECTSVA(1,14688),VECTSVP(1,14688),(VECTS
VA(1,14688)-
VECTSVA(1,14400)),VECTEPTLA(1,14688),VECTEPTLP(1,14688),(V
ECTEPTLA(1,14688)-VECTEPTLA(1,14400));

52,VECTFVA(1,14976),VECTFVP(1,14976),(VECTFVA(1,14976)-
VECTFVA(1,14688)),VECTSVA(1,14976),VECTSVP(1,14976),(VECTS
VA(1,14976)-
VECTSVA(1,14688)),VECTEPTLA(1,14976),VECTEPTLP(1,14976),(V
ECTEPTLA(1,14976)-VECTEPTLA(1,14688));

53,VECTFVA(1,15264),VECTFVP(1,15264),(VECTFVA(1,15264)-
VECTFVA(1,14976)),VECTSVA(1,15264),VECTSVP(1,15264),(VECTS
VA(1,15264)-
VECTSVA(1,14976)),VECTEPTLA(1,15264),VECTEPTLP(1,15264),(V
ECTEPTLA(1,15264)-VECTEPTLA(1,14976));

54,VECTFVA(1,15552),VECTFVP(1,15552),(VECTFVA(1,15552)-
VECTFVA(1,15264)),VECTSVA(1,15552),VECTSVP(1,15552),(VECTS
VA(1,15552)-
VECTSVA(1,15264)),VECTEPTLA(1,15552),VECTEPTLP(1,15552),(V
ECTEPTLA(1,15552)-VECTEPTLA(1,15264));

55,VECTFVA(1,15840),VECTFVP(1,15840),(VECTFVA(1,15840)-
VECTFVA(1,15552)),VECTSVA(1,15840),VECTSVP(1,15840),(VECTS
VA(1,15840)-
VECTSVA(1,15552)),VECTEPTLA(1,15840),VECTEPTLP(1,15840),(V
ECTEPTLA(1,15840)-VECTEPTLA(1,15552));

56,VECTFVA(1,16128),VECTFVP(1,16128),(VECTFVA(1,16128)-
VECTFVA(1,15840)),VECTSVA(1,16128),VECTSVP(1,16128),(VECTS
VA(1,16128)-
```

```
VECTSVA(1,15840)),VECTEPTLA(1,16128),VECTEPTLP(1,16128),(V
ECTEPTLA(1,16128)-VECTEPTLA(1,15840));

57,VECTFVA(1,16416),VECTFVP(1,16416),(VECTFVA(1,16416)-
VECTFVA(1,16128)),VECTSVA(1,16416),VECTSVP(1,16416),(VECTS
VA(1,16416)-
VECTSVA(1,16128)),VECTEPTLA(1,16416),VECTEPTLP(1,16416),(V
ECTEPTLA(1,16416)-VECTEPTLA(1,16128));

58,VECTFVA(1,16704),VECTFVP(1,16704),(VECTFVA(1,16704)-
VECTFVA(1,16416)),VECTSVA(1,16704),VECTSVP(1,16704),(VECTS
VA(1,16704)-
VECTSVA(1,16416)),VECTEPTLA(1,16704),VECTEPTLP(1,16704),(V
ECTEPTLA(1,16704)-VECTEPTLA(1,16416));

59,VECTFVA(1,16992),VECTFVP(1,16992),(VECTFVA(1,16992)-
VECTFVA(1,16704)),VECTSVA(1,16992),VECTSVP(1,16992),(VECTS
VA(1,16992)-
VECTSVA(1,16704)),VECTEPTLA(1,16992),VECTEPTLP(1,16992),(V
ECTEPTLA(1,16992)-VECTEPTLA(1,16704));

60,VECTFVA(1,17280),VECTFVP(1,17280),(VECTFVA(1,17280)-
VECTFVA(1,16992)),VECTSVA(1,17280),VECTSVP(1,17280),(VECTS
VA(1,17280)-
VECTSVA(1,16992)),VECTEPTLA(1,17280),VECTEPTLP(1,17280),(V
ECTEPTLA(1,17280)-VECTEPTLA(1,16992));

61,VECTFVA(1,17568),VECTFVP(1,17568),(VECTFVA(1,17568)-
VECTFVA(1,17280)),VECTSVA(1,17568),VECTSVP(1,17568),(VECTS
VA(1,17568)-
VECTSVA(1,17280)),VECTEPTLA(1,17568),VECTEPTLP(1,17568),(V
ECTEPTLA(1,17568)-VECTEPTLA(1,17280));

62,VECTFVA(1,17856),VECTFVP(1,17856),(VECTFVA(1,17856)-
VECTFVA(1,17568)),VECTSVA(1,17856),VECTSVP(1,17856),(VECTS
VA(1,17856)-
VECTSVA(1,17568)),VECTEPTLA(1,17856),VECTEPTLP(1,17856),(V
ECTEPTLA(1,17856)-VECTEPTLA(1,17568));

63,VECTFVA(1,18144),VECTFVP(1,18144),(VECTFVA(1,18144)-
VECTFVA(1,17856)),VECTSVA(1,18144),VECTSVP(1,18144),(VECTS
VA(1,18144)-
VECTSVA(1,17856)),VECTEPTLA(1,18144),VECTEPTLP(1,18144),(V
ECTEPTLA(1,18144)-VECTEPTLA(1,17856));};

ftop2= figure('name' , 'Top Layer Diagnostics');
atab1 = uitable('columnname', col, 'data', dat2);
```

```
table_extent = get(atab1,'Extent');
set(atab1,'Position',[1 -25 table_extent(3)
table_extent(4)+40]);
figure_size = get(ftop2,'outerposition');
desired_fig_size = [(figure_size(1)+150)
(figure_size(2)+150) (table_extent(3)+155)
(table_extent(4)+100)];
set(ftop2,'outerposition', desired_fig_size);
saveas(atab1, 'DIAGTop2.pdf')

%Grafiek percentages en aantallen Soil Layer
col2 = {'Day' , '#EP', '%EP', '?#EP', '#SP', '%SP',
'?#SP', '#BP', '%BP', '?#BP'};

dat3 = {0,488198,0.0,0,1,0,0.0,0,0,0,;
       1,VECTEPA(1,288),VECTEPP(1,288),(VECTEPA(1,288)-
488198), VECTSPA(1,288),VECTSPP(1,288),(VECTSPA(1,288)-
0),VECTBPA(1,288),VECTBPP(1,288),(VECTBPA(1,288)-0);
       2,VECTEPA(1,576),VECTEPP(1,576),(VECTEPA(1,576)-
VECTEPA(1,288)),VECTSPA(1,576),VECTSPP(1,576),(VECTSPA(1,5
76)-
VECTSPA(1,288)),VECTBPA(1,576),VECTBPP(1,576),(VECTBPA(1,5
76)-VECTBPA(1,288));
       3,VECTEPA(1,864),VECTEPP(1,864),(VECTEPA(1,864)-
VECTEPA(1,576)),VECTSPA(1,864),VECTSPP(1,864),(VECTSPA(1,8
64)-
VECTSPA(1,576)),VECTBPA(1,864),VECTBPP(1,864),(VECTBPA(1,8
64)-VECTBPA(1,576));
       4,VECTEPA(1,1152),VECTEPP(1,1152),(VECTEPA(1,1152)-
VECTEPA(1,864)),VECTSPA(1,1152),VECTSPP(1,1152),(VECTSPA(1
,1152)-
VECTSPA(1,864)),VECTBPA(1,1152),VECTBPP(1,1152),(VECTBPA(1
,1152)-VECTBPA(1,864));
       5,VECTEPA(1,1440),VECTEPP(1,1440),(VECTEPA(1,1440)-
VECTEPA(1,1152)),VECTSPA(1,1440),VECTSPP(1,1440),(VECTSPA(
1,1440)-
VECTSPA(1,1152)),VECTBPA(1,1440),VECTBPP(1,1440),(VECTBPA(
1,1440)-VECTBPA(1,1152));
       6,VECTEPA(1,1728),VECTEPP(1,1728),(VECTEPA(1,1728)-
VECTEPA(1,1440)),VECTSPA(1,1728),VECTSPP(1,1728),(VECTSPA(
1,1728)-
VECTSPA(1,1440)),VECTBPA(1,1728),VECTBPP(1,1728),(VECTBPA(
1,1728)-VECTBPA(1,1440));
       7,VECTEPA(1,2016),VECTEPP(1,2016),(VECTEPA(1,2016)-
VECTEPA(1,1728)),VECTSPA(1,2016),VECTSPP(1,2016),(VECTSPA(
1,2016)-
```

```
VECTSPA(1,1728)),VECTBPA(1,2016),VECTBPP(1,2016),(VECTBPA(
1,2016)-VECTBPA(1,1728));
       8,VECTEPA(1,2304),VECTEPP(1,2304),(VECTEPA(1,2304)-
VECTEPA(1,2016)),VECTSPA(1,2304),VECTSPP(1,2304),(VECTSPA(
1,2304)-
VECTSPA(1,2016)),VECTBPA(1,2304),VECTBPP(1,2304),(VECTBPA(
1,2304)-VECTBPA(1,2016));
       9,VECTEPA(1,2592),VECTEPP(1,2592),(VECTEPA(1,2592)-
VECTEPA(1,2304)),VECTSPA(1,2592),VECTSPP(1,2592),(VECTSPA(
1,2592)-
VECTSPA(1,2304)),VECTBPA(1,2592),VECTBPP(1,2592),(VECTBPA(
1,2592)-VECTBPA(1,2304));

10,VECTEPA(1,2880),VECTEPP(1,2880),(VECTEPA(1,2880)-
VECTEPA(1,2592)),VECTSPA(1,2880),VECTSPP(1,2880),(VECTSPA(
1,2880)-
VECTSPA(1,2592)),VECTBPA(1,2880),VECTBPP(1,2880),(VECTBPA(
1,2880)-VECTBPA(1,2592));

11,VECTEPA(1,3168),VECTEPP(1,3168),(VECTEPA(1,3168)-
VECTEPA(1,2880)),VECTSPA(1,3168),VECTSPP(1,3168),(VECTSPA(
1,3168)-
VECTSPA(1,2880)),VECTBPA(1,3168),VECTBPP(1,3168),(VECTBPA(
1,3168)-VECTBPA(1,2880));

12,VECTEPA(1,3456),VECTEPP(1,3456),(VECTEPA(1,3456)-
VECTEPA(1,3168)),VECTSPA(1,3456),VECTSPP(1,3456),(VECTSPA(
1,3456)-
VECTSPA(1,3168)),VECTBPA(1,3456),VECTBPP(1,3456),(VECTBPA(
1,3456)-VECTBPA(1,3168));

13,VECTEPA(1,3744),VECTEPP(1,3744),(VECTEPA(1,3744)-
VECTEPA(1,3456)),VECTSPA(1,3744),VECTSPP(1,3744),(VECTSPA(
1,3744)-
VECTSPA(1,3456)),VECTBPA(1,3744),VECTBPP(1,3744),(VECTBPA(
1,3744)-VECTBPA(1,3456));

14,VECTEPA(1,4032),VECTEPP(1,4032),(VECTEPA(1,4032)-
VECTEPA(1,3744)),VECTSPA(1,4032),VECTSPP(1,4032),(VECTSPA(
1,4032)-
VECTSPA(1,3744)),VECTBPA(1,4032),VECTBPP(1,4032),(VECTBPA(
1,4032)-VECTBPA(1,3744));

15,VECTEPA(1,4320),VECTEPP(1,4320),(VECTEPA(1,4320)-
VECTEPA(1,4032)),VECTSPA(1,4320),VECTSPP(1,4320),(VECTSPA(
1,4320)-
```

```
VECTSPA(1,4032)),VECTBPA(1,4320),VECTBPP(1,4320),(VECTBPA(
1,4320)-VECTBPA(1,4032));

16,VECTEPA(1,4608),VECTEPP(1,4608),(VECTEPA(1,4608)-
VECTEPA(1,4320)),VECTSPA(1,4608),VECTSPP(1,4608),(VECTSPA(
1,4608)-
VECTSPA(1,4320)),VECTBPA(1,4608),VECTBPP(1,4608),(VECTBPA(
1,4608)-VECTBPA(1,4320));

17,VECTEPA(1,4896),VECTEPP(1,4896),(VECTEPA(1,4896)-
VECTEPA(1,4608)),VECTSPA(1,4896),VECTSPP(1,4896),(VECTSPA(
1,4896)-
VECTSPA(1,4608)),VECTBPA(1,4896),VECTBPP(1,4896),(VECTBPA(
1,4896)-VECTBPA(1,4608));

18,VECTEPA(1,5184),VECTEPP(1,5184),(VECTEPA(1,5184)-
VECTEPA(1,4896)),VECTSPA(1,5184),VECTSPP(1,5184),(VECTSPA(
1,5184)-
VECTSPA(1,4896)),VECTBPA(1,5184),VECTBPP(1,5184),(VECTBPA(
1,5184)-VECTBPA(1,4896));

19,VECTEPA(1,5472),VECTEPP(1,5472),(VECTEPA(1,5472)-
VECTEPA(1,5184)),VECTSPA(1,5472),VECTSPP(1,5472),(VECTSPA(
1,5472)-
VECTSPA(1,5184)),VECTBPA(1,5472),VECTBPP(1,5472),(VECTBPA(
1,5472)-VECTBPA(1,5184));

20,VECTEPA(1,5760),VECTEPP(1,5760),(VECTEPA(1,5760)-
VECTEPA(1,5472)),VECTSPA(1,5760),VECTSPP(1,5760),(VECTSPA(
1,5760)-
VECTSPA(1,5472)),VECTBPA(1,5760),VECTBPP(1,5760),(VECTBPA(
1,5760)-VECTBPA(1,5472));

21,VECTEPA(1,6048),VECTEPP(1,6048),(VECTEPA(1,6048)-
VECTEPA(1,5760)),VECTSPA(1,6048),VECTSPP(1,6048),(VECTSPA(
1,6048)-
VECTSPA(1,5760)),VECTBPA(1,6048),VECTBPP(1,6048),(VECTBPA(
1,6048)-VECTBPA(1,5760));

22,VECTEPA(1,6336),VECTEPP(1,6336),(VECTEPA(1,6336)-
VECTEPA(1,6048)),VECTSPA(1,6336),VECTSPP(1,6336),(VECTSPA(
1,6336)-
VECTSPA(1,6048)),VECTBPA(1,6336),VECTBPP(1,6336),(VECTBPA(
1,6336)-VECTBPA(1,6048));

23,VECTEPA(1,6624),VECTEPP(1,6624),(VECTEPA(1,6624)-
VECTEPA(1,6336)),VECTSPA(1,6624),VECTSPP(1,6624),(VECTSPA(
```

```
1,6624)-
VECTSPA(1,6336)),VECTBPA(1,6624),VECTBPP(1,6624),(VECTBPA(
1,6624)-VECTBPA(1,6336));

24,VECTEPA(1,6912),VECTEPP(1,6912),(VECTEPA(1,6912)-
VECTEPA(1,6624)),VECTSPA(1,6912),VECTSPP(1,6912),(VECTSPA(
1,6912)-
VECTSPA(1,6624)),VECTBPA(1,6912),VECTBPP(1,6912),(VECTBPA(
1,6912)-VECTBPA(1,6624));

25,VECTEPA(1,7200),VECTEPP(1,7200),(VECTEPA(1,7200)-
VECTEPA(1,6912)),VECTSPA(1,7200),VECTSPP(1,7200),(VECTSPA(
1,7200)-
VECTSPA(1,6912)),VECTBPA(1,7200),VECTBPP(1,7200),(VECTBPA(
1,7200)-VECTBPA(1,6912));

26,VECTEPA(1,7488),VECTEPP(1,7488),(VECTEPA(1,7488)-
VECTEPA(1,7200)),VECTSPA(1,7488),VECTSPP(1,7488),(VECTSPA(
1,7488)-
VECTSPA(1,7200)),VECTBPA(1,7488),VECTBPP(1,7488),(VECTBPA(
1,7488)-VECTBPA(1,7200));

27,VECTEPA(1,7776),VECTEPP(1,7776),(VECTEPA(1,7776)-
VECTEPA(1,7488)),VECTSPA(1,7776),VECTSPP(1,7776),(VECTSPA(
1,7776)-
VECTSPA(1,7488)),VECTBPA(1,7776),VECTBPP(1,7776),(VECTBPA(
1,7776)-VECTBPA(1,7488));

28,VECTEPA(1,8064),VECTEPP(1,8064),(VECTEPA(1,8064)-
VECTEPA(1,7776)),VECTSPA(1,8064),VECTSPP(1,8064),(VECTSPA(
1,8064)-
VECTSPA(1,7776)),VECTBPA(1,8064),VECTBPP(1,8064),(VECTBPA(
1,8064)-VECTBPA(1,7776));

29,VECTEPA(1,8352),VECTEPP(1,8352),(VECTEPA(1,8352)-
VECTEPA(1,8064)),VECTSPA(1,8352),VECTSPP(1,8352),(VECTSPA(
1,8352)-
VECTSPA(1,8064)),VECTBPA(1,8352),VECTBPP(1,8352),(VECTBPA(
1,8352)-VECTBPA(1,8064));

30,VECTEPA(1,8640),VECTEPP(1,8640),(VECTEPA(1,8640)-
VECTEPA(1,8352)),VECTSPA(1,8640),VECTSPP(1,8640),(VECTSPA(
1,8640)-
VECTSPA(1,8352)),VECTBPA(1,8640),VECTBPP(1,8640),(VECTBPA(
1,8640)-VECTBPA(1,8352));

31,VECTEPA(1,8928),VECTEPP(1,8928),(VECTEPA(1,8928)-
```

```
VECTEPA(1,8640)),VECTSPA(1,8928),VECTSPP(1,8928),(VECTSPA(
1,8928)-
VECTSPA(1,8640)),VECTBPA(1,8928),VECTBPP(1,8928),(VECTBPA(
1,8928)-VECTBPA(1,8640));

32,VECTEPA(1,9216),VECTEPP(1,9216),(VECTEPA(1,9216)-
VECTEPA(1,8928)),VECTSPA(1,9216),VECTSPP(1,9216),(VECTSPA(
1,9216)-
VECTSPA(1,8928)),VECTBPA(1,9216),VECTBPP(1,9216),(VECTBPA(
1,9216)-VECTBPA(1,8928));

33,VECTEPA(1,9504),VECTEPP(1,9504),(VECTEPA(1,9504)-
VECTEPA(1,9216)),VECTSPA(1,9504),VECTSPP(1,9504),(VECTSPA(
1,9504)-
VECTSPA(1,9216)),VECTBPA(1,9504),VECTBPP(1,9504),(VECTBPA(
1,9504)-VECTBPA(1,9216));

34,VECTEPA(1,9792),VECTEPP(1,9792),(VECTEPA(1,9792)-
VECTEPA(1,9504)),VECTSPA(1,9792),VECTSPP(1,9792),(VECTSPA(
1,9792)-
VECTSPA(1,9504)),VECTBPA(1,9792),VECTBPP(1,9792),(VECTBPA(
1,9792)-VECTBPA(1,9504));

35,VECTEPA(1,10080),VECTEPP(1,10080),(VECTEPA(1,10080)-
VECTEPA(1,9792)),VECTSPA(1,10080),VECTSPP(1,10080),(VECTSP
A(1,10080)-
VECTSPA(1,9792)),VECTBPA(1,10080),VECTBPP(1,10080),(VECTBP
A(1,10080)-VECTBPA(1,9792));};

fsoil= figure('name' , 'Soil Layer Diagnostics');
btab1 = uitable('columnname', col2, 'data', dat3);
table_extent = get(btab1,'Extent');
set(btab1,'Position',[1 -25 table_extent(3)
table_extent(4)+40])
figure_size = get(fsoil,'outerposition');
desired_fig_size = [(figure_size(1)+150)
(figure_size(2)+150) (table_extent(3)+155)
(table_extent(4)+100)];
set(fsoil,'outerposition', desired_fig_size);
saveas(btab1, 'DIAGSoil1.pdf')

dat4 =
{36,VECTEPA(1,10368),VECTEPP(1,10368),(VECTEPA(1,10368)-
VECTEPA(1,10080)),VECTSPA(1,10368),VECTSPP(1,10368),(VECTS
PA(1,10368)-
VECTSPA(1,10080)),VECTBPA(1,10368),VECTBPP(1,10368),(VECTB
PA(1,10368)-VECTBPA(1,10080));
```

```
37,VECTEPA(1,10658),VECTEPP(1,10658),(VECTEPA(1,10658)-
VECTEPA(1,10368)),VECTSPA(1,10658),VECTSPP(1,10658),(VECTS
PA(1,10658)-
VECTSPA(1,10368)),VECTBPA(1,10658),VECTBPP(1,10658),(VECTB
PA(1,10658)-VECTBPA(1,10368));

38,VECTEPA(1,10944),VECTEPP(1,10944),(VECTEPA(1,10944)-
VECTEPA(1,10658)),VECTSPA(1,10944),VECTSPP(1,10944),(VECTS
PA(1,10944)-
VECTSPA(1,10658)),VECTBPA(1,10944),VECTBPP(1,10944),(VECTB
PA(1,10944)-VECTBPA(1,10658));

39,VECTEPA(1,11232),VECTEPP(1,11232),(VECTEPA(1,11232)-
VECTEPA(1,10944)),VECTSPA(1,11232),VECTSPP(1,11232),(VECTS
PA(1,11232)-
VECTSPA(1,10944)),VECTBPA(1,11232),VECTBPP(1,11232),(VECTB
PA(1,11232)-VECTBPA(1,10944));

40,VECTEPA(1,11520),VECTEPP(1,11520),(VECTEPA(1,11520)-
VECTEPA(1,11232)),VECTSPA(1,11520),VECTSPP(1,11520),(VECTS
PA(1,11520)-
VECTSPA(1,11232)),VECTBPA(1,11520),VECTBPP(1,11520),(VECTB
PA(1,11520)-VECTBPA(1,11232));

41,VECTEPA(1,11808),VECTEPP(1,11808),(VECTEPA(1,11808)-
VECTEPA(1,11520)),VECTSPA(1,11808),VECTSPP(1,11808),(VECTS
PA(1,11808)-
VECTSPA(1,11520)),VECTBPA(1,11808),VECTBPP(1,11808),(VECTB
PA(1,11808)-VECTBPA(1,11520));

42,VECTEPA(1,12096),VECTEPP(1,12096),(VECTEPA(1,12096)-
VECTEPA(1,11808)),VECTSPA(1,12096),VECTSPP(1,12096),(VECTS
PA(1,12096)-
VECTSPA(1,11808)),VECTBPA(1,12096),VECTBPP(1,12096),(VECTB
PA(1,12096)-VECTBPA(1,11808));

43,VECTEPA(1,12384),VECTEPP(1,12384),(VECTEPA(1,12384)-
VECTEPA(1,12096)),VECTSPA(1,12384),VECTSPP(1,12384),(VECTS
PA(1,12384)-
VECTSPA(1,12096)),VECTBPA(1,12384),VECTBPP(1,12384),(VECTB
PA(1,12384)-VECTBPA(1,12096));

44,VECTEPA(1,12672),VECTEPP(1,12672),(VECTEPA(1,12672)-
VECTEPA(1,12384)),VECTSPA(1,12672),VECTSPP(1,12672),(VECTS
PA(1,12672)-
```

```
VECTSPA(1,12384)),VECTBPA(1,12672),VECTBPP(1,12672),(VECTB
PA(1,12672)-VECTBPA(1,12384));

45,VECTEPA(1,12960),VECTEPP(1,12960),(VECTEPA(1,12960)-
VECTEPA(1,12672)),VECTSPA(1,12960),VECTSPP(1,12960),(VECTS
PA(1,12960)-
VECTSPA(1,12672)),VECTBPA(1,12960),VECTBPP(1,12960),(VECTB
PA(1,12960)-VECTBPA(1,12672));

46,VECTEPA(1,13248),VECTEPP(1,13248),(VECTEPA(1,13248)-
VECTEPA(1,12960)),VECTSPA(1,13248),VECTSPP(1,13248),(VECTS
PA(1,13248)-
VECTSPA(1,12960)),VECTBPA(1,13248),VECTBPP(1,13248),(VECTB
PA(1,13248)-VECTBPA(1,12960));

47,VECTEPA(1,13536),VECTEPP(1,13536),(VECTEPA(1,13536)-
VECTEPA(1,13248)),VECTSPA(1,13536),VECTSPP(1,13536),(VECTS
PA(1,13536)-
VECTSPA(1,13248)),VECTBPA(1,13536),VECTBPP(1,13536),(VECTB
PA(1,13536)-VECTBPA(1,13248));

48,VECTEPA(1,13824),VECTEPP(1,13824),(VECTEPA(1,13824)-
VECTEPA(1,13536)),VECTSPA(1,13824),VECTSPP(1,13824),(VECTS
PA(1,13824)-
VECTSPA(1,13536)),VECTBPA(1,13824),VECTBPP(1,13824),(VECTB
PA(1,13824)-VECTBPA(1,13536));

49,VECTEPA(1,14112),VECTEPP(1,14112),(VECTEPA(1,14112)-
VECTEPA(1,13824)),VECTSPA(1,14112),VECTSPP(1,14112),(VECTS
PA(1,14112)-
VECTSPA(1,13824)),VECTBPA(1,14112),VECTBPP(1,14112),(VECTB
PA(1,14112)-VECTBPA(1,13824));

50,VECTEPA(1,14400),VECTEPP(1,14400),(VECTEPA(1,14400)-
VECTEPA(1,14112)),VECTSPA(1,14400),VECTSPP(1,14400),(VECTS
PA(1,14400)-
VECTSPA(1,14112)),VECTBPA(1,14400),VECTBPP(1,14400),(VECTB
PA(1,14400)-VECTBPA(1,14112));

51,VECTEPA(1,14688),VECTEPP(1,14688),(VECTEPA(1,14688)-
VECTEPA(1,14400)),VECTSPA(1,14688),VECTSPP(1,14688),(VECTS
PA(1,14688)-
VECTSPA(1,14400)),VECTBPA(1,14688),VECTBPP(1,14688),(VECTB
PA(1,14688)-VECTBPA(1,14400));

52,VECTEPA(1,14976),VECTEPP(1,14976),(VECTEPA(1,14976)-
VECTEPA(1,14688)),VECTSPA(1,14976),VECTSPP(1,14976),(VECTS
```

```
PA(1,14976)-
VECTSPA(1,14688)),VECTBPA(1,14976),VECTBPP(1,14976),(VECTB
PA(1,14976)-VECTBPA(1,14688));

53,VECTEPA(1,15264),VECTEPP(1,15264),(VECTEPA(1,15264)-
VECTEPA(1,14976)),VECTSPA(1,15264),VECTSPP(1,15264),(VECTS
PA(1,15264)-
VECTSPA(1,14976)),VECTBPA(1,15264),VECTBPP(1,15264),(VECTB
PA(1,15264)-VECTBPA(1,14976));

54,VECTEPA(1,15552),VECTEPP(1,15552),(VECTEPA(1,15552)-
VECTEPA(1,15264)),VECTSPA(1,15552),VECTSPP(1,15552),(VECTS
PA(1,15552)-
VECTSPA(1,15264)),VECTBPA(1,15552),VECTBPP(1,15552),(VECTB
PA(1,15552)-VECTBPA(1,15264));

55,VECTEPA(1,15840),VECTEPP(1,15840),(VECTEPA(1,15840)-
VECTEPA(1,15552)),VECTSPA(1,15840),VECTSPP(1,15840),(VECTS
PA(1,15840)-
VECTSPA(1,15552)),VECTBPA(1,15840),VECTBPP(1,15840),(VECTB
PA(1,15840)-VECTBPA(1,15552));

56,VECTEPA(1,16128),VECTEPP(1,16128),(VECTEPA(1,16128)-
VECTEPA(1,15840)),VECTSPA(1,16128),VECTSPP(1,16128),(VECTS
PA(1,16128)-
VECTSPA(1,15840)),VECTBPA(1,16128),VECTBPP(1,16128),(VECTB
PA(1,16128)-VECTBPA(1,15840));

57,VECTEPA(1,16416),VECTEPP(1,16416),(VECTEPA(1,16416)-
VECTEPA(1,16128)),VECTSPA(1,16416),VECTSPP(1,16416),(VECTS
PA(1,16416)-
VECTSPA(1,16128)),VECTBPA(1,16416),VECTBPP(1,16416),(VECTB
PA(1,16416)-VECTBPA(1,16128));

58,VECTEPA(1,16704),VECTEPP(1,16704),(VECTEPA(1,16704)-
VECTEPA(1,16416)),VECTSPA(1,16704),VECTSPP(1,16704),(VECTS
PA(1,16704)-
VECTSPA(1,16416)),VECTBPA(1,16704),VECTBPP(1,16704),(VECTB
PA(1,16704)-VECTBPA(1,16416));

59,VECTEPA(1,16992),VECTEPP(1,16992),(VECTEPA(1,16992)-
VECTEPA(1,16704)),VECTSPA(1,16992),VECTSPP(1,16992),(VECTS
PA(1,16992)-
VECTSPA(1,16704)),VECTBPA(1,16992),VECTBPP(1,16992),(VECTB
PA(1,16992)-VECTBPA(1,16704));

60,VECTEPA(1,17280),VECTEPP(1,17280),(VECTEPA(1,17280)-
```

```
VECTEPA(1,16992)),VECTSPA(1,17280),VECTSPP(1,17280),(VECTS
PA(1,17280)-
VECTSPA(1,16992)),VECTBPA(1,17280),VECTBPP(1,17280),(VECTB
PA(1,17280)-VECTBPA(1,16992));

61,VECTEPA(1,17568),VECTEPP(1,17568),(VECTEPA(1,17568)-
VECTEPA(1,17280)),VECTSPA(1,17568),VECTSPP(1,17568),(VECTS
PA(1,17568)-
VECTSPA(1,17280)),VECTBPA(1,17568),VECTBPP(1,17568),(VECTB
PA(1,17568)-VECTBPA(1,17280));

62,VECTEPA(1,17856),VECTEPP(1,17856),(VECTEPA(1,17856)-
VECTEPA(1,17568)),VECTSPA(1,17856),VECTSPP(1,17856),(VECTS
PA(1,17856)-
VECTSPA(1,17568)),VECTBPA(1,17856),VECTBPP(1,17856),(VECTB
PA(1,17856)-VECTBPA(1,17568));

63,VECTEPA(1,18144),VECTEPP(1,18144),(VECTEPA(1,18144)-
VECTEPA(1,17856)),VECTSPA(1,18144),VECTSPP(1,18144),(VECTS
PA(1,18144)-
VECTSPA(1,17856)),VECTBPA(1,18144),VECTBPP(1,18144),(VECTB
PA(1,18144)-VECTBPA(1,17856));};

fsoil= figure('name' , 'Soil Layer Diagnostics');
btab2 = uitable('columnname', col2, 'data', dat4);
table_extent = get(btab2,'Extent');
set(btab2,'Position',[1 -25 table_extent(3)
table_extent(4)+40])
figure_size = get(fsoil,'outerposition');
desired_fig_size = [(figure_size(1)+150)
(figure_size(2)+150) (table_extent(3)+155)
(table_extent(4)+100)];
set(fsoil,'outerposition', desired_fig_size);
saveas(btab2, 'DIAGSoil2.pdf')

%Table ?b
col3 = {'Day', '#SP&BP', '?#SP&BP', '?b', '??b'};

dat5 = [0,0,0,0,0;
       1, VECTSPBPA(1,288), (VECTSPBPA(1,288)-0),
VECTSPBPP(1,288), (VECTSPBPP(1,288)-0);
       2, VECTSPBPA(1,576), (VECTSPBPA(1,576)-
VECTSPBPA(1,288)), VECTSPBPP(1,576), (VECTSPBPP(1,576)-
VECTSPBPP(1,288));
       3, VECTSPBPA(1,864), (VECTSPBPA(1,864)-
VECTSPBPA(1,576)), VECTSPBPP(1,864), (VECTSPBPP(1,864)-
VECTSPBPP(1,576));
```

```
       4, VECTSPBPA(1,1152), (VECTSPBPA(1,1152)-
VECTSPBPA(1,864)), VECTSPBPP(1,1152), (VECTSPBPP(1,1152)-
VECTSPBPP(1,864));
       5, VECTSPBPA(1,1440), (VECTSPBPA(1,1440)-
VECTSPBPA(1,1152)), VECTSPBPP(1,1440), (VECTSPBPP(1,1440)-
VECTSPBPP(1,1152));
       6,VECTSPBPA(1,1728),(VECTSPBPA(1,1728)-
VECTSPBPA(1,1440)),VECTSPBPP(1,1728),(VECTSPBPP(1,1728)-
VECTSPBPP(1,1440));
       7,VECTSPBPA(1,2016),(VECTSPBPA(1,2016)-
VECTSPBPA(1,1728)),VECTSPBPP(1,2016),(VECTSPBPP(1,2016)-
VECTSPBPP(1,1728));
       8,VECTSPBPA(1,2304),(VECTSPBPA(1,2304)-
VECTSPBPA(1,2016)),VECTSPBPP(1,2304),(VECTSPBPP(1,2304)-
VECTSPBPP(1,2016));
       9,VECTSPBPA(1,2592),(VECTSPBPA(1,2592)-
VECTSPBPA(1,2304)),VECTSPBPP(1,2592),(VECTSPBPP(1,2592)-
VECTSPBPP(1,2304));
       10,VECTSPBPA(1,2880),(VECTSPBPA(1,2880)-
VECTSPBPA(1,2592)),VECTSPBPP(1,2880),(VECTSPBPP(1,2880)-
VECTSPBPP(1,2592));
       11,VECTSPBPA(1,3168),(VECTSPBPA(1,3168)-
VECTSPBPA(1,2880)),VECTSPBPP(1,3168),(VECTSPBPP(1,3168)-
VECTSPBPP(1,2880));
       12,VECTSPBPA(1,3456),(VECTSPBPA(1,3456)-
VECTSPBPA(1,3168)),VECTSPBPP(1,3456),(VECTSPBPP(1,3456)-
VECTSPBPP(1,3168));
       13,VECTSPBPA(1,3744),(VECTSPBPA(1,3744)-
VECTSPBPA(1,3456)),VECTSPBPP(1,3744),(VECTSPBPP(1,3744)-
VECTSPBPP(1,3456));
       14,VECTSPBPA(1,4032),(VECTSPBPA(1,4032)-
VECTSPBPA(1,3744)),VECTSPBPP(1,4032),(VECTSPBPP(1,4032)-
VECTSPBPP(1,3744));
       15,VECTSPBPA(1,4320),(VECTSPBPA(1,4320)-
VECTSPBPA(1,4032)),VECTSPBPP(1,4320),(VECTSPBPP(1,4320)-
VECTSPBPP(1,4032));
       16,VECTSPBPA(1,4608),(VECTSPBPA(1,4608)-
VECTSPBPA(1,4320)),VECTSPBPP(1,4608),(VECTSPBPP(1,4608)-
VECTSPBPP(1,4320));
       17,VECTSPBPA(1,4896),(VECTSPBPA(1,4896)-
VECTSPBPA(1,4608)),VECTSPBPP(1,4896),(VECTSPBPP(1,4896)-
VECTSPBPP(1,4608));
       18,VECTSPBPA(1,5184),(VECTSPBPA(1,5184)-
VECTSPBPA(1,4896)),VECTSPBPP(1,5184),(VECTSPBPP(1,5184)-
VECTSPBPP(1,4896));
```

```
       19,VECTSPBPA(1,5472),(VECTSPBPA(1,5472)-
VECTSPBPA(1,5184)),VECTSPBPP(1,5472),(VECTSPBPP(1,5472)-
VECTSPBPP(1,5184));
       20,VECTSPBPA(1,5760),(VECTSPBPA(1,5760)-
VECTSPBPA(1,5472)),VECTSPBPP(1,5760),(VECTSPBPP(1,5760)-
VECTSPBPP(1,5472));
       21,VECTSPBPA(1,6048),(VECTSPBPA(1,6048)-
VECTSPBPA(1,5760)),VECTSPBPP(1,6048),(VECTSPBPP(1,6048)-
VECTSPBPP(1,5760));
       22,VECTSPBPA(1,6336),(VECTSPBPA(1,6336)-
VECTSPBPA(1,6048)),VECTSPBPP(1,6336),(VECTSPBPP(1,6336)-
VECTSPBPP(1,6048));
       23,VECTSPBPA(1,6624),(VECTSPBPA(1,6624)-
VECTSPBPA(1,6336)),VECTSPBPP(1,6624),(VECTSPBPP(1,6624)-
VECTSPBPP(1,6336));
       24,VECTSPBPA(1,6912),(VECTSPBPA(1,6912)-
VECTSPBPA(1,6624)),VECTSPBPP(1,6912),(VECTSPBPP(1,6912)-
VECTSPBPP(1,6624));
       25,VECTSPBPA(1,7200),(VECTSPBPA(1,7200)-
VECTSPBPA(1,6912)),VECTSPBPP(1,7200),(VECTSPBPP(1,7200)-
VECTSPBPP(1,6912));
       26,VECTSPBPA(1,7488),(VECTSPBPA(1,7488)-
VECTSPBPA(1,7200)),VECTSPBPP(1,7488),(VECTSPBPP(1,7488)-
VECTSPBPP(1,7200));
       27,VECTSPBPA(1,7776),(VECTSPBPA(1,7776)-
VECTSPBPA(1,7488)),VECTSPBPP(1,7776),(VECTSPBPP(1,7776)-
VECTSPBPP(1,7488));
       28,VECTSPBPA(1,8064),(VECTSPBPA(1,8064)-
VECTSPBPA(1,7776)),VECTSPBPP(1,8064),(VECTSPBPP(1,8064)-
VECTSPBPP(1,7776));
       29,VECTSPBPA(1,8352),(VECTSPBPA(1,8352)-
VECTSPBPA(1,8064)),VECTSPBPP(1,8352),(VECTSPBPP(1,8352)-
VECTSPBPP(1,8064));
       30,VECTSPBPA(1,8640),(VECTSPBPA(1,8640)-
VECTSPBPA(1,8352)),VECTSPBPP(1,8640),(VECTSPBPP(1,8640)-
VECTSPBPP(1,8352));
       31,VECTSPBPA(1,8928),(VECTSPBPA(1,8928)-
VECTSPBPA(1,8640)),VECTSPBPP(1,8928),(VECTSPBPP(1,8928)-
VECTSPBPP(1,8640));
       32,VECTSPBPA(1,9216),(VECTSPBPA(1,9216)-
VECTSPBPA(1,8928)),VECTSPBPP(1,9216),(VECTSPBPP(1,9216)-
VECTSPBPP(1,8928));
       33,VECTSPBPA(1,9504),(VECTSPBPA(1,9504)-
VECTSPBPA(1,9216)),VECTSPBPP(1,9504),(VECTSPBPP(1,9504)-
VECTSPBPP(1,9216));
```

```
       34,VECTSPBPA(1,9792),(VECTSPBPA(1,9792)-
VECTSPBPA(1,9504)),VECTSPBPP(1,9792),(VECTSPBPP(1,9792)-
VECTSPBPP(1,9504));
       35,VECTSPBPA(1,10080),(VECTSPBPA(1,10080)-
VECTSPBPA(1,9792)),VECTSPBPP(1,10080),(VECTSPBPP(1,10080)-
VECTSPBPP(1,9792));];

fspbp= figure('name' , 'SP&BP Diagnostics');
ctab1 = uitable('columnname', col3, 'data', dat5);
table_extent = get(ctab1,'Extent');
set(ctab1,'Position',[1 -25 table_extent(3)
table_extent(4)+40])
figure_size = get(fspbp,'outerposition');
desired_fig_size = [(figure_size(1)+150)
(figure_size(2)+150) (table_extent(3)+155)
(table_extent(4)+100)];
set(fspbp,'outerposition', desired_fig_size);
saveas(ctab1, 'DIAGspbp1.pdf')

dat6 = [36,VECTSPBPA(1,10368),(VECTSPBPA(1,10368)-
VECTSPBPA(1,10080)),VECTSPBPP(1,10368),(VECTSPBPP(1,10368)
-VECTSPBPP(1,10080));
       37,VECTSPBPA(1,10656),(VECTSPBPA(1,10656)-
VECTSPBPA(1,10368)),VECTSPBPP(1,10656),(VECTSPBPP(1,10656)
-VECTSPBPP(1,10368));
       38,VECTSPBPA(1,10944),(VECTSPBPA(1,10944)-
VECTSPBPA(1,10656)),VECTSPBPP(1,10944),(VECTSPBPP(1,10944)
-VECTSPBPP(1,10656));
       39,VECTSPBPA(1,11232),(VECTSPBPA(1,11232)-
VECTSPBPA(1,10944)),VECTSPBPP(1,11232),(VECTSPBPP(1,11232)
-VECTSPBPP(1,10944));
       40,VECTSPBPA(1,11520),(VECTSPBPA(1,11520)-
VECTSPBPA(1,11232)),VECTSPBPP(1,11520),(VECTSPBPP(1,11520)
-VECTSPBPP(1,11232));
       41,VECTSPBPA(1,11808),(VECTSPBPA(1,11808)-
VECTSPBPA(1,11520)),VECTSPBPP(1,11808),(VECTSPBPP(1,11808)
-VECTSPBPP(1,11520));
       42,VECTSPBPA(1,12096),(VECTSPBPA(1,12096)-
VECTSPBPA(1,11808)),VECTSPBPP(1,12096),(VECTSPBPP(1,12096)
-VECTSPBPP(1,11808));
       43,VECTSPBPA(1,12384),(VECTSPBPA(1,12384)-
VECTSPBPA(1,12096)),VECTSPBPP(1,12384),(VECTSPBPP(1,12384)
-VECTSPBPP(1,12096));
       44,VECTSPBPA(1,12672),(VECTSPBPA(1,12672)-
VECTSPBPA(1,12384)),VECTSPBPP(1,12672),(VECTSPBPP(1,12672)
-VECTSPBPP(1,12384));
```

```
       45,VECTSPBPA(1,12960),(VECTSPBPA(1,12960)-
VECTSPBPA(1,12672)),VECTSPBPP(1,12960),(VECTSPBPP(1,12960)
-VECTSPBPP(1,12672));
       46,VECTSPBPA(1,13248),(VECTSPBPA(1,13248)-
VECTSPBPA(1,12960)),VECTSPBPP(1,13248),(VECTSPBPP(1,13248)
-VECTSPBPP(1,12960));
       47,VECTSPBPA(1,13536),(VECTSPBPA(1,13536)-
VECTSPBPA(1,13248)),VECTSPBPP(1,13536),(VECTSPBPP(1,13536)
-VECTSPBPP(1,13248));
       48,VECTSPBPA(1,13824),(VECTSPBPA(1,13824)-
VECTSPBPA(1,13536)),VECTSPBPP(1,13824),(VECTSPBPP(1,13824)
-VECTSPBPP(1,13536));
       49,VECTSPBPA(1,14112),(VECTSPBPA(1,14112)-
VECTSPBPA(1,13824)),VECTSPBPP(1,14112),(VECTSPBPP(1,14112)
-VECTSPBPP(1,13824));
       50,VECTSPBPA(1,14400),(VECTSPBPA(1,14400)-
VECTSPBPA(1,14112)),VECTSPBPP(1,14400),(VECTSPBPP(1,14400)
-VECTSPBPP(1,14112));
       51,VECTSPBPA(1,14688),(VECTSPBPA(1,14688)-
VECTSPBPA(1,14400)),VECTSPBPP(1,14688),(VECTSPBPP(1,14688)
-VECTSPBPP(1,14400));
       52,VECTSPBPA(1,14976),(VECTSPBPA(1,14976)-
VECTSPBPA(1,14688)),VECTSPBPP(1,14976),(VECTSPBPP(1,14976)
-VECTSPBPP(1,14688));
       53,VECTSPBPA(1,15264),(VECTSPBPA(1,15264)-
VECTSPBPA(1,14976)),VECTSPBPP(1,15264),(VECTSPBPP(1,15264)
-VECTSPBPP(1,14976));
       54,VECTSPBPA(1,15552),(VECTSPBPA(1,15552)-
VECTSPBPA(1,15264)),VECTSPBPP(1,15552),(VECTSPBPP(1,15552)
-VECTSPBPP(1,15264));
       55,VECTSPBPA(1,15840),(VECTSPBPA(1,15840)-
VECTSPBPA(1,15552)),VECTSPBPP(1,15840),(VECTSPBPP(1,15840)
-VECTSPBPP(1,15552));
       56,VECTSPBPA(1,16128),(VECTSPBPA(1,16128)-
VECTSPBPA(1,15840)),VECTSPBPP(1,16128),(VECTSPBPP(1,16128)
-VECTSPBPP(1,15840));
       57,VECTSPBPA(1,16416),(VECTSPBPA(1,16416)-
VECTSPBPA(1,16128)),VECTSPBPP(1,16416),(VECTSPBPP(1,16416)
-VECTSPBPP(1,16128));
       58,VECTSPBPA(1,16704),(VECTSPBPA(1,16704)-
VECTSPBPA(1,16416)),VECTSPBPP(1,16704),(VECTSPBPP(1,16704)
-VECTSPBPP(1,16416));
       59,VECTSPBPA(1,16992),(VECTSPBPA(1,16992)-
VECTSPBPA(1,16704)),VECTSPBPP(1,16992),(VECTSPBPP(1,16992)
-VECTSPBPP(1,16704));
```

```
       60,VECTSPBPA(1,17280),(VECTSPBPA(1,17280)-
VECTSPBPA(1,16992)),VECTSPBPP(1,17280),(VECTSPBPP(1,17280)
-VECTSPBPP(1,16992));
       61,VECTSPBPA(1,17568),(VECTSPBPA(1,17568)-
VECTSPBPA(1,17280)),VECTSPBPP(1,17568),(VECTSPBPP(1,17568)
-VECTSPBPP(1,17280));
       62,VECTSPBPA(1,17856),(VECTSPBPA(1,17856)-
VECTSPBPA(1,17568)),VECTSPBPP(1,17856),(VECTSPBPP(1,17856)
-VECTSPBPP(1,17568));
       63,VECTSPBPA(1,18144),(VECTSPBPA(1,18144)-
VECTSPBPA(1,17856)),VECTSPBPP(1,18144),(VECTSPBPP(1,18144)
-VECTSPBPP(1,17856));];

fspbp= figure('name' , 'SP&BP Diagnostics');
ctab2 = uitable('columnname', col3, 'data', dat6);
table_extent = get(ctab2,'Extent');
set(ctab2,'Position',[1 -25 table_extent(3)
table_extent(4)+40])
figure_size = get(fspbp,'outerposition');
desired_fig_size = [(figure_size(1)+150)
(figure_size(2)+150) (table_extent(3)+155)
(table_extent(4)+100)];
set(fspbp,'outerposition', desired_fig_size);
saveas(ctab2, 'DIAGspbp2.pdf')
```